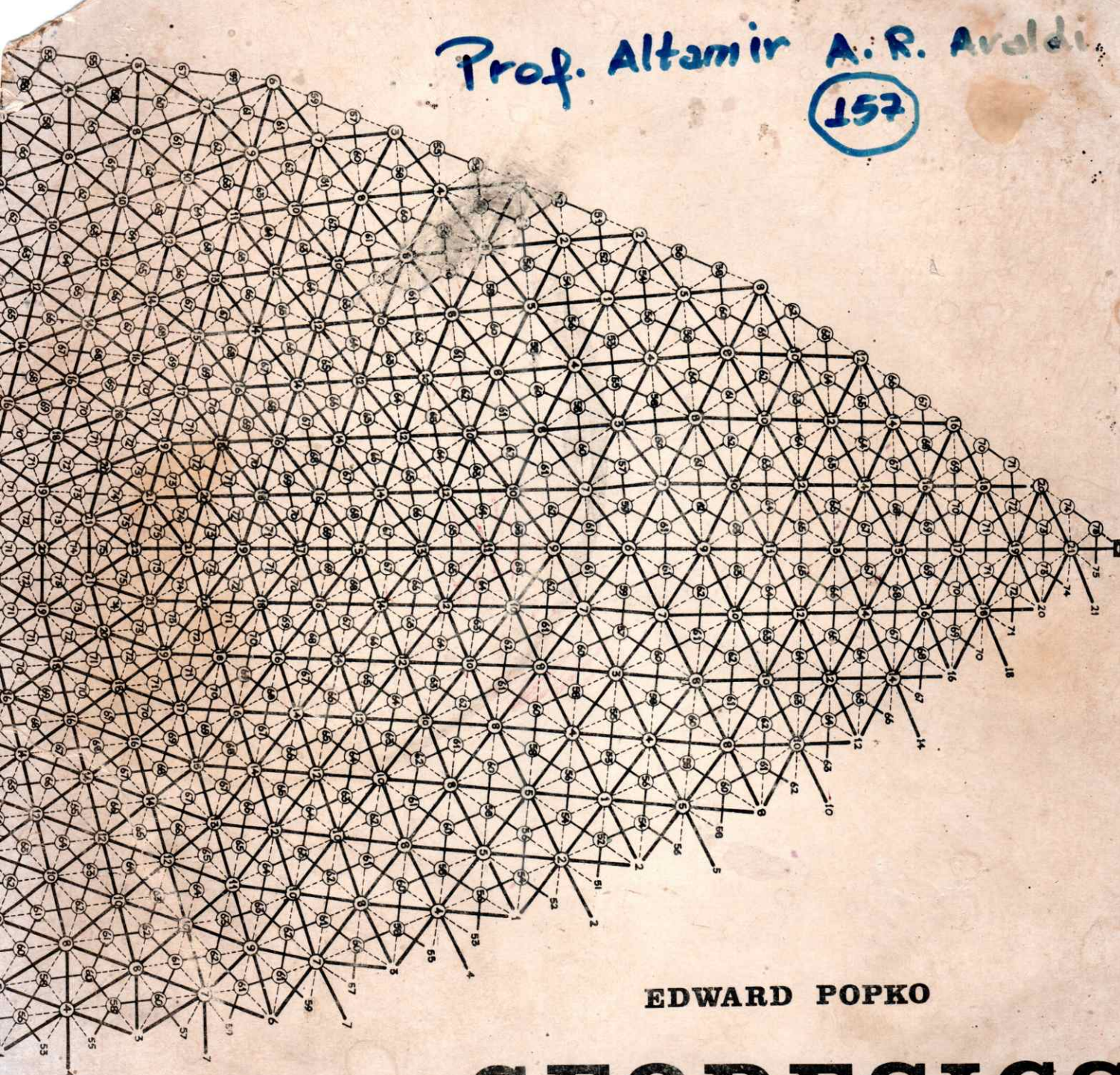

EDWARD POPKO

GEODESICS

GEODESICS

EDWARD POPKO

Industrialization and Technology
Course Supplement Number I
School of Architecture
University of Detroit
Detroit, Michigan

INTRODUCTION

The term geodesics is a contemporary geometric title ascribed to the arcs on a spherical surface which represent the shortest distance between any two points on that surface. When applied to architectural spanning devices it becomes, "...a frame of generally spherical form in which the main structural elements are interconnected in a geodesic pattern of approximate great circle arcs intersecting to form a three-way grid,..." (From R. B. Fuller, U.S. Pat. No. 2-682-235)

The following primer concerns itself with some of the basic principles which have underlined investigations into geodesic structures. Although the scope is somewhat limited, the author wishes to relate sufficient background so as to familiarize the reader with criterion necessary to spherical design. In an attempt to offset supplementary references we have treated geodesic domes as developments of polyhedra and it is at this point our investigation begins.

Many of the examples contained herein embody patented principles of Richard Buckminister Fuller. These projects represent the work of many individuals as part of a continuing process of search by the offices established by Mr. Fuller. I wish to thank the organizations of Geometric Incorporated, Synergetics Incorporated, and R. Buckminister Fuller - Sadao Incorporated for their aid in securing material and to John Borrago and the National Endowment for the Arts for their encouragement.

Edward Popko
School of Architecture
University of Detroit
Detroit, Michigan

TO R.B.F.

POLYHEDRA

To initiate our investigation into geodesic structures we must first concern ourselves with the basic polyhedra whose spherical versions form the basis for all geometric development. Polyhedra are basically three dimensional constructions embodying various degrees of geometrical restraint. Three such families present themselves most directly: the platonic, archimedian, and archimedian duals.

The five platonic solids Row 1 Fig. 1, are the most basic of polyhedra. Each possesses regular congruent faces, equal face angles, and equal dihedral angles. The thirteen archimedian solids, Rows 2, 3 and 4 Fig. 1, are similar forms retaining the regular face restraint, but allowing more than one regular face polygon. Equal face and dihedral angle restrains no longer apply, however, both platonic and archimedian polyhedra maintain equal edge length throughout. We include also Euler's law which relates topologically the various restraints.

Every polyhedra, whether platonic or archimedian, has a dual to it, that is, there exists another polyhedra whose faces correspond to edges, vertexes, and faces of the original polyhedra. Figure 2 diagramatically illustrates three dual conditions. Upon closer inspection of the vertex, face, and edge counts under the polyhedra of Fig. 1 several reoccuring phenomena take place. Note that the dodecahedron evenly distributes 20 vertex points, 12 faces, and 30 edges, while the icosahedron merely rearranges the count, 12 vertex points, 20 faces, and 30 edges. These two polyhedra therefore are duals. Column 1, Fig. 2 demonstrates this by circumscribing the icosahedron about the dodecahedron, every icosa-vertex positioning itself about the mid dodeca-face and vice-versa. The inscribed dodecahedron could have circumscribed the icosahedron just as easily. Thus both the icosahedron and the dodecahedron are mutually related by their common geometric nature and are said to be duals.

Column 2, Fig. 2 could have reversed the column 1 situation circumscribing the dodecahedron about the icosahedron; however, a third dual figure, the rhombic

triacontahedron (not shown in Fig. 1), is noteworthy of our attention. This polyhedron distributes 32 vertexes, 30 faces, and 60 edges possessing dual characteristics to both the dodecahedron and the icosahedron. With respect to the column 2 Fig. 2 illustration we find that the rhombic triacontahedron distributes 30 diamond faces, the long axis of which corresponds to the icosa-edge. While distributing a face for every icosa-edge not only are the icosa vertexes retained but an additional 20 vertexes are added, one for each mid-icosa face point. Having previously established the dodeca-icosa dual, it naturally follows that the rhombic triacontahedron relates similarity to the dodecahedron. In this case the rhombic triacontahedron displaces a face, the narrow axis of which corresponds to dodeca-edges. This three way duality must not be overlooked for it is upon this geometrical inter-relation that the geodesic principles lie. Departing momentarly from Fig. 2, we glance at the upper row diagrams of Fig. 7, here spherical versions of the dodecahedron, icosahedron and rhombic triacontahedron have been cumulatively superimposed in their respective positions of duality to create a combined sphere. This combined sphere, as we will discover shortly, is the basic geodesic sphere for its edges represent great circles intersections, 15 in all. The darkened portion of the sphere represents the area shared commonly by the three spherical polyhedra leading to the combined form. We will reserve discussion of this triangle till later. Returning again to Fig. 2, the icosa-dodecahedron and the rhombic triacontahedron dual is indicated in column 3. Although not as common as the previous two cases of duality, none-the-less, a face addition in Row 1 does not alter the dual characteristics.

ORIENTATION

Although somewhat basic, it is necessary in our development from polyhedra to spherical structures to point out that spherical bodies may orientate themselves in an infinite number of positions in space. In dealing with domes, however, only three basic conditions are considered: edge, face and vertex zenith. In the combined sphere (icosahedron, dodecahedron, rhombic triacontahedron), the heavy rhombic triacontahedron diamonds, the long axis of which delineates the icosa edge and the

short axis the dodeca edge, indicate the basic orientations. We will return again to Fig. 3 in the following section, while discussing frequencies when these orientations become useful as an aid to describing points in space.

To this point our concern has primarily been with basic icosahedral forms and their related duals. We have chosen to limit ourselves to this category of geometry for this family offers the greatest degree of regularity when translated into spherical structures of which member length and joinery conditions become factors.

BREAKDOWN

In dealing with the great range of conditions that the dome must geometrically satisfy (span and height most commonly) it becomes readily apparent that the basic icosahedron cannot remain in a pure state. This brings us to the matter of a geometrical breakdown. This can best be described as an attempt to expand the icosahedral form to satisfy the space requirements and allow the components from which it is made to remain within structural fabrication and erection limits.

A logical starting point would be to reduce the icosahedron to the greatest number of equal components. Having already accomplished this by coincidence, through the dual exercises of Fig. 2 and 7 Row 1, we find that the greatest number of equal faces that both planar and spherical icosahedrons can be subdivided into is 120. This is true for any sphere. In Fig. 7, Row 1, we noted earlier that this basic right spherical triangle (shaded area) was the common area shared by the superimposition of the dodecahedron, icosahedron, and rhombic triacontahedron. It turns out that this is the least common area to which an icosahedral form can be reduced, noting further that 60 of the 120 faces are left-handed right triangles and 60 are right-handed right triangles. This shaded portion represents 1/6 of an icosa face, 1/10 of a dodeca face and 1/4 of a rhombic tricontahedron face. A spherical description of this right triangle appears in Fig. 7 mid-page. Topologically speaking, the combined superimposition sphere consists of 15 great circle intersections.

By reducing the icosahedral surface to its smallest basic triangle we have only partially succeeded in our goal. Equal member lengths and vertex angles have yet to be satisfied. Although not fulfilling all criteria, it is noteworthy that this basic right triangle is identical throughout the entire surface subdivision. It is therefore possible and common practice, to describe any subdivision of the surface of the sphere in terms of the basic grid triangle. Information (geometrically or mathematically), can readily be passed throughout the surface by its rotating and/or mirroring about the sphere.

Our attention must again return to reducing the icosahedron to equal components. Two basic subdivision methods present themselves most directly, the Triacon and the Alternate. The Triacon divides the icosa face about its mediam lines, see Fig. 5 column 1. This subdivision resenbles the rhombic triacontahedron with the addition of a diamond narrow axis member. It is perhaps from this dual the name was derived. In its most basic form the Triacon subdivision distributes two near equalateral faces over every icosa edge. The third diagram in column 1 indicates members of equal length. Note that the icosa edge no longer remains a part of the final form.

In the second method the Alternate, the icosa-face is subdivided by faces whose edges are parallel to the icosa edge. Unlike the Triacon breakdown, the icosa edge remains a part of the final form. The third figure column 2 indicates members of equal length. The third subdivision, the Hex-Pent breakdown, is but a special case of the Alternate breakdown and will be discussed later. Throughout Fig. 5 Row 3 the grid triangle has remained to demonstrate that enough breakdown information is contained within it to adequately define the entire spherical surface.

The breakdown process, as we have seen, merely reduces the icosahedron to smaller and smaller nearly identical pieces. This process could theoretically be carried on indefinitely which brings us to the matter of frequency or the degree to which the icosahedron has been subdivided. A capsulized comparison of Triacon and Alternate breakdowns can be found on Fig. 8.

FREQUENCY

Almost synonymous with breakdown is the notion of frequency. Frequency is merely the number of segments the icosa edge, whether a real member or not, has been divided by a particular breakdown.

The frequency of any particular sphere is graphically designated by the number of times the icosa edge has been segmented and a superscript V, i.e., 3^V. Referring to Fig. 5 once more, both columns 1 and 2 would therefore be 2^V breakdowns, the icosa edge being segmented twice.

Breakdown and frequency are of particular concern to the spherical designer not only from a geometrical standpoint, but also in regard to erection and fabrication. As the frequency of a particular subdivision increases, member length or face edges reduce, the number of components increase and the numbers of different vertex angles increase. Finally the basic icosahedron which distributed 12 vertices on the sphere is now distributing many more vertices and could be said to be evolving from a faceted polyhedron to a pure sphere.

Special notice must be taken of non-triangular breakdowns for it is upon their triangulated versions that frequency counts are made. Figure 6 illustrates that while diamonds, hexagons, and pentagons are dominant, pattern-wise they are merely the result of a triangulated grid in which members were omitted. Column 1 Fig. 6 presents the three principle patterns obtainable from the Alternate breakdown method, while column 2 demonstrates the Triacon breakdown. Note that in the Alternate diamond breakdown and all Triacon cases the breakdown patterns overlap into adjacent icosa faces.

Carrying the subdivision patterns a bit further, note the subtle relationships that exists between the final pattern and the frequency. The Alternate method permits any frequency of triangular breakdown while the Triacon permits only even-numbered frequencies. The fact that the median lines are the axis of Triacon division proves

this (see Fig. 7, mid-page) frequencies 6^V, and 14^V were omitted to allow a graphic comparison of doubling frequencies.

In diamond facets the Alternate requires a minimum 3^V while the Triacon only a 2^V. Similar minimum frequencies exist for the Hex-Pent breakdowns; 3^V and 4^V respectfully. It is worth noting here that every icosahedron vertex consists of the intersection of five edges. The triangular faces which remain at the icosahedron vertex during the subdivision process, group together in the completed icosahedron to form a pentagon. This accounts for the hexagon and triangular patterns in Fig. 5 Row 3 being called Hex-Pent.

This phenomena is technically worth re-examining, for it aids in identifying a dome's frequency. By locating any five-way or pentagonal vertices in the dome, the icosa vertices are found. By connecting any two adjacent five-way vertices an icosa-edge is formed. This edge may or may not be an actual dome component. Where this icosa edge is coincidental with the structural pattern, the breakdown is Alternate. When the triangular patterning lies across the icosa-edge the breakdown is Triacon. Again where the facets of the dome appear as diamonds, pentagons, or hexagons it is necessarily to mentally polt in the pattern of triangulation before the original breakdown frequency can be determined.

Examples of various frequencies and breakdowns can be found on Figs. 7, 9, 10, 11 and 12, not to mention scattered examples throughout the text.* In all cases the members contributing to the pentagonal icosa vertices and the icosa face are delineated. Figure 9 allows for comparison of vertex and edge zenith orientations. Figure 13 has been included to point out that sub assembly domes do not alter our methods of identification.

---

*In light of breakdown and frequency, the truncated icosahedron and icosadodecahedron of Fig. 1 are respectfully 3^V and 2^V Alternate spheres.

BASE TRUNCATIONS

In the architectonic state, domes appear as truncated spheres. When considering the results of passing a horizontal datum plane normal to the polar axis at various points from north to south poles, we find base truncation regulates the proportion of surface area, volumetric enclosure and horizontal floor area. The least surface area and volume per unit gain of floor area exists in the first 1/3 sphere. As the datum approaches equatorial truncations, surface area and volume contained are rapidly increasing while the rate of floor area gain is diminishing, at the equator maximum floor area is reached. As the datum approaches the south pole, surface area and volume are approaching maximums while floor area reduces to infinity at the pole.

In terms of construction and maintenance of dome structures these variables have economic consequences. Surface area is proportional to structure, while volume may become an environmental control consideration. The most economical range surface and volume wise per floor area has been the 1/3 sphere icosa-cap or pent-cap* truncations. Beyond this point the accumulation of structure and needless volume prohibit spherical use in many cases. This fact accounts for a rather large number of pent-cap or 1/3 spheres beyond the 150 foot span range. Figs. 69, 73, 77, 79, and 82 represent projects that have utilized these proportions.

Referring to our systems of breakdown, the Triacon and the Alternate systems offer truncation limits. Since, in the Triacon breakdown, no complete great circle is delineated naturally by the structural pattern, such as the equatorial obtainable in even number alternate breakdowns, truncated base members must be used in every case. The Expo '67 dome Fig. 88 is an attempt to alleviate this problem. (See net explanation Fig. 89).

---

*Any icosa-vertex and its five tangent faces form a pentagonal cap; the icosahedron is made up of 12 overlapping pent caps. A pent-cap dome would of necessity have a vertex zenith and five pent points at the base.

Alternate breakdown in even frequencies delineate an equatorial line with members. Since the icosa-edge remains a part of the final form, base rings are naturally delineated in pent-cap truncations.

CHORD FACTORS

Up to now we have treated spherical bodies as topologically unified bodies of proportion without definite scale. Breakdowns in Figs. 9, 10, 11 and 12 could conceivably represent domes from one foot to 50 feet in diameter. The question of scale must therefore come to terms with proportion. It is possible, and the intent of spherical designers to describe members and vertex relationships in terms of surface and arc functions. The grid triangle on Fig. 7, bottom right, is just such a description. Each 12^V Triacon member and surface angle are described as occupying or displacing so many degrees, minutes, and seconds of spherical arc and angle. The surface angles for any given frequency remain constant irrespective of the dome's scale. Scale therefore is solely a function of member length. Note that at all times the total of spherical degrees around any vertex is 360.

To convert arc lengths into chords or straight structural members joining two points on the spherical surface, the chord factors shown tabulated in Fig. 7 are used. The chord length is obtained by multiplying the given chord factor by the radius of the desired dome or sphere. A member with a chord factor of .10120562, such as member F G, for a 100 foot radius sphere would be 10.120562 feet long. To obtain chord factors from arcs:

$$CF = 2 \sin \measuredangle / 2, \text{ where } \measuredangle = \text{angle of arc.}$$

The chord factor therefore is a means of respecting the scale-less proportions of spherical bodies while at the same time obtaining definitive member lengths through ratios of chord lengths to spherical radius. We see also that a five frequency's chord factors serve for any scale sphere or dome as long as members are within structural

limits. Having converted the spherical surface into triangular facets bounded by chords, the planar angles are worked out by planar trigonometry from the side lenghts of the triangles. These are included at the vertices of the triangle. (Bottom right Fig. 7).

In using the basic grid triangle of Fig. 7, several inter-relationships are noteworthy. For the Triacon breakdown, triangles on each successive parallel row are congruent but mirrored from left to right. That is, triangle BCH is the same as CIH, mirrored about the CH line. Triangle IJM is equal to BCH, JNM is equal to CIH and so forth across the row. The icosa edge triangles are the only true isosceles triangles, AB = AB' etc.

High frequency grid triangles may contain sufficient information for use as lower frequency members, the grid triangles contains adequate information for 2^V and 4^V breakdowns. For 4^V use, only members AD, DG, GP, DP and icosa edge PA are necessary. Vertex angles can be added as well as cumulative arc lengths for member length obtained. New cord factors must be obtained from formula, for chord factors are not additive or subtractive.

Thus far our attention has been focused upon the theoretical aspects of geodesic domes. Sufficient data has been presented to see that the icosahedral form is a generative framework for these braced domes. Our attention must now turn to the architectonic forms these principles represent. The remainder of the text Figs. 14 - 106 takes an editorial air as examples are presented and identified. Through this process the author wishes to both parallel and encourage the re-examination of the previous discussions in light of examples.

ILLUSTRATIONS

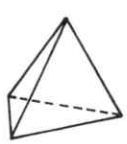

TETRAHEDRON
V4 F4 E6

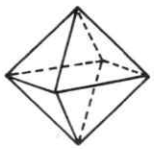

OCTAHEDRON
V6 F8 E12

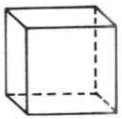

HEXAHEDRON
V8 F6 E12

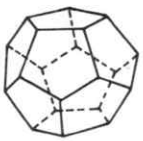

DODECAHEDRON
V20 F12 E30

ICOSAHEDRON
V12 F20 E30

TRUNCATED TETRAHEDRON
V12 F8 E18

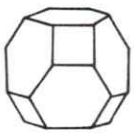

TRUNCATED OCTAHEDRON
V24 F14 E36

TRUNCATED CUBE
V24 F14 E36

TRUNCATED DODECAHEDRON
V60 F32 E90

TRUNCATED ICOSAHEDRON
V60 F32 E90

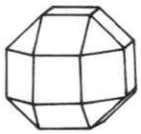

RHOMBICUBOCTAHEDRON
V24 F26 E48

CUBOCTAHEDRON
V12 F14 E24

RHOMBICOSIDODECAHEDRON
V60 F62 E120

ICOSADODECAHEDRON
V30 F32 E60

TRUNCATED CUBOCTAHEDRON
V48 F26 E72

SNUB CUBE
V24 F38 E60

SNUB DODECAHEDRON
V60 F92 E105

TRUNCATED ICOSADODECAHEDRON
V120 F62 E108

EULER'S LAW

$$V + F : E + 2$$

NO. OF VERTEXES — NO. OF FACES — NO. OF EDGES

Fig. No. 1 Basic polyhedra, Row 1 the five Platonic solids. Rows 2, 3, 4 the thirteen Archimedian solids.

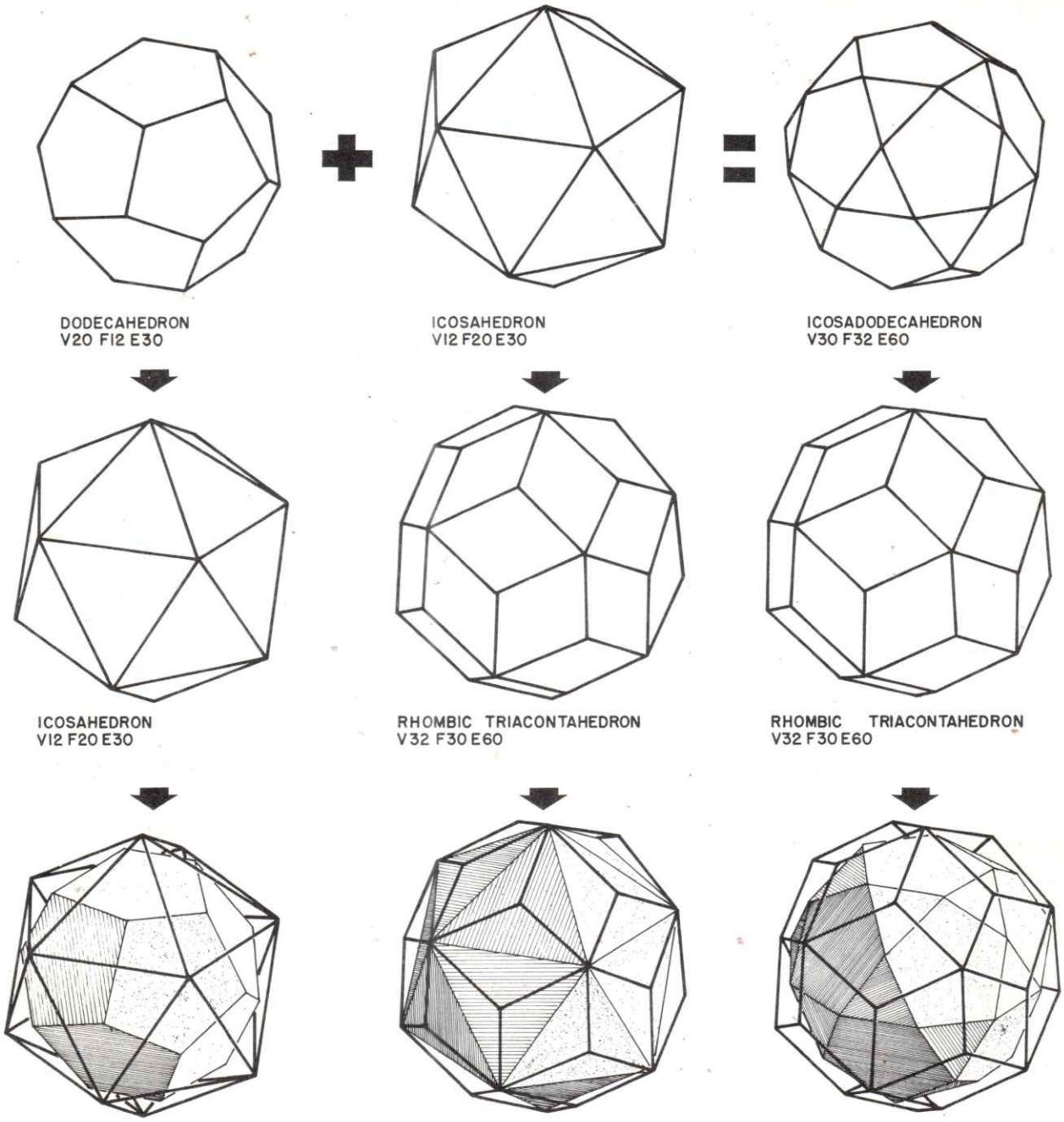

Fig. No. 2 Evolution of dual polyhedra through face addition.

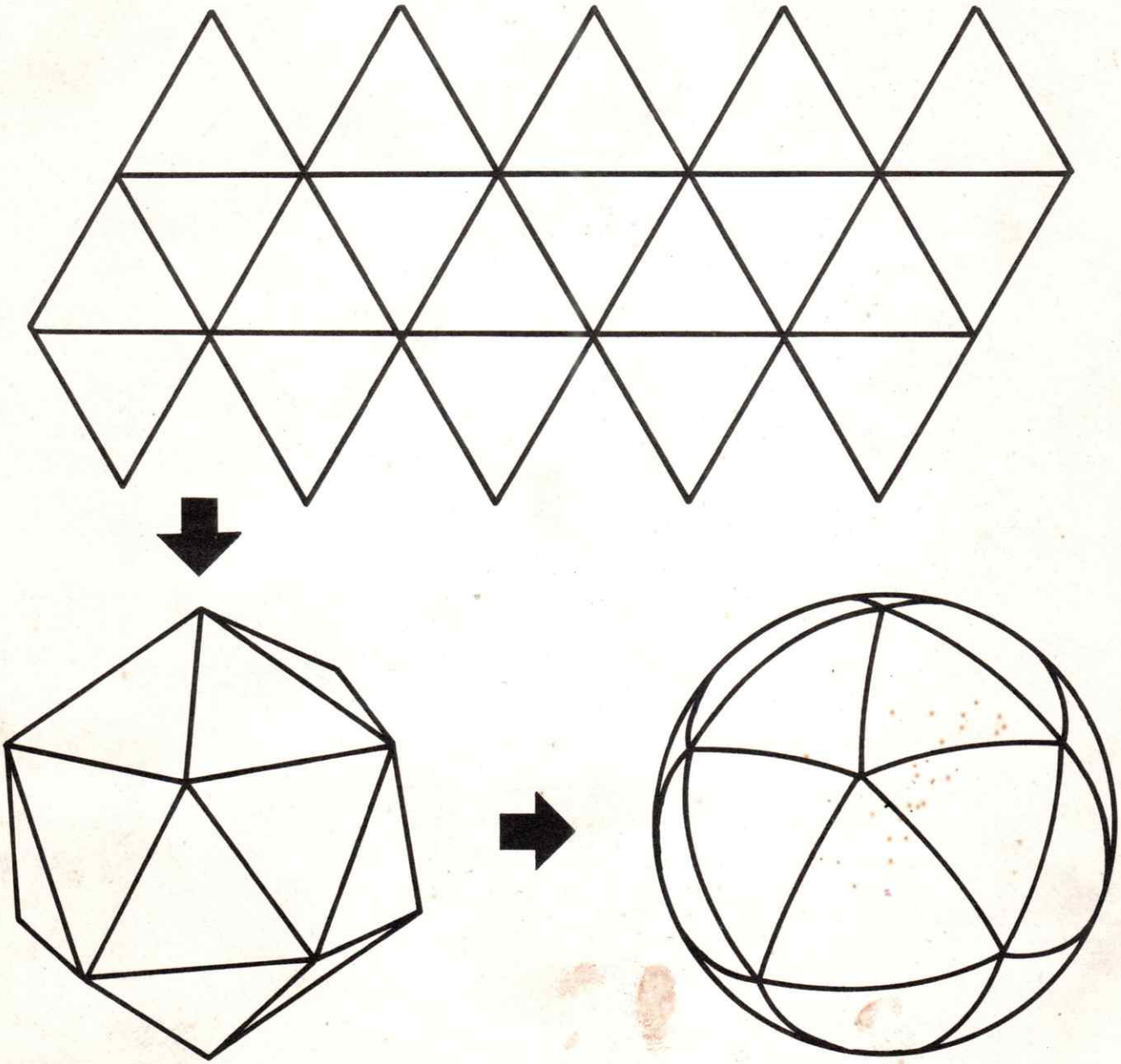

Fig. No. 3 Polyhedra and spherical nomenclature. Top: Two dimensional "net" of icosahedron. Bottom: Planar and spherical icosahedron.

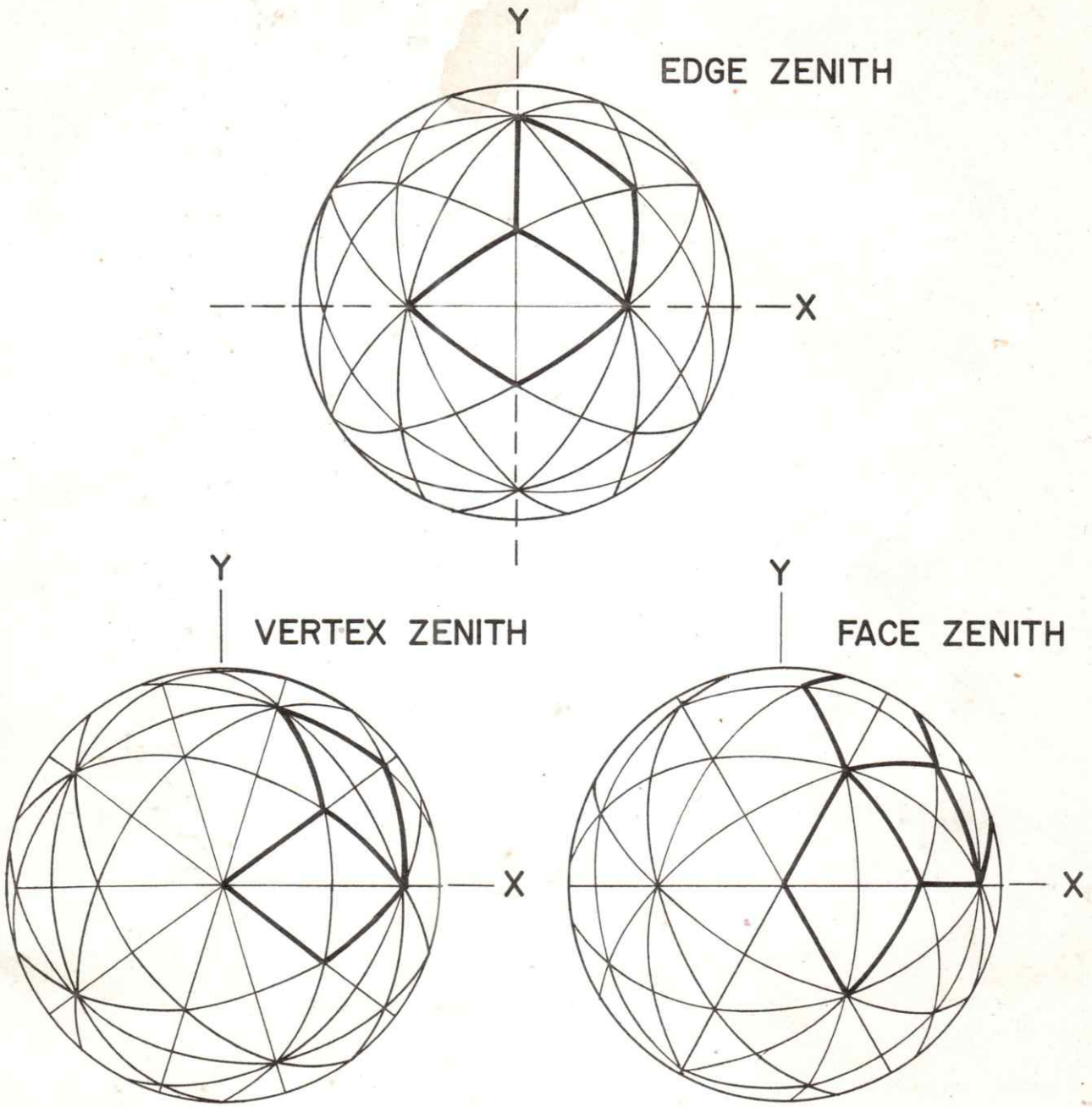

Fig. No. 4 Spherical orientation x, y, z, edge zenith, vertex zenith, and face zenith.

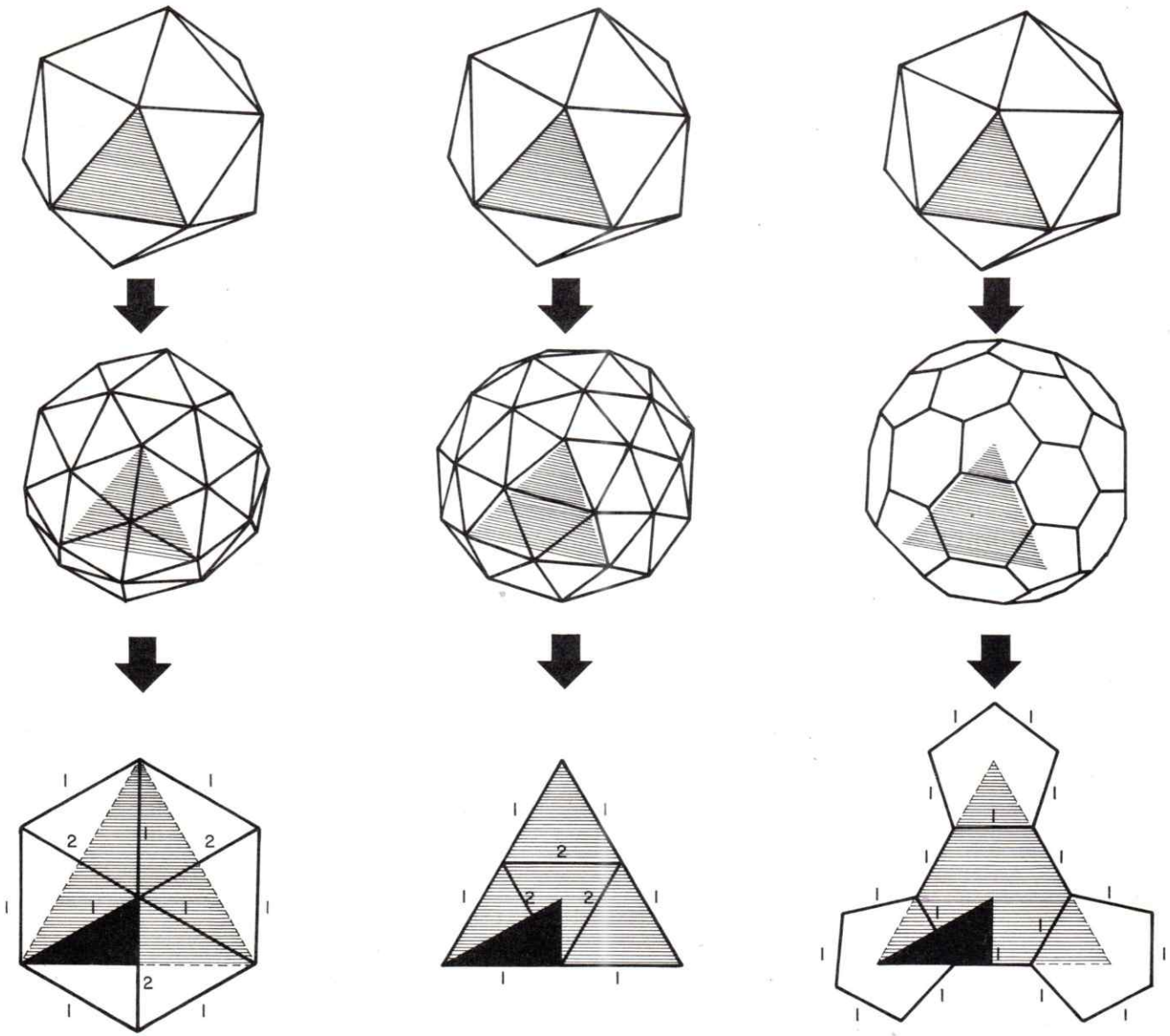

Fig. No. 5 Icosahedron breakdowns generated about the edge, face and vertex.

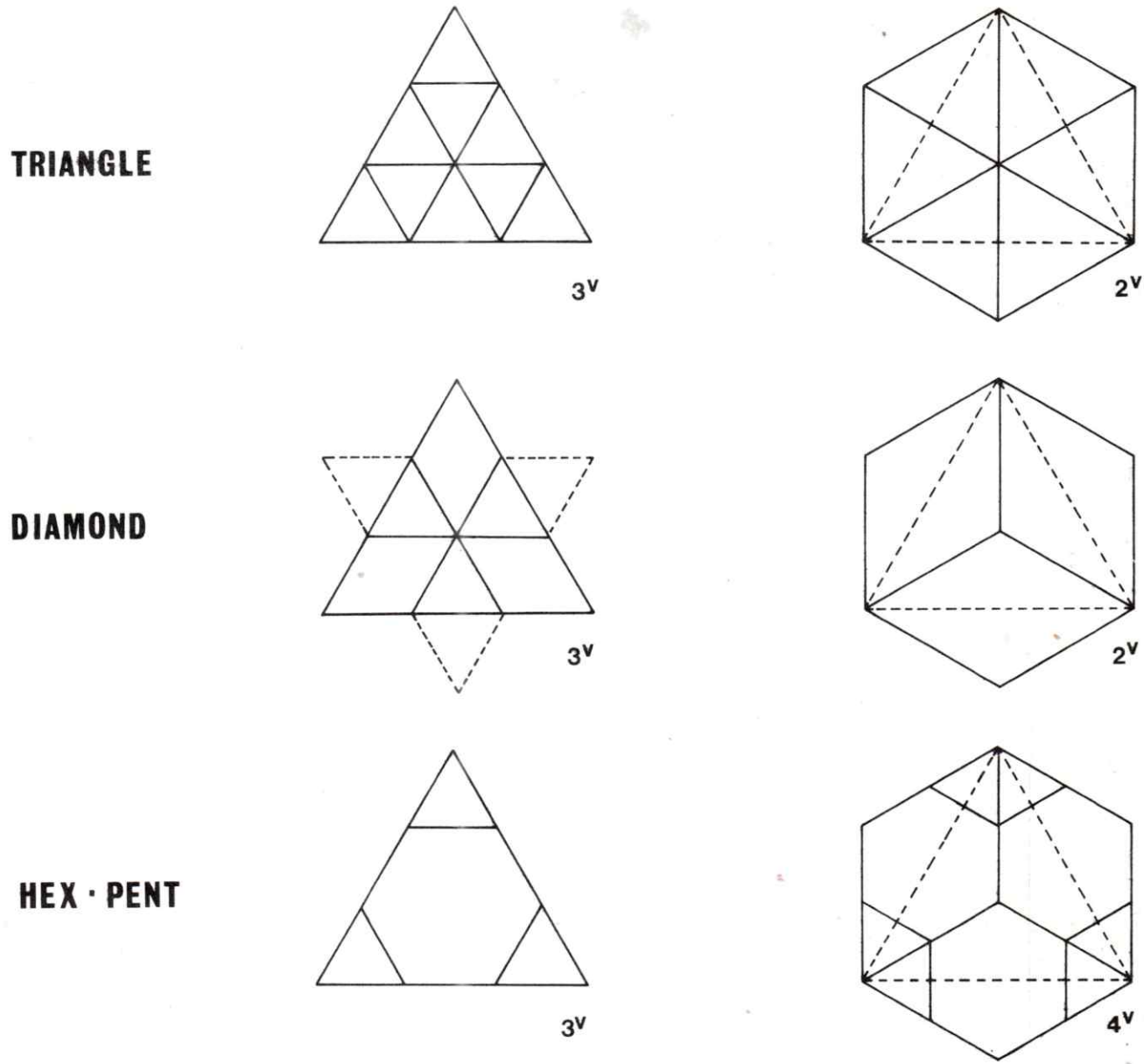

Fig. No. 6 Comparative breakdown of icosahedron face Alternate and Triacon methods.

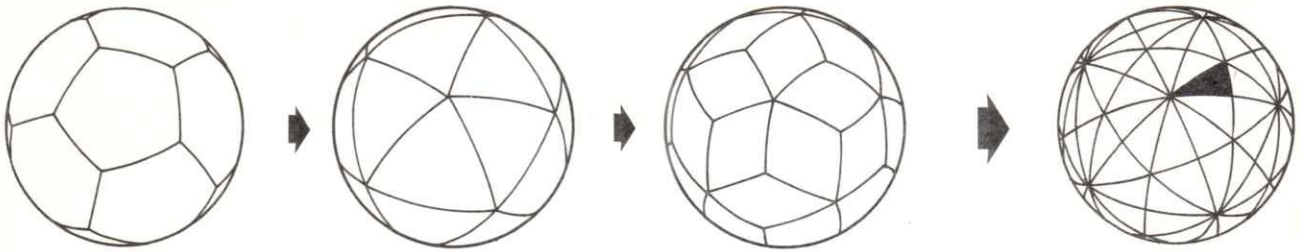

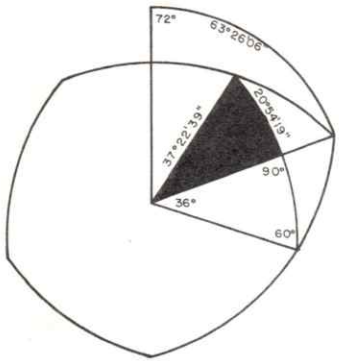

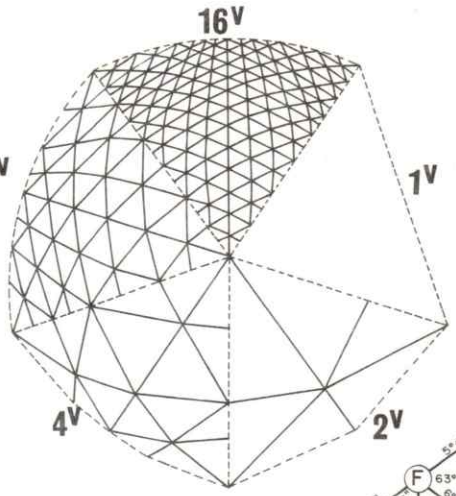

MEMBER	ARC °	'	"	CHORD FACTOR
AB BH HI IM MN NP	6	31	19.00	.11376180
BC CI IJ JN NO	6	28	14.27	.11286902
CD DJ JK KO	6	21	16.39	.11084914
DE EK KI	6	12	12.16	.10821876
EF FL	6	01	31.43	.10512192
FG	5	48	05.29	.10120562
BB' II' NN'	7	38	22.22	.13322738
CH JM OP	7	35	40.20	.13244426
DI KN	7	24	28.09	.12919580
EJ LO	7	05	31.40	.12370174
FK	6	41	33.09	.11674520
GL	6	13	07.11	.10848440
AB· HB· HI· MI· MN·	5	17	10.49	
BB· II· NN·	3	49	11.11	

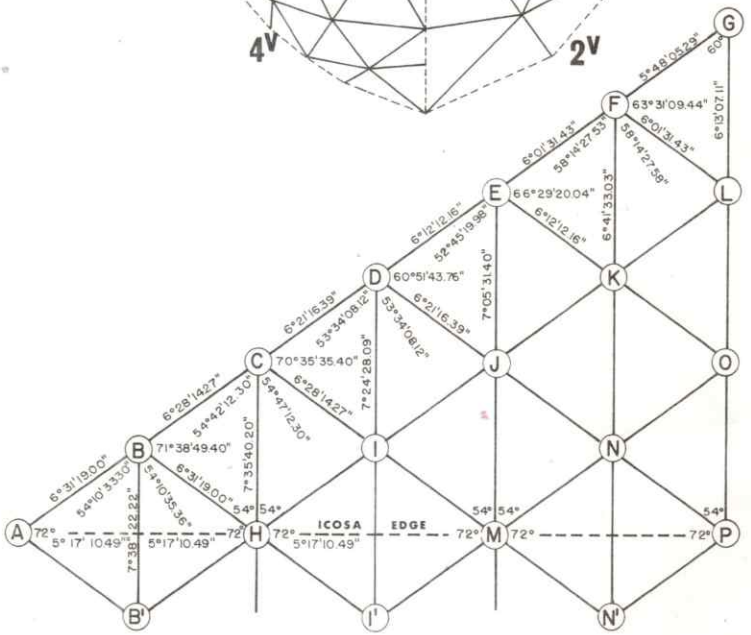

Fig. No. 7 Top: Cumulative superimposition of dodecahedron, icosahedron, and rhombic triacontahedron to achieve smallest common triangle. Mid-page: Basic spherical triangle, multiple frequency comparison. Bottom: Typical geometrical data for 12^{V} Triacon breakdown. Same chart is good for 2^{V} Tricon eliminating unnecessary members. New chord factors are needed.

The Triacon Breakdown

The Triacon breakdown has these advantages over the other breakdowns

a. A minimum number of different components

b. A symmetry of relationship of adjacent faces making easy combination into diamonds.

and the following disadvantages:

a. A greater variation of member length than with the Alternate system.

b. No complete great circle delineated naturally by the structural pattern - such as the equatorial obtainable on the even number Alternate breakdowns. Consequently truncated base members must be used in every case.

c. Frequencies must always run in an even number - therefore there is less graduation in scale than is available with the Alternate breakdown.

In practice, the advantages of the Triacon become more and more emphatic in the higher frequencies - usually this means in the larger diameter structures such as those 100 feet or more. In the Triacon, the relationship of number of different component lengths to the frequency, is an arithmetical one. With the Alternate breakdown this relationship is geometric.

The disadvantages of Triacon also tend to be minimised in proportion to the diameter of the structure. Larger structures are not usually hemispherical, as the head space so generated is not required. In conditions other than hemispheres, both Triacon and Alternate breakdowns need special base members. Also at higher frequencies, the lack of the odd numbered frequencies is minimized. A four frequency member is usually much longer in proportion to a six frequency one, but a fourteen frequency member is only slightly larger than a sixteen frequency one. A rule of thumb concerning the numbers of different length of struts, angular conditions at vertices and faces: frequency (1) equals number of different length of struts, (2) is about 1/2 number of angular conditions at vertices, (3) is about twice number of different faces when triangulated. An 8^V Triacon triangular grid has eight different lengths of struts, 15 angular conditions at vertices and four different faces.

The Alternate Breakdown

The Alternate breakdown has the following advantages:

a. A minimum variation in member length, and except for the pent joints, less variation in face angles.

b. In even frequencies, a continuous equator is delineated, so achieving hemispheres without the need for truncated members at the base.

c. As odd and even number frequencies are both obtainable, a more gradual variation in scale of breakdown is available.

Disadvantages:

a. The number of different components in relation to frequency increase on a geometric scale. In frequencies from six to eight upwards this number becomes considerably greater than with the same frequency Triacon. This factor can be somewhat reduced by distorting the regularly plotted breakdown to minimize the number of components, for example: a normal four frequency has five member lengths, six different faces and four vertexes. By slight distortions of the pattern this can be reduced to four in each case.

Fig. No. 8 Triacon and Alternate breakdown comparison.

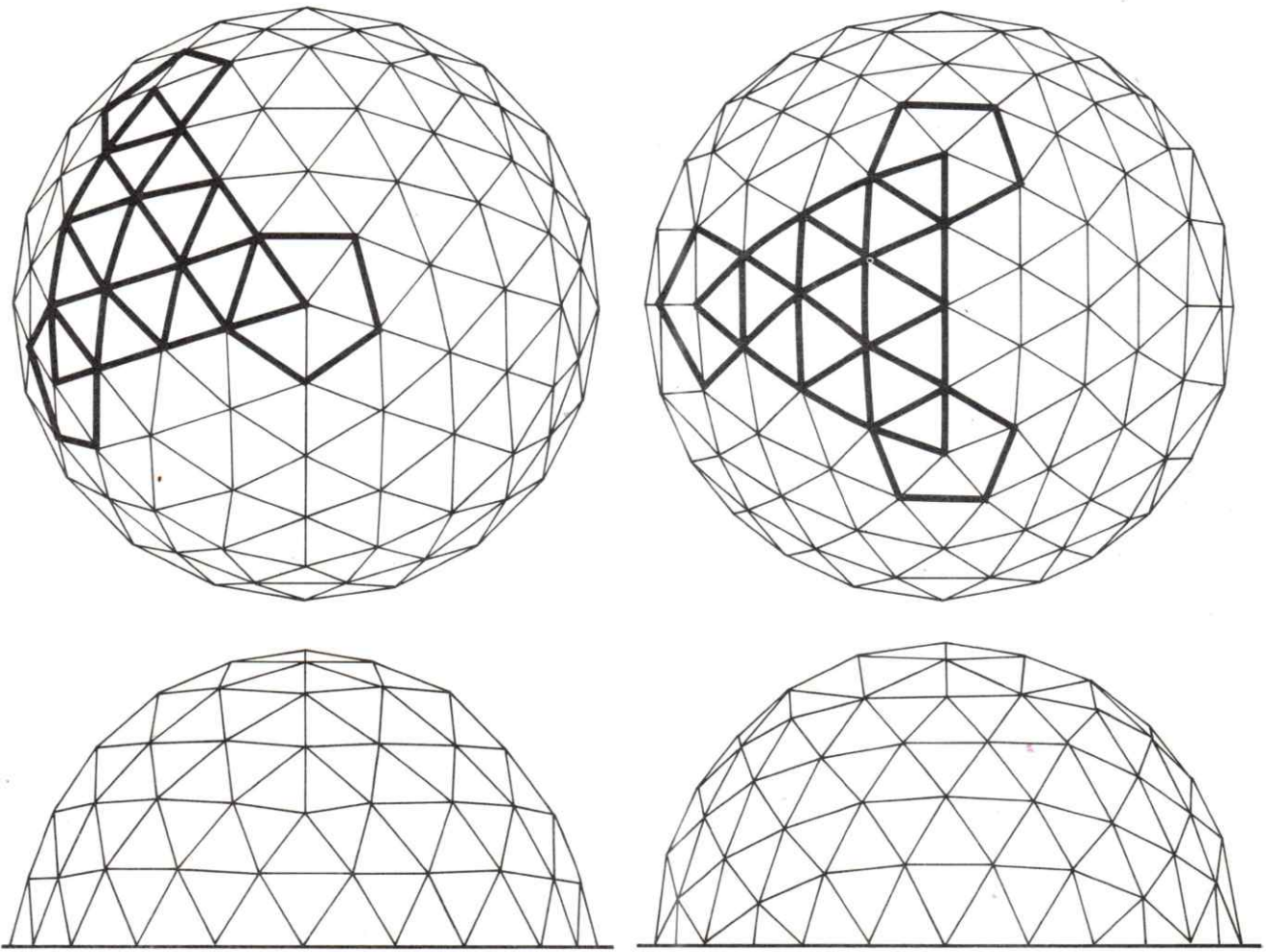

Fig. No. 9 Plans and elevations of 4^V Alternate breakdown domes with vertex and edge zenith comparison, icosahedron face with pentagonal vertex cues outlined.

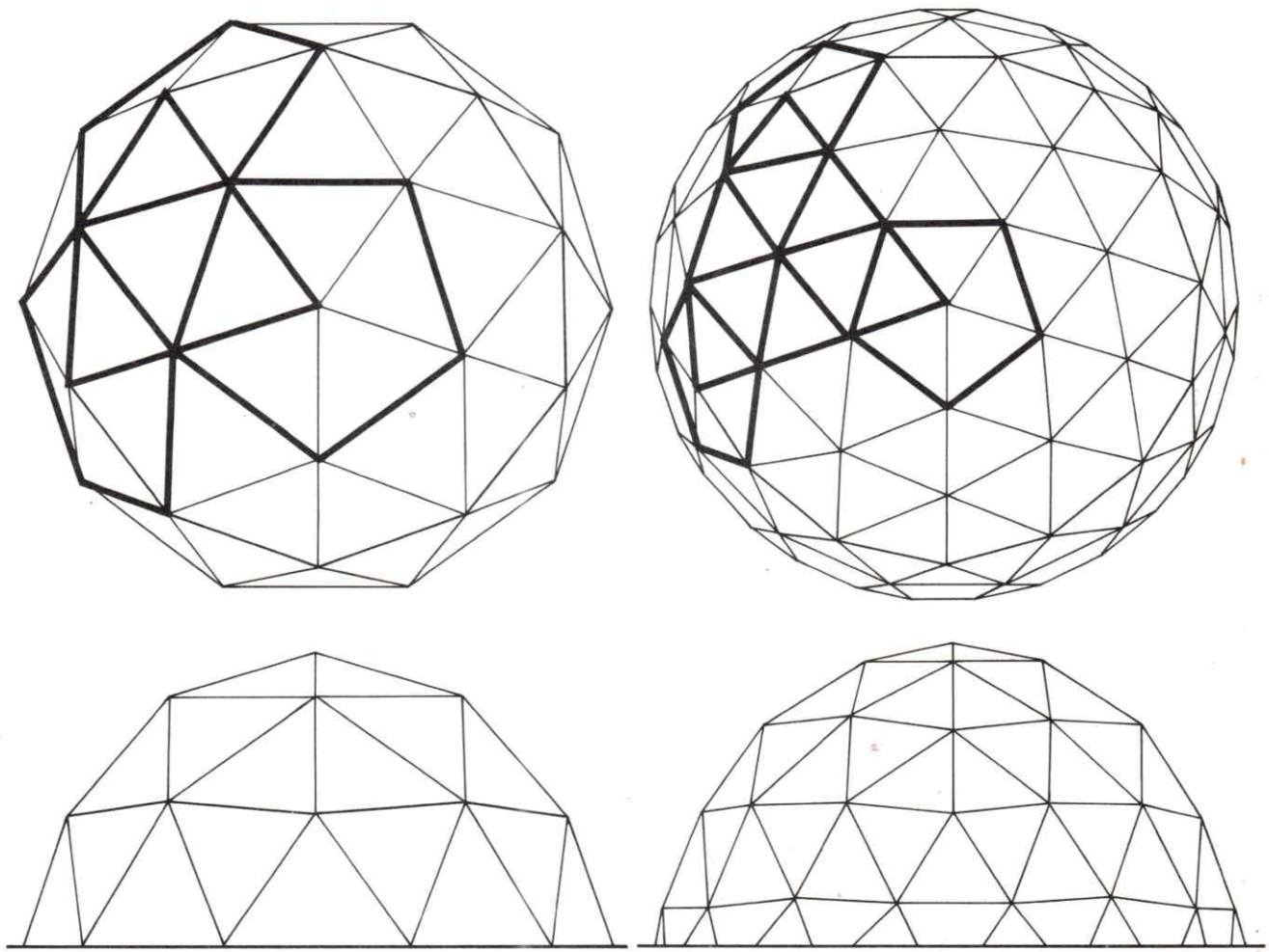

Fig. No. 10 Plans and elevations of 2^V and 3^V Alternate breakdown, vertex zenith domes. Icosahedron face breakdown with pentagonal vertex cues outlined.

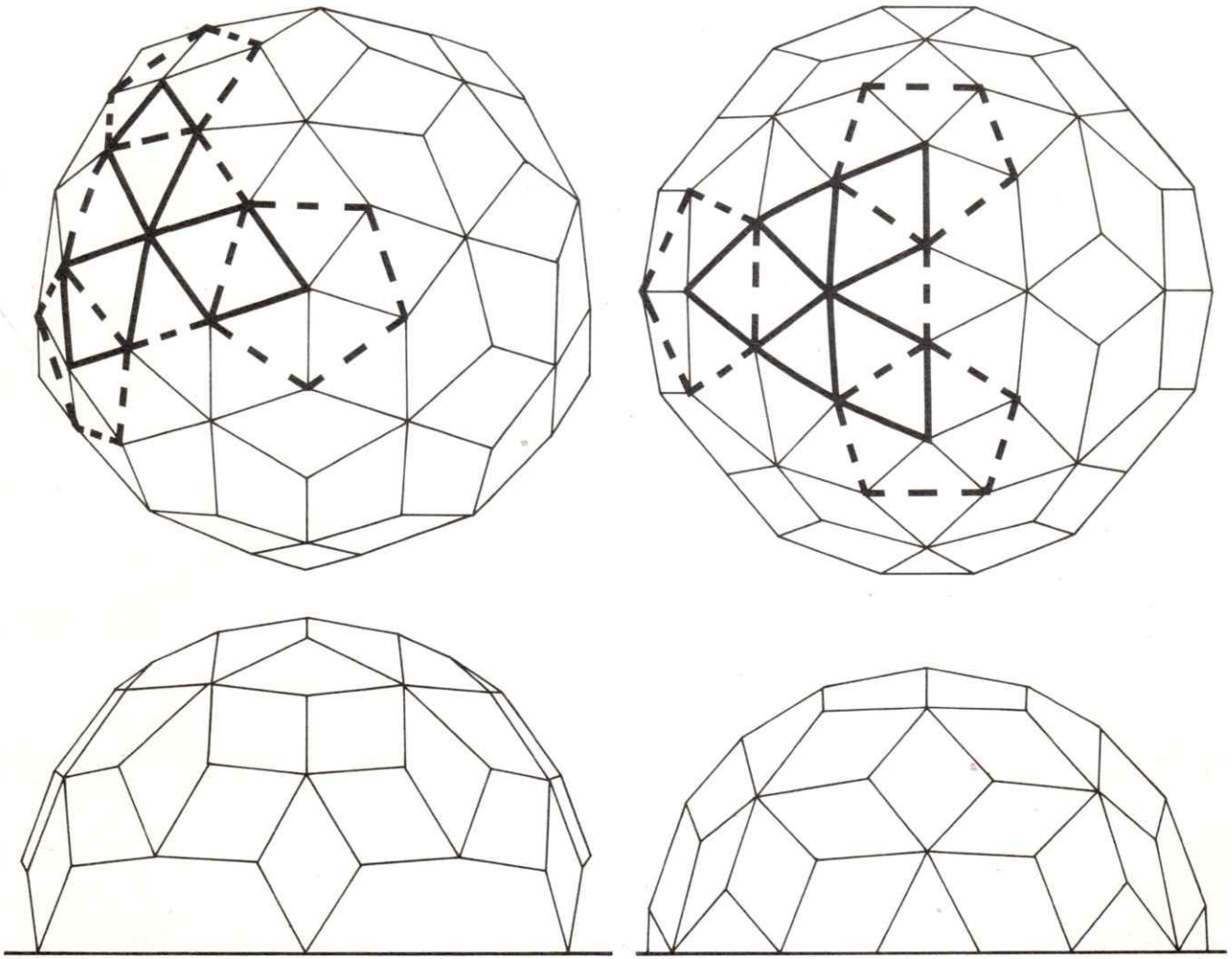

Fig. No. 11 Plans and elevation of 3^V Alternate breakdown domes with vertex and edge zenith comparison. Icosahedron face diamond patterns with pentagonal vertex cues outlined.

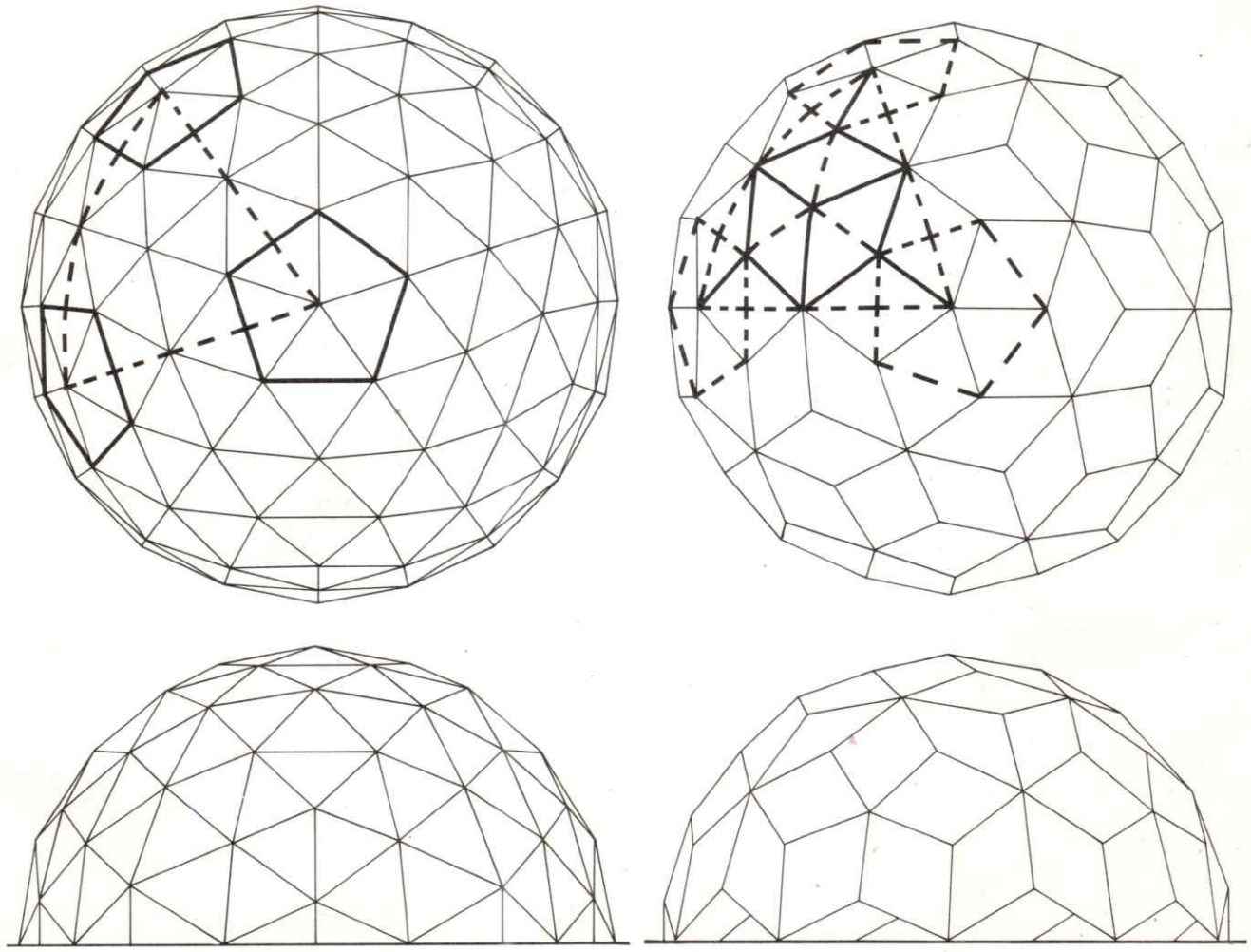

Fig. No. 12 Plans and elevations of 4^V Triacon, vertex zenith domes with triangular and diamond breakdowns compared. Icosahedron face patterns and pentagonal vertex cues outlined.

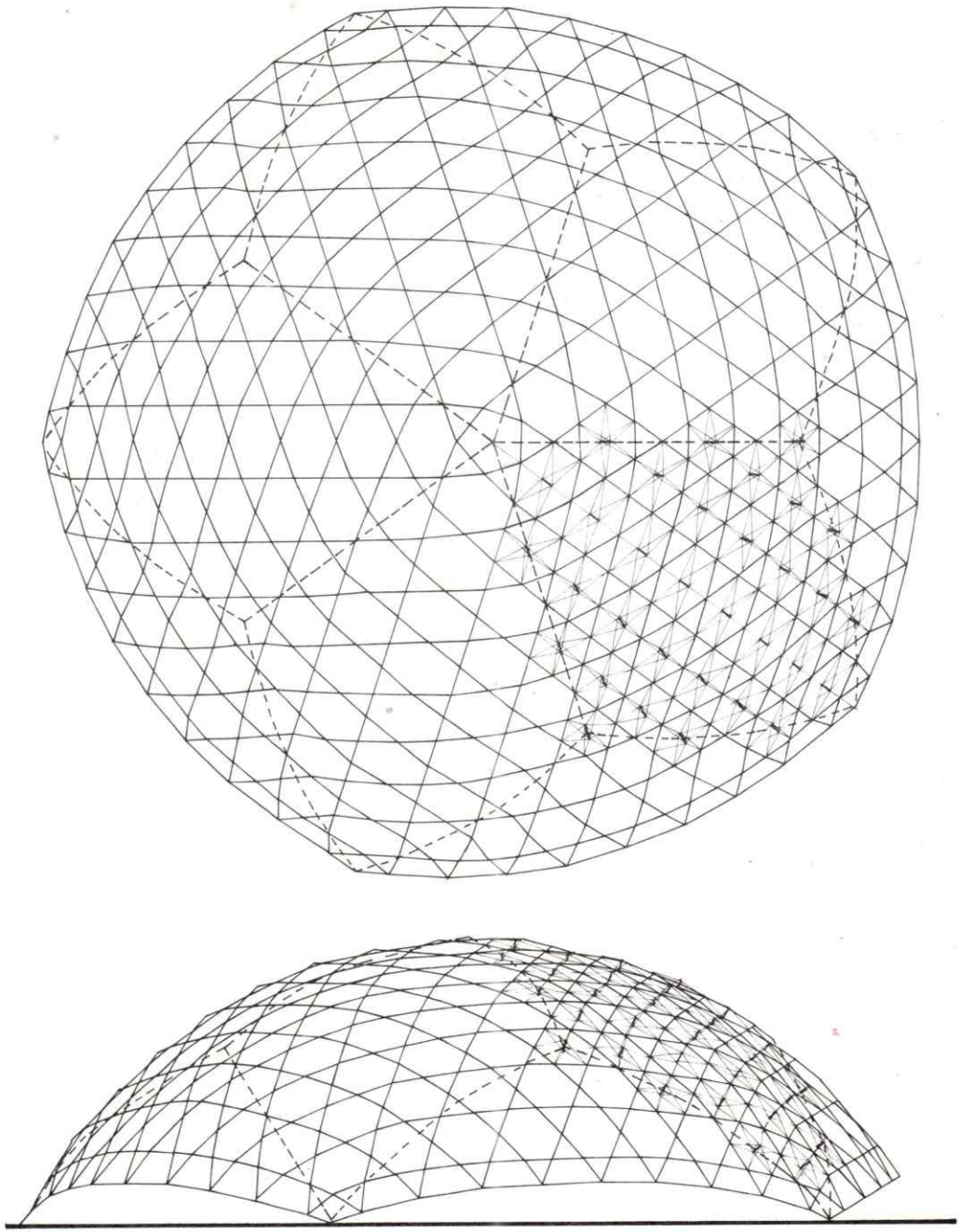

Fig. No. 13 Plan and elevation of 18^{V} Triacon Hex-Pent dome. Rhombic triacontahedron faces dotted, icosa vertexes at ends of long diamond axis.

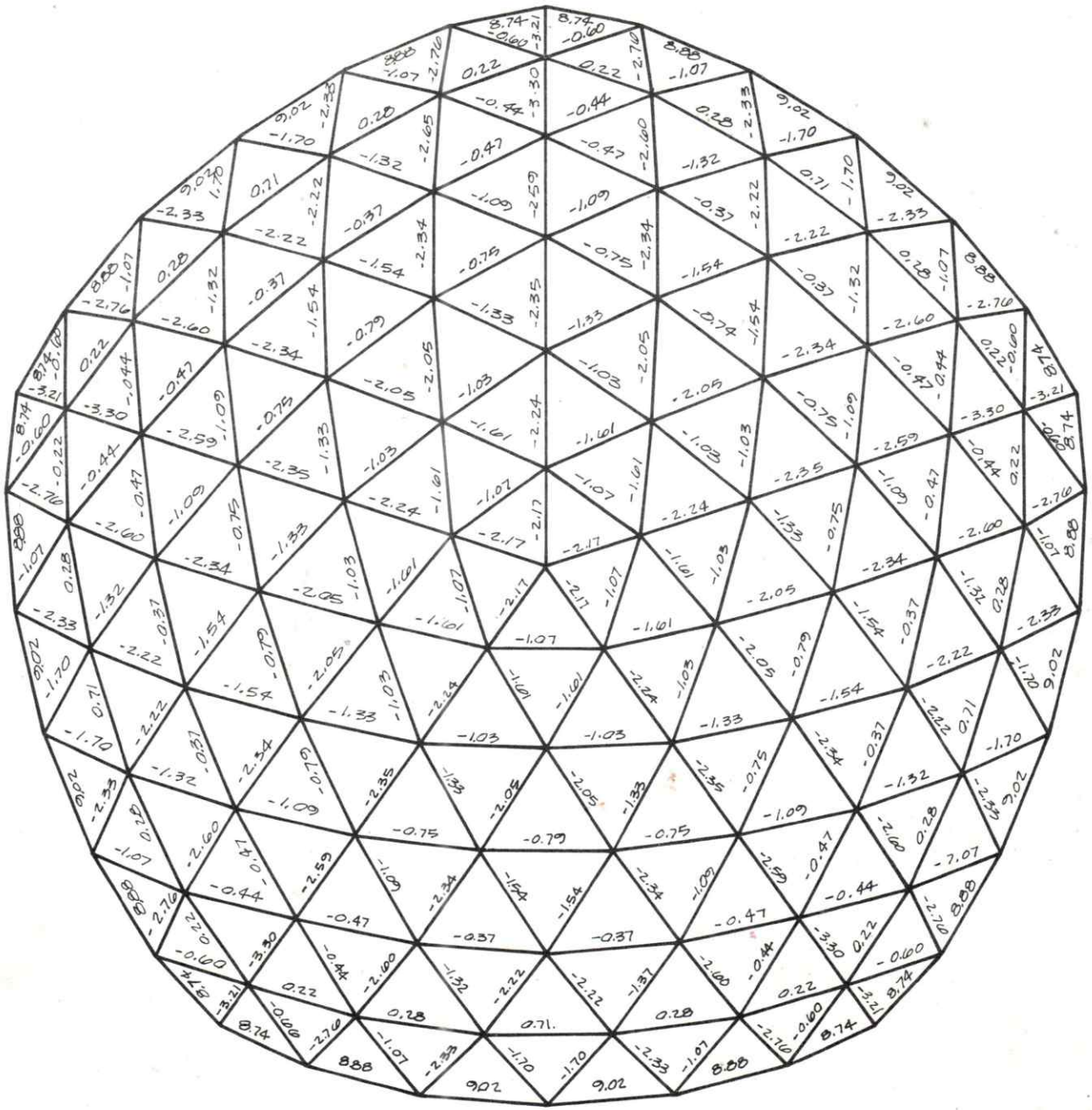

Fig. No. 14 Axial load results from one unit vertical load applied at every vertex of 6^V Alternate strut dome. Plus tension, minus compression. Note five main zenith radials have highest stress, other members act as semi-structural infill.

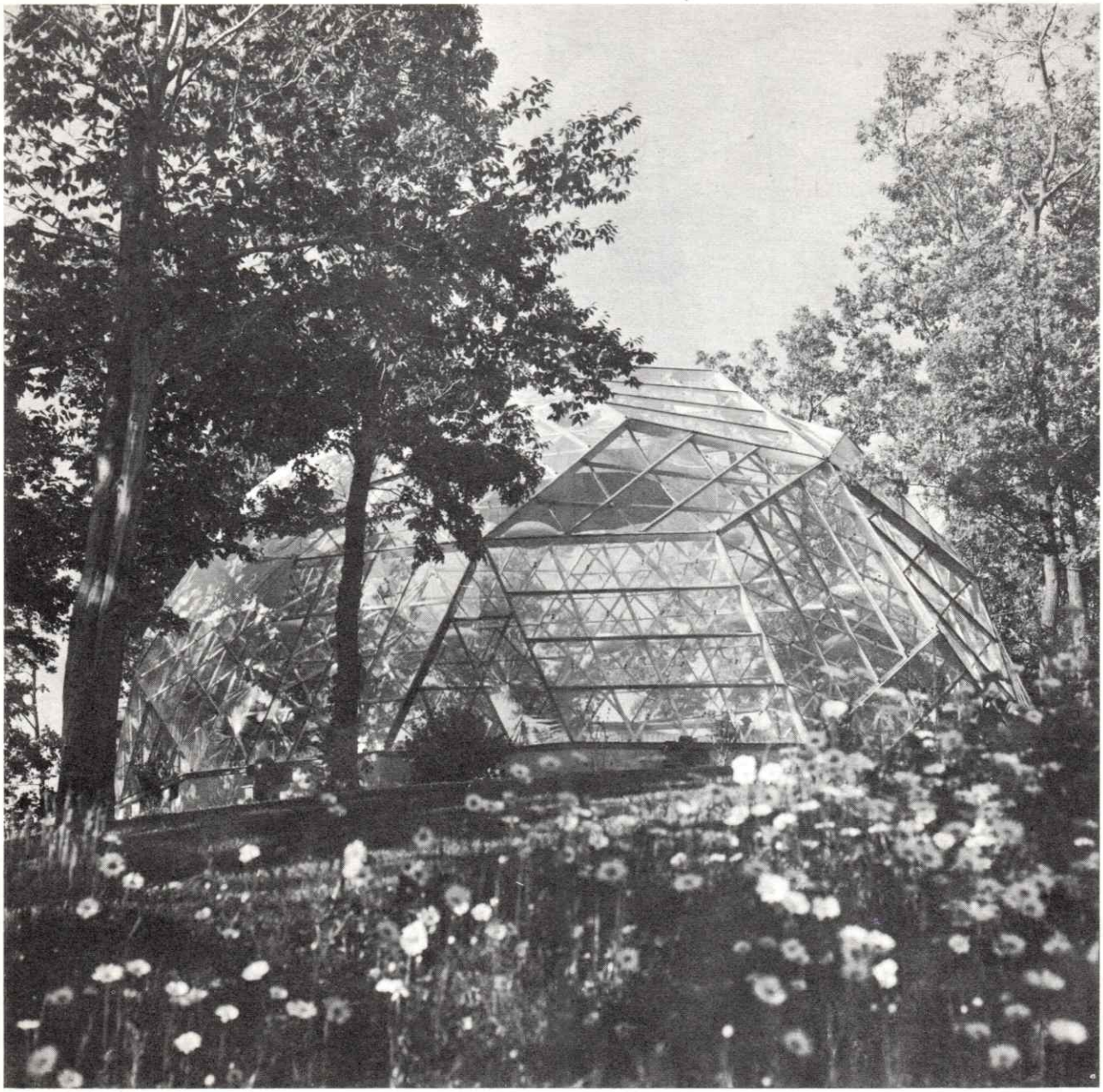

Fig. No. 15 Woods Hole dome, Woods Hole, Massachusetts, 1953-54. Fifty-five foot diameter, wood and mylar hyperbolic parabola dome.

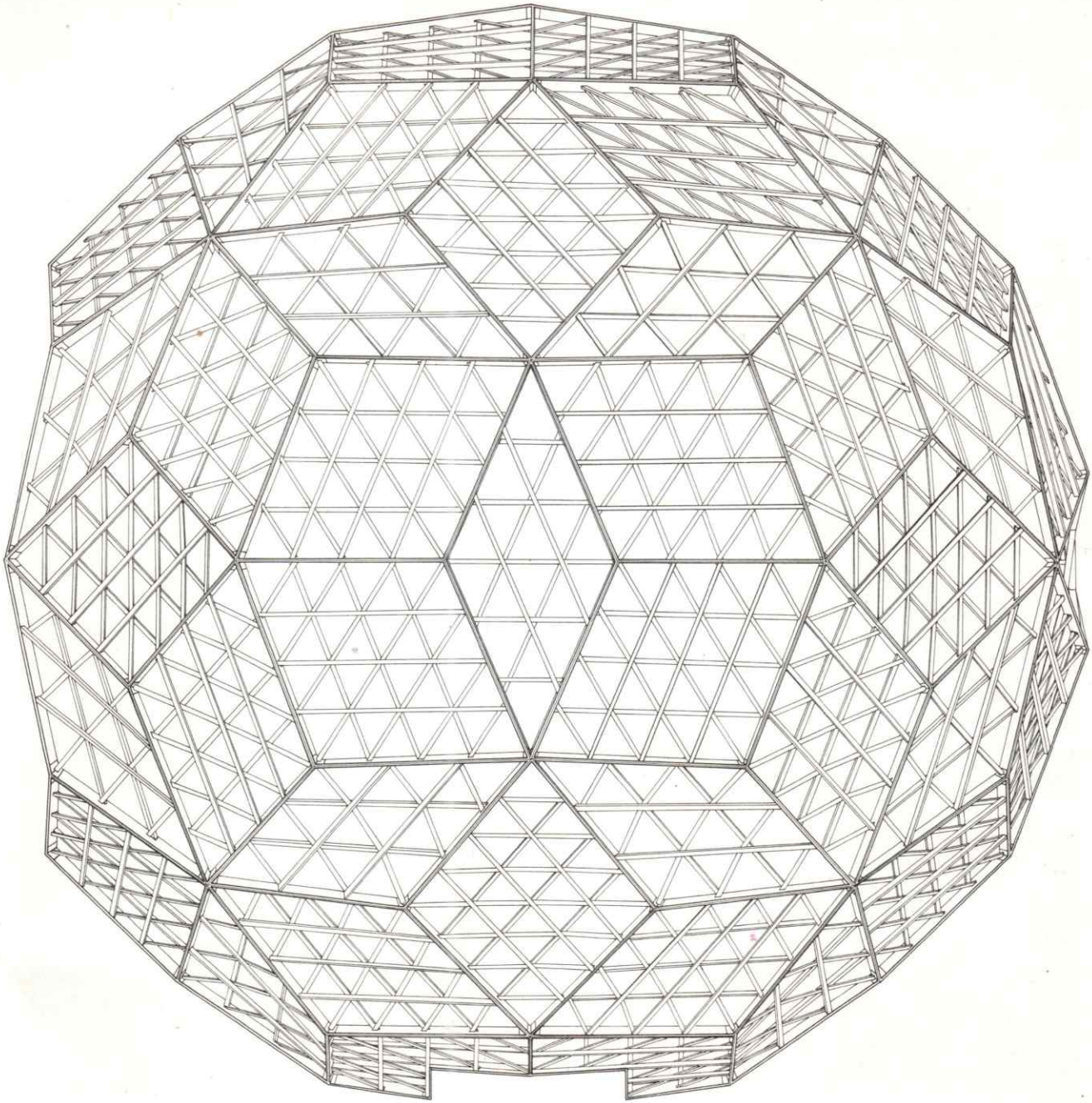

Fig. No. 16 Plan, basic hyperbolic parabola diamonds composed of 1" x 8", 2" x 3" and 1" x 2" members diamonds are approximately 10' to an edge.

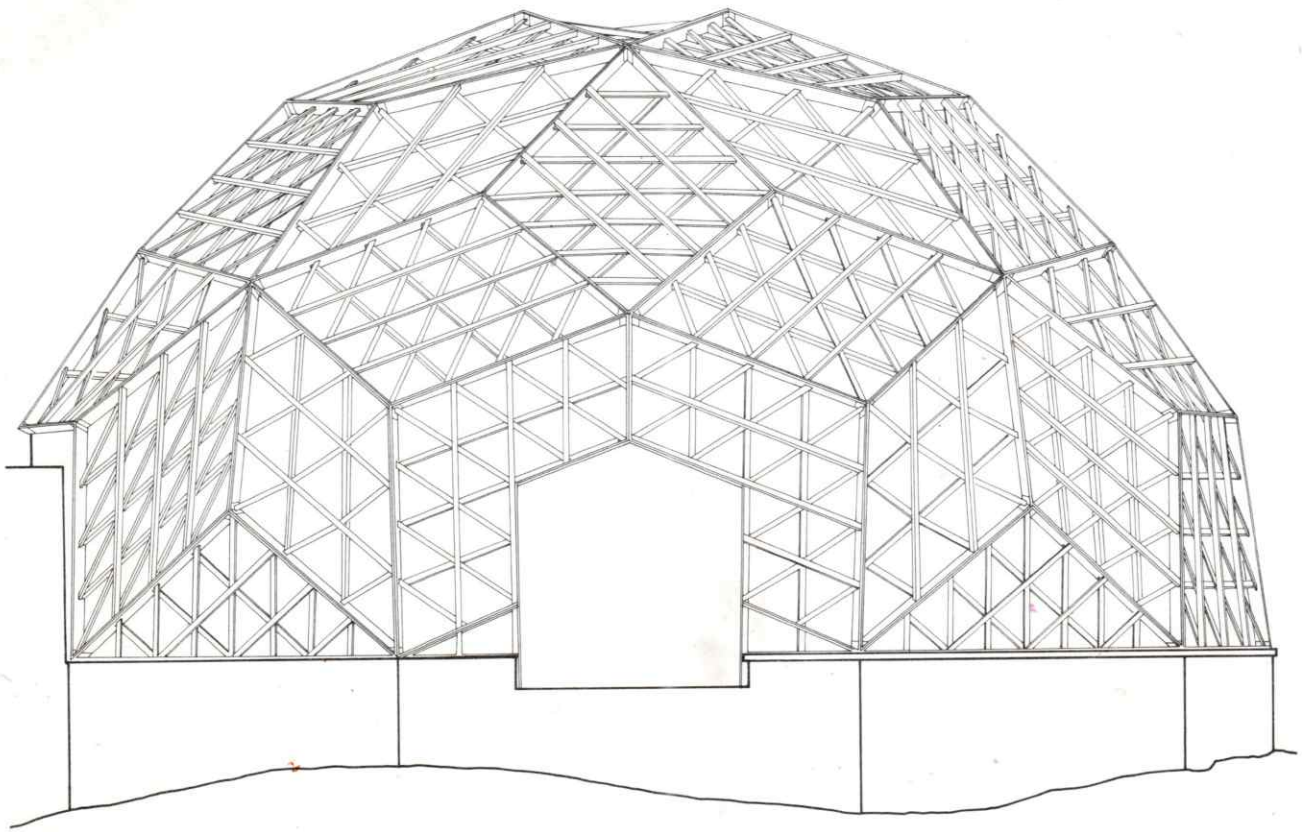

Fig. No. 17 Elevation.

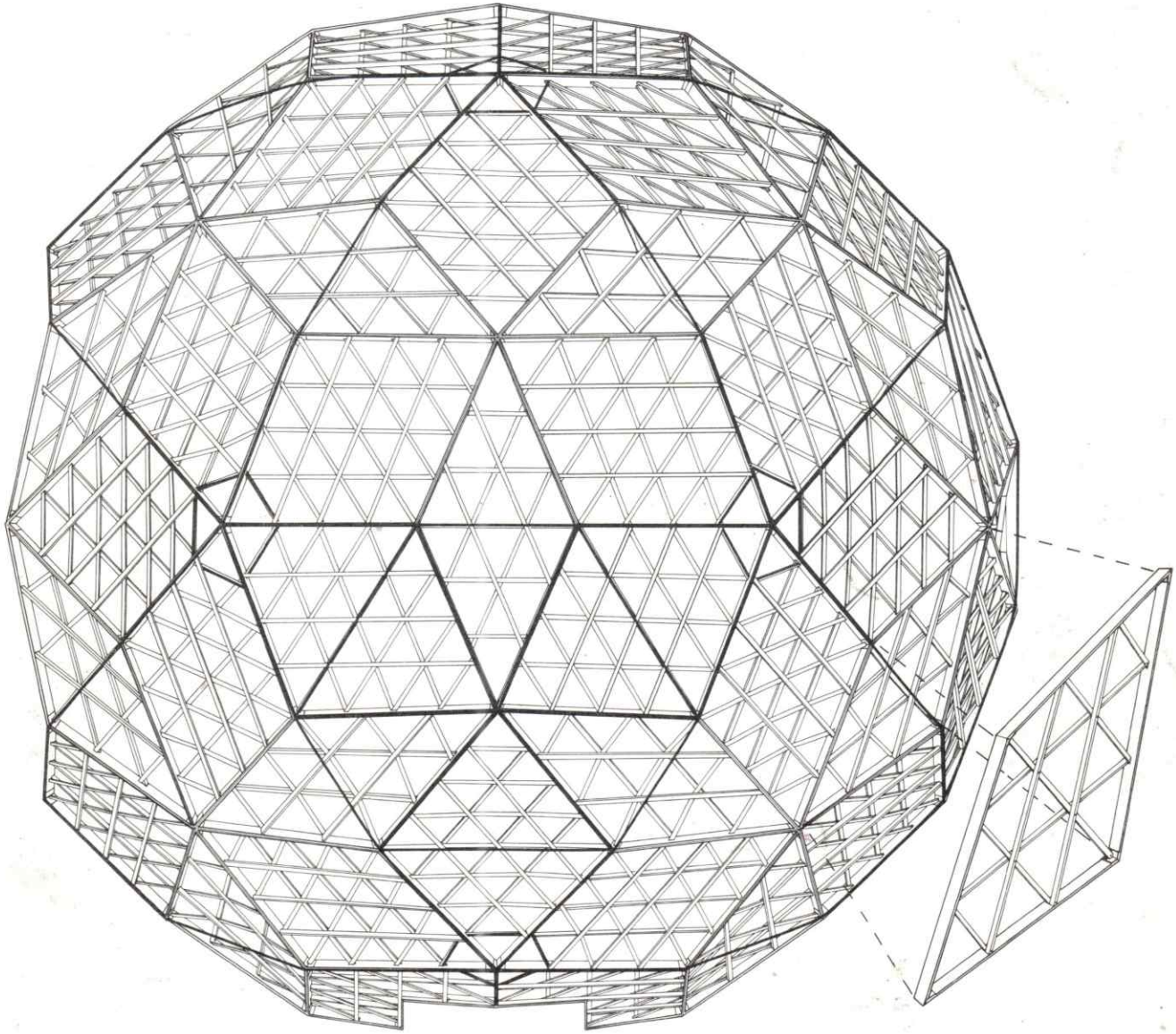

Fig. No. 18 Geometric explanation of dome, A 3^V Alternate edge zenith breakdown. Basic hyperbolic parabola diamond withdrawn.

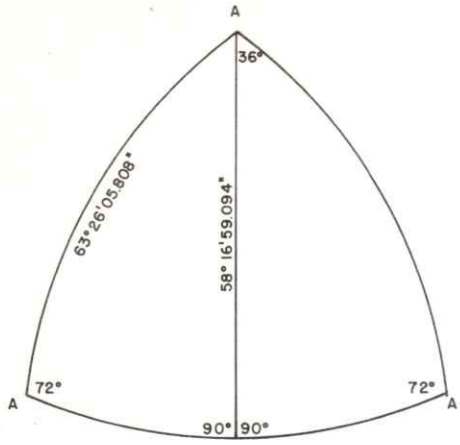

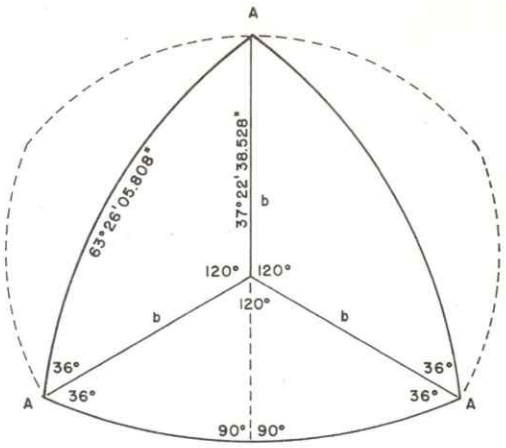

DETERMINATION OF ARC OF ICOSA EDGE $\widehat{A\text{-}A}$

$\text{SIN } \widehat{AA} = \text{COT } 72° \cdot \text{COT } 36°$

$\widehat{AA} = 63°\,26'\,05.808"$

DETERMINATION OF ARC DISTANCE OF CENTROID FROM ICOSA VERTEX $\widehat{b}$

$\text{SIN}(90°-\widehat{b}) = \text{COT } 36° \cdot \text{COT } 60°$

$\widehat{b} = 37°\,22'\,38.528"$

DETERMINATION OF MEDIAN OF ICOSA FACE $\widehat{a}$

$$\frac{\text{SIN } \widehat{a}}{\text{SIN } 72°} = \frac{\text{SIN } 63°\,26'\,05.808"}{\text{SIN } 90°}$$

$\widehat{a} = 58°\,16'\,59.094"$

DISTANCE OF CENTROID FROM ICOSA EDGE $\widehat{c}$

$\widehat{c} = (58°\,16'\,59.094") - (37°\,22'\,38.528")$

$\widehat{c} = 20°\,54'\,18.566"$

FAT DIAMOND

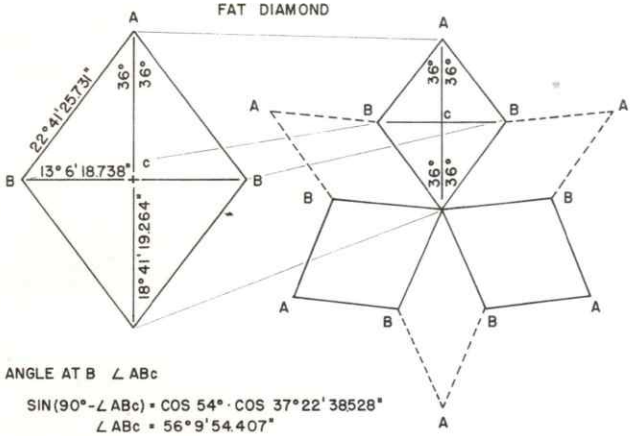

ANGLE AT B $\angle ABc$

$\text{SIN}(90°-\angle ABc) = \text{COS } 54° \cdot \text{COS } 37°22'38528"$

$\angle ABc = 56°\,9'\,54.407"$

DIAMOND EDGE $\widehat{AB}$

$\text{SIN}(90°-\widehat{AB}) = \text{COT } 56°\,9'\,56.407" \cdot \text{COT } 54°$

$\widehat{AB} = 22°\,41'\,25.731"$

SHORT DIAGONAL $\widehat{BB}$

$$\frac{\text{SIN } \widehat{BB}}{2} = \text{COT } 56°\,9'\,56.407" \cdot \text{TAN } 18°41'\,19.264"$$

$$\frac{\widehat{BB}}{2} = 13°6'\,18.738"$$

$\widehat{BB} = 26°\,12'\,39.476"$

THIN DIAMOND

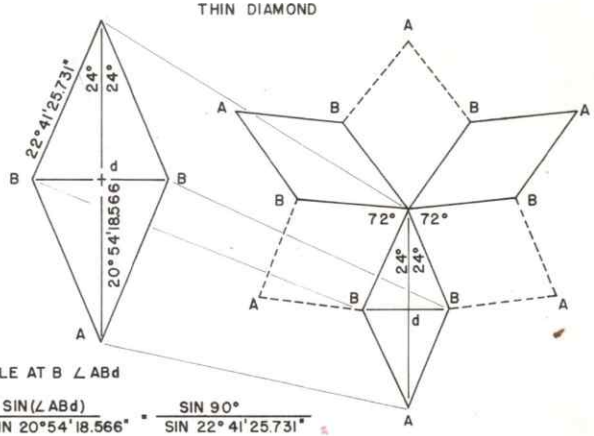

ANGLE AT B $\angle ABd$

$$\frac{\text{SIN}(\angle ABd)}{\text{SIN } 20°54'\,18.566"} = \frac{\text{SIN } 90°}{\text{SIN } 22°\,41'\,25.731"}$$

$\angle ABd = 67°\,40'\,7.187"$

SHORT DIAGONAL $\widehat{BB}$

$$\frac{\text{SIN } \widehat{BB}}{2} = \text{COT } 67°40'\,7.187" \cdot \text{TAN } 20°54'\,18.566"$$

$$\frac{\widehat{BB}}{2} = 9°1'\,37.173"$$

$\widehat{BB} = 18°3'\,14.346"$

Fig. No. 19 Basic calculations for the icosahedron subdivision. Note that normally near equalateral triangles for Alternate breakdown are modified to produce fat and thin diamonds. The two different diamond faces have a common edge length, though different length diagonals.

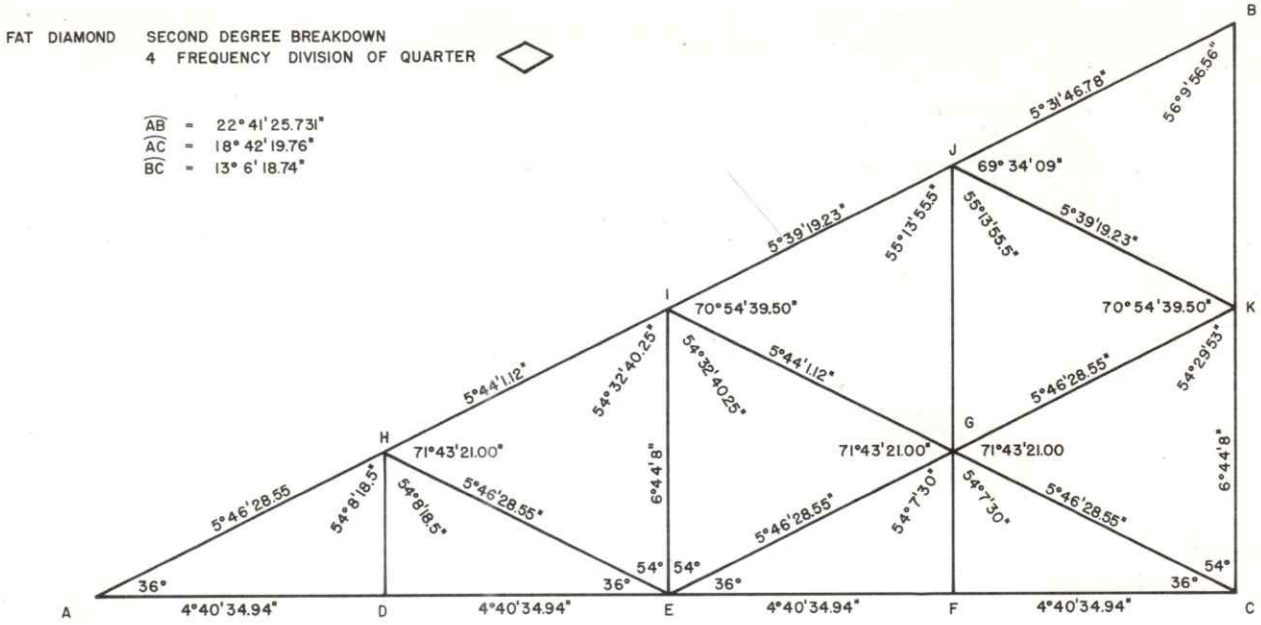

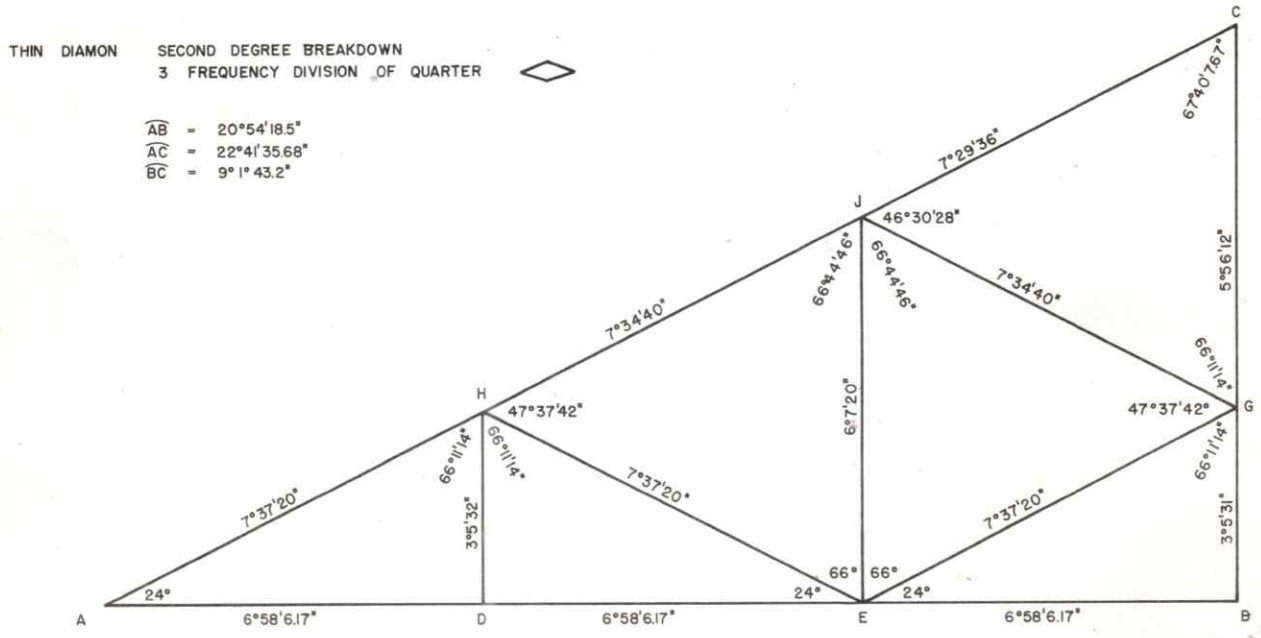

Fig. No. 20 Grid triangle calculations for fat and thin diamonds. Chord factor formula converts arc lengths to chord lengths when multiplied by the desired dome radius. Project by Geodesics Incorporated.

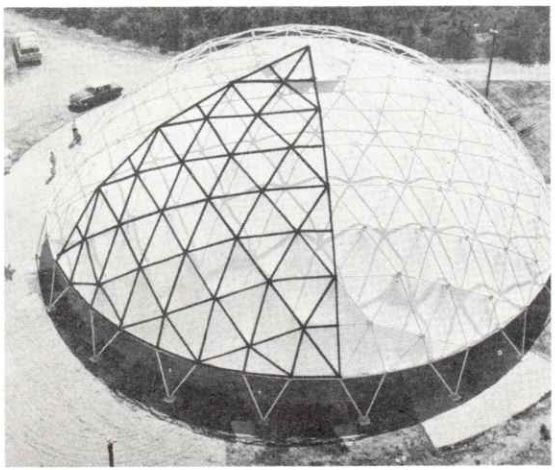

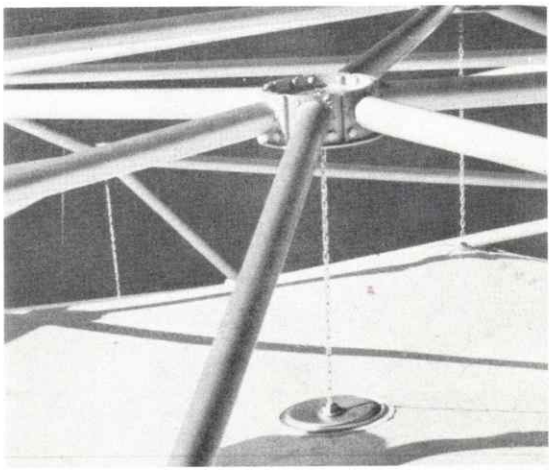

Fig. No. 21 One hundred twenty foot diameter strut and membrane dome. An 8^V Triacon breakdown, vertex zenith truncated along pent-cap. Struts have square flange ends bolt to cylinder ring, pull chain to membrane secures and adjusts membrane tension. A Synergetics Incorporated project.

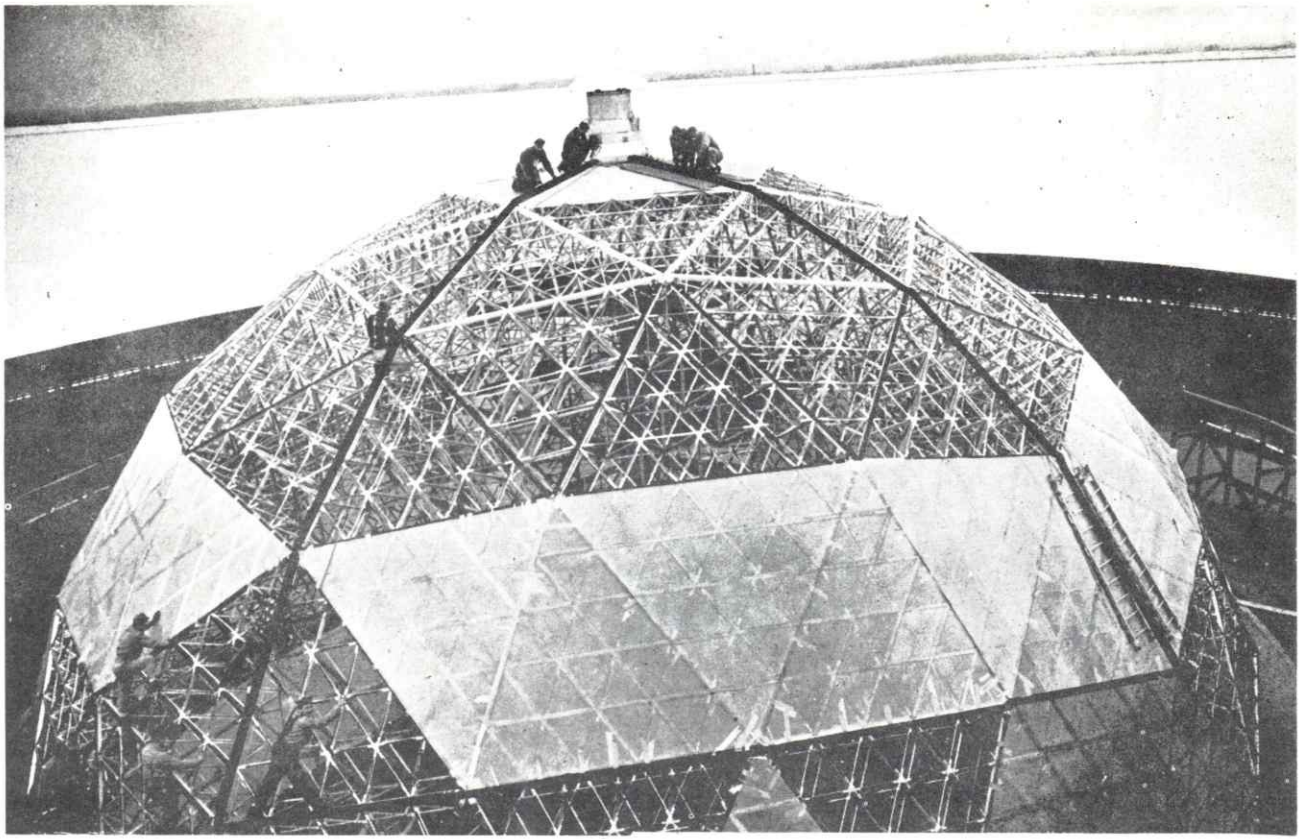

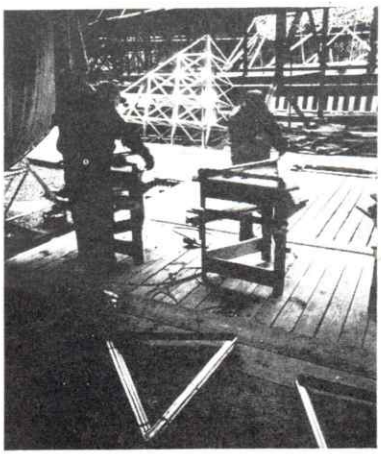

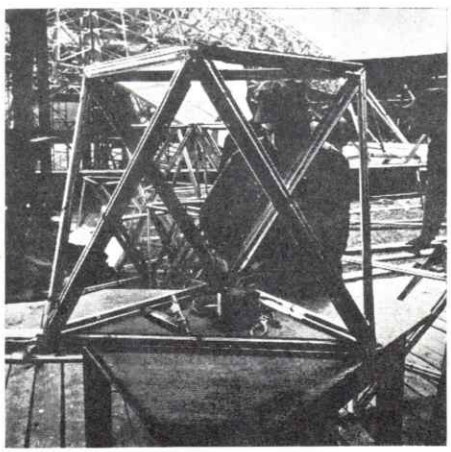

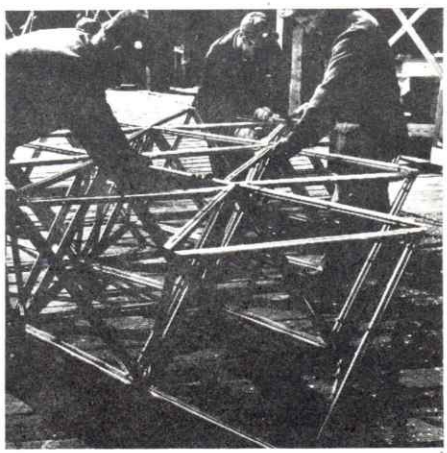

Fig. No. 22 Top: Partial construction of Ford Rotunda Dome. A single layer 3^V Alternate (icosa triangle outlined) 93' diameter dome infilled with double grid. Octahedron - tetrahedron truss, mylar covering water proofs enclosure. Infill truss is not a spherical generation, therefore dome appears to have planar facets in every Alternate breakdown triangle. Bottom: 1) Jiging table for infill truss, note finished section in background. 2) Basic octahedral unit. 3) Truss assembly. Infill trusses average 2 1/2 depth, 123 struts and 65 pounds in weight. Completed infill truss about 15' to a side. Project by Geodesics, Incorporated.

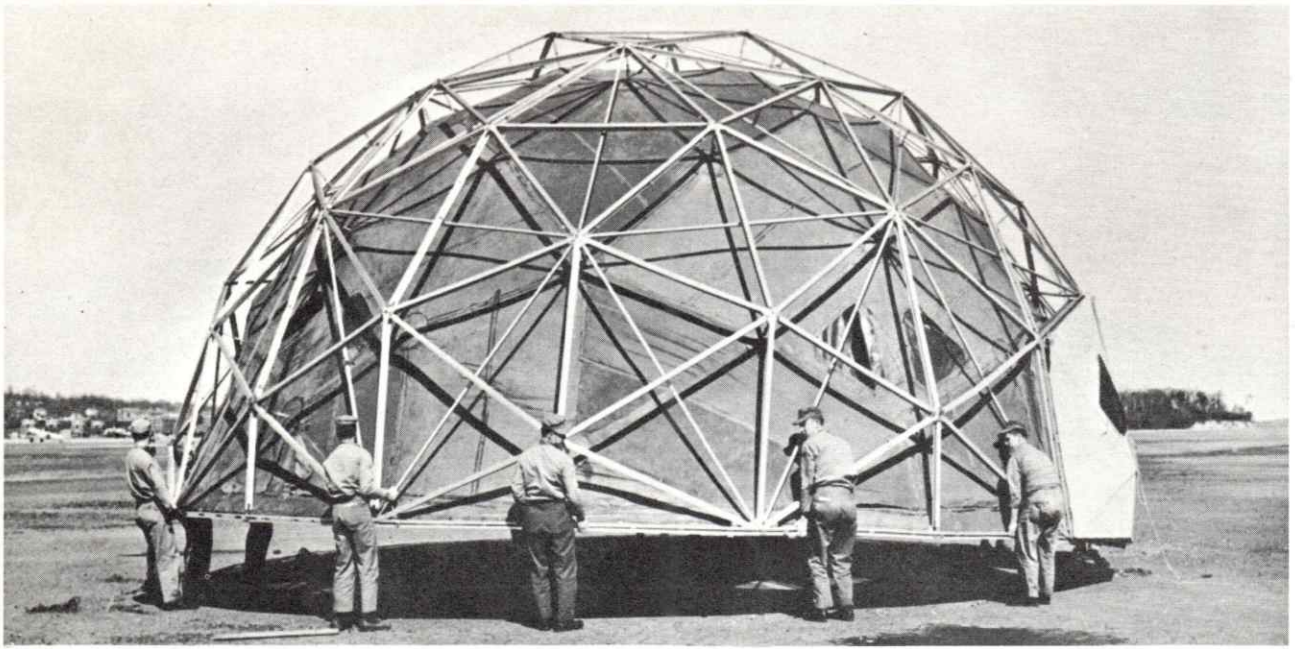

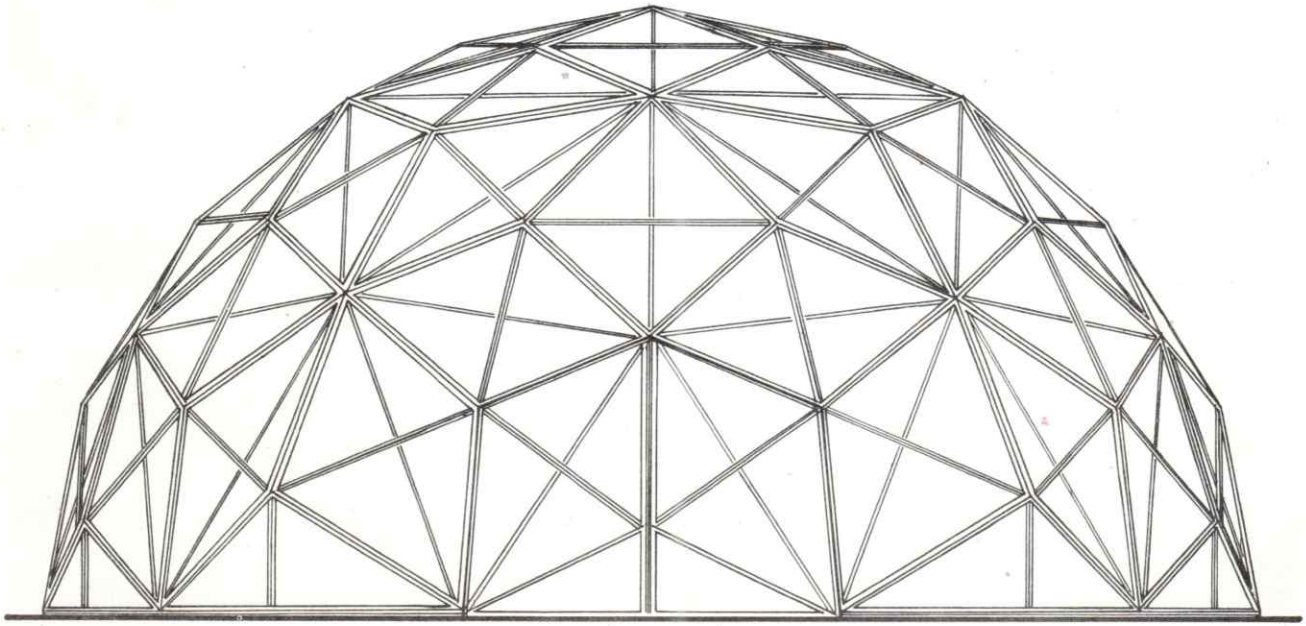

Fig. No. 23 Thirty-five foot diameter hemispherical personnel shelter developed for the Marine Corps Aviation, 1955. Development studies through numerous university research projects formally initiated large scale geodesic studies under R. B. Fuller. Numerous material, fabrication and erection discoveries were direct results of this series.

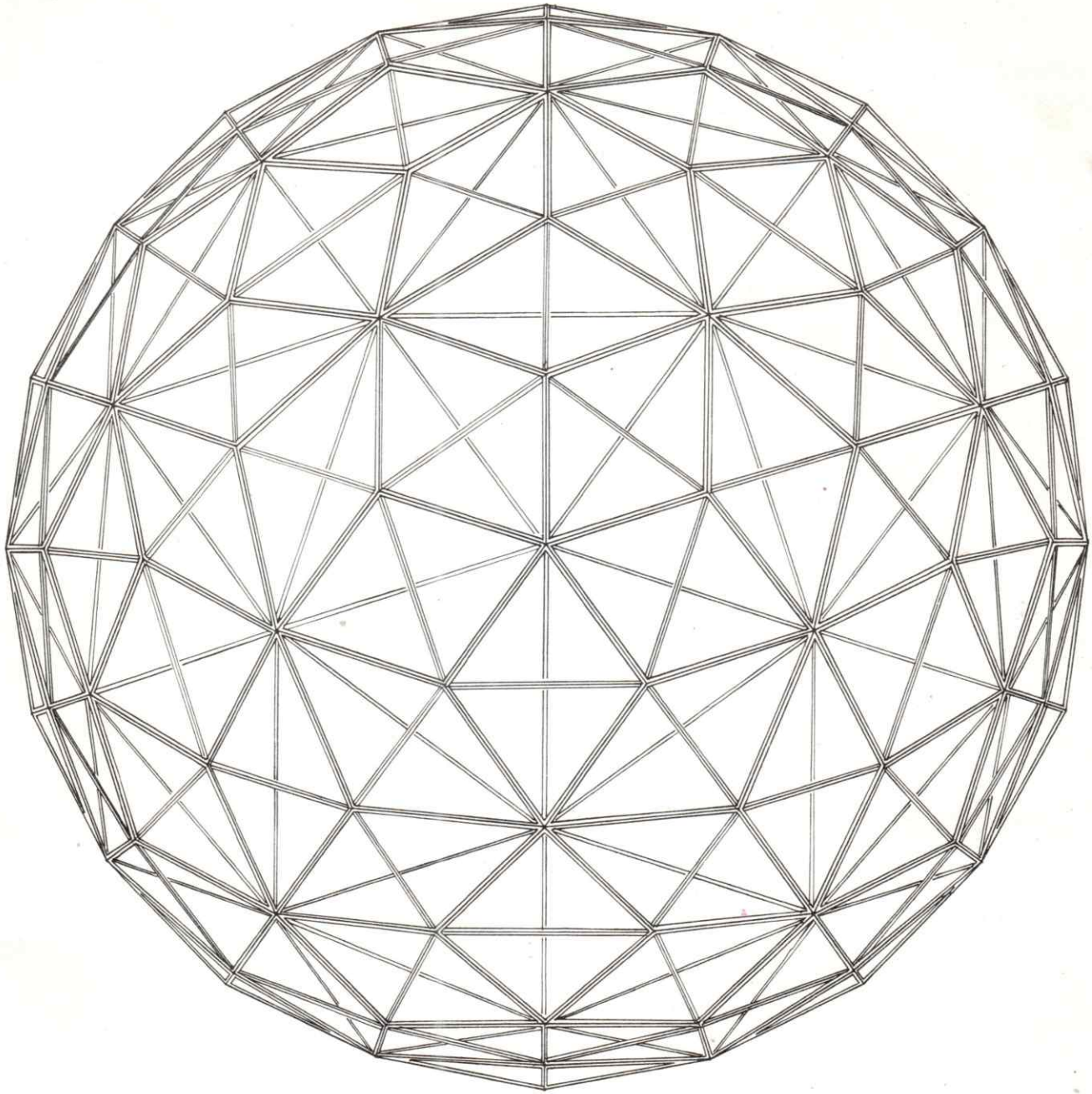

Fig. No. 24 Plan. Dome consists of an outer structural framework and interior membrane suspension. Fifty-five diamond units and ten half-diamond base pieces make up outer frame. Total erection of dome including membrane is about three man hours.

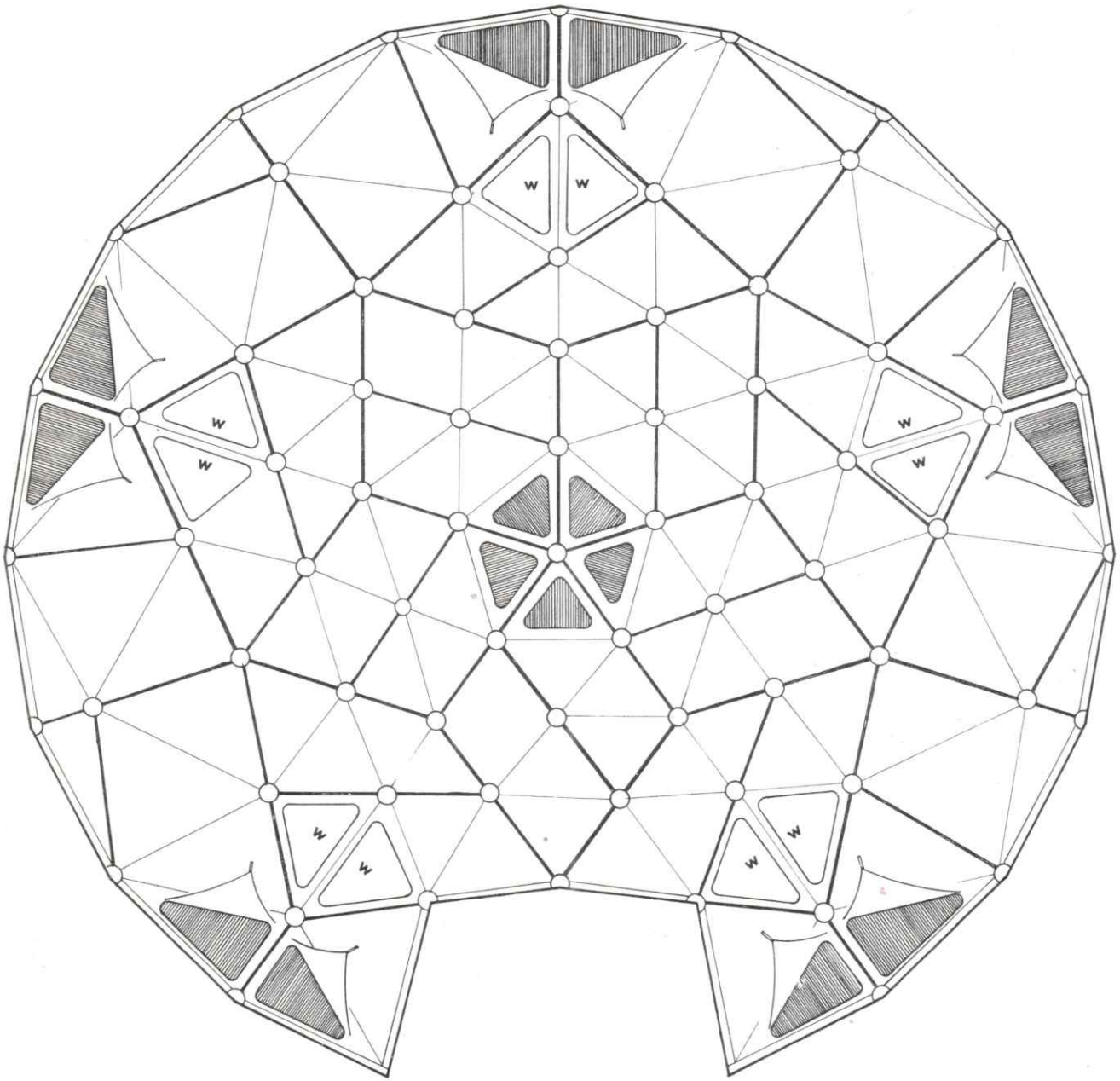

Fig. No. 25 Plan of interior membrane with vertex pick up points (similar chain and clamp device Fig. 21) windows and vents are indicated, dome encloses 1, 018 square feet, 10, 300 cubic feet, weights 1, 313 pounds and packs into 176 cubic feet, Strut efficiency is gained by supporting membrane only at vertexes. Enclosures inducing bending in struts call for almost 100% material increase.

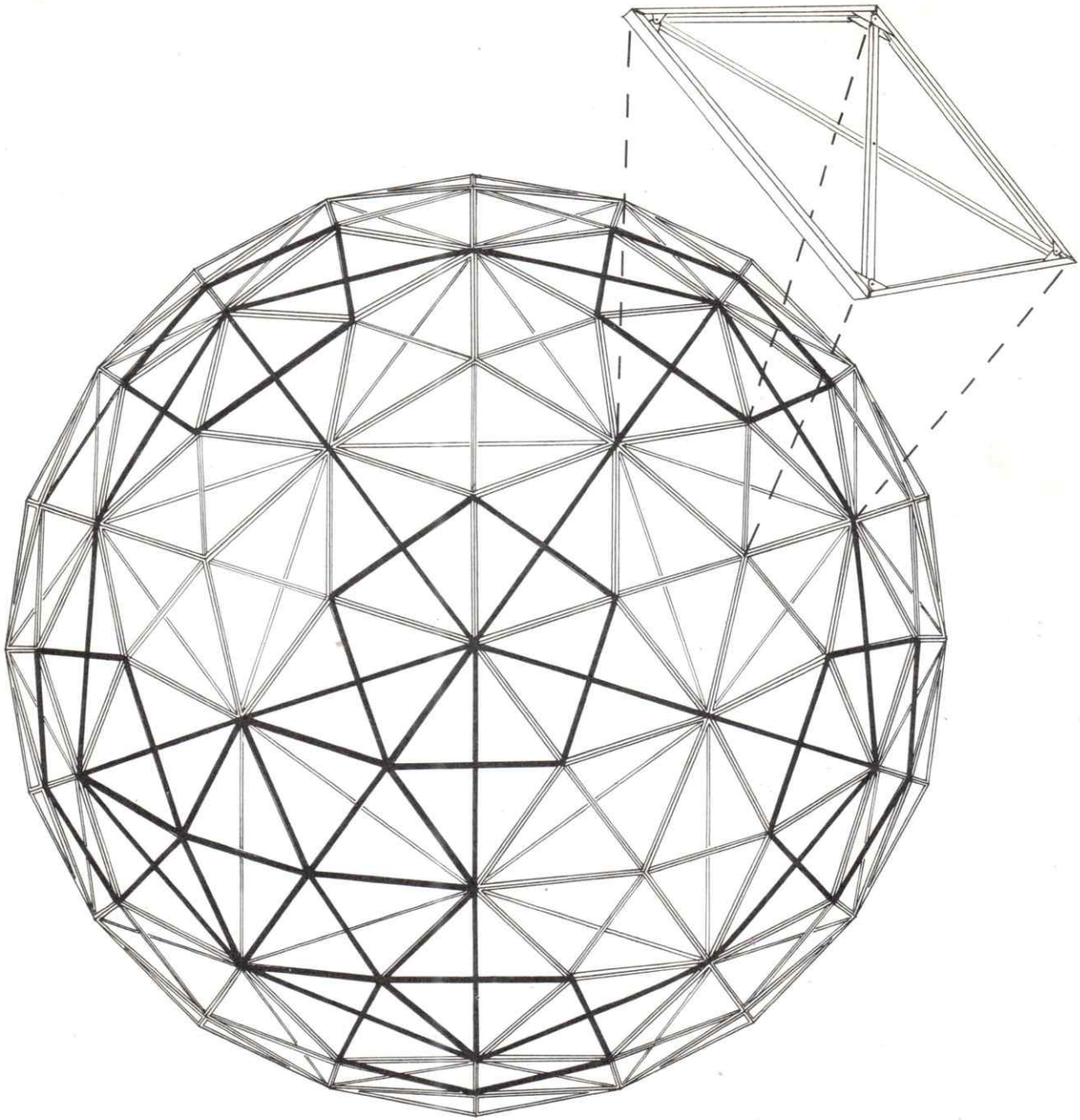

Fig. No. 26 Plan of geometry 4^V Triacon, vertex zenith, basic diamond component withdrawn.

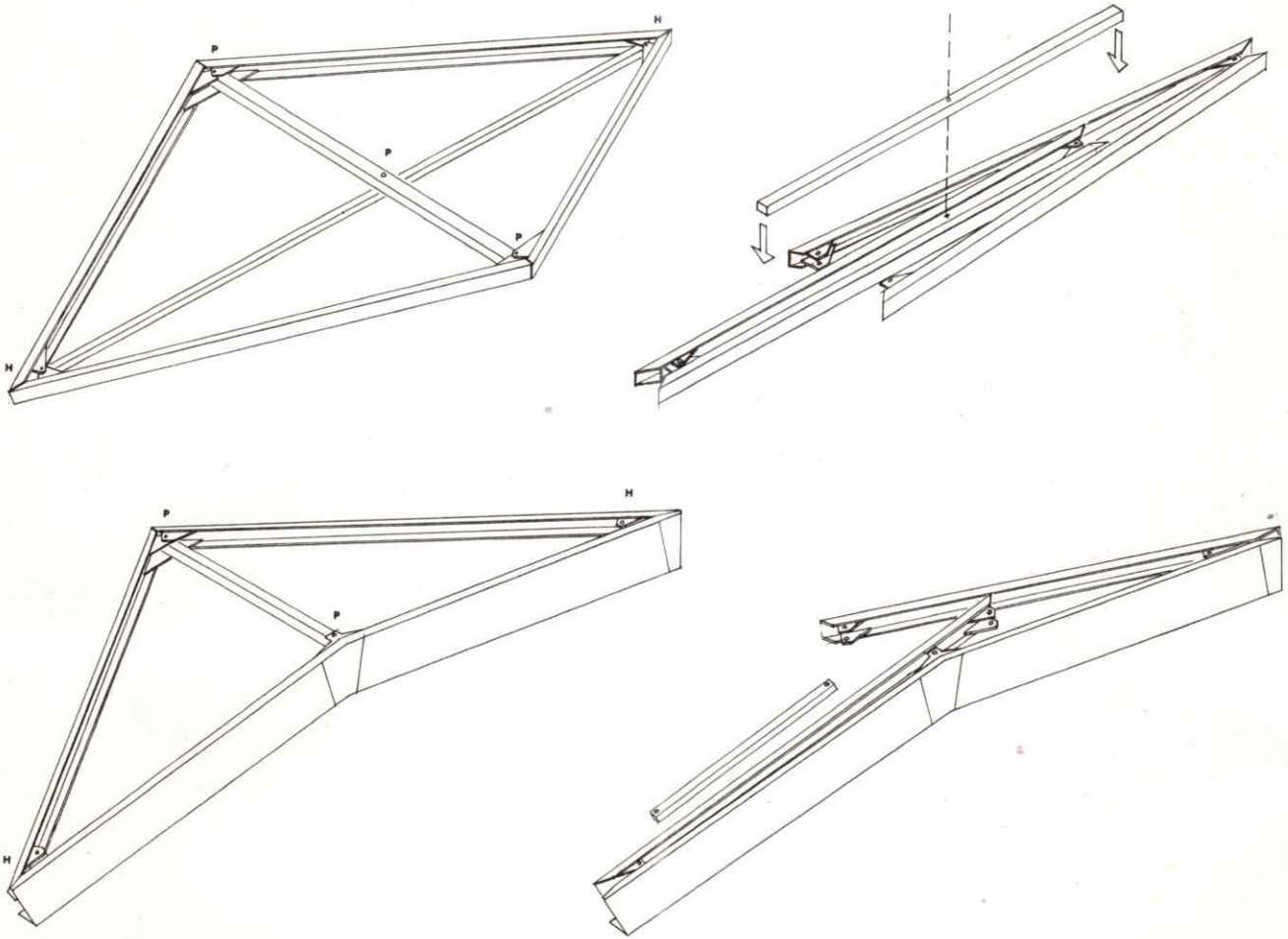

Fig. No. 27 Diamond packaging sequence, an ingenious pin and hinge system allows diamond components to partially disassemble reducing packaging volume, typical diamond and base support shown. A Fuller Research Foundation Project.

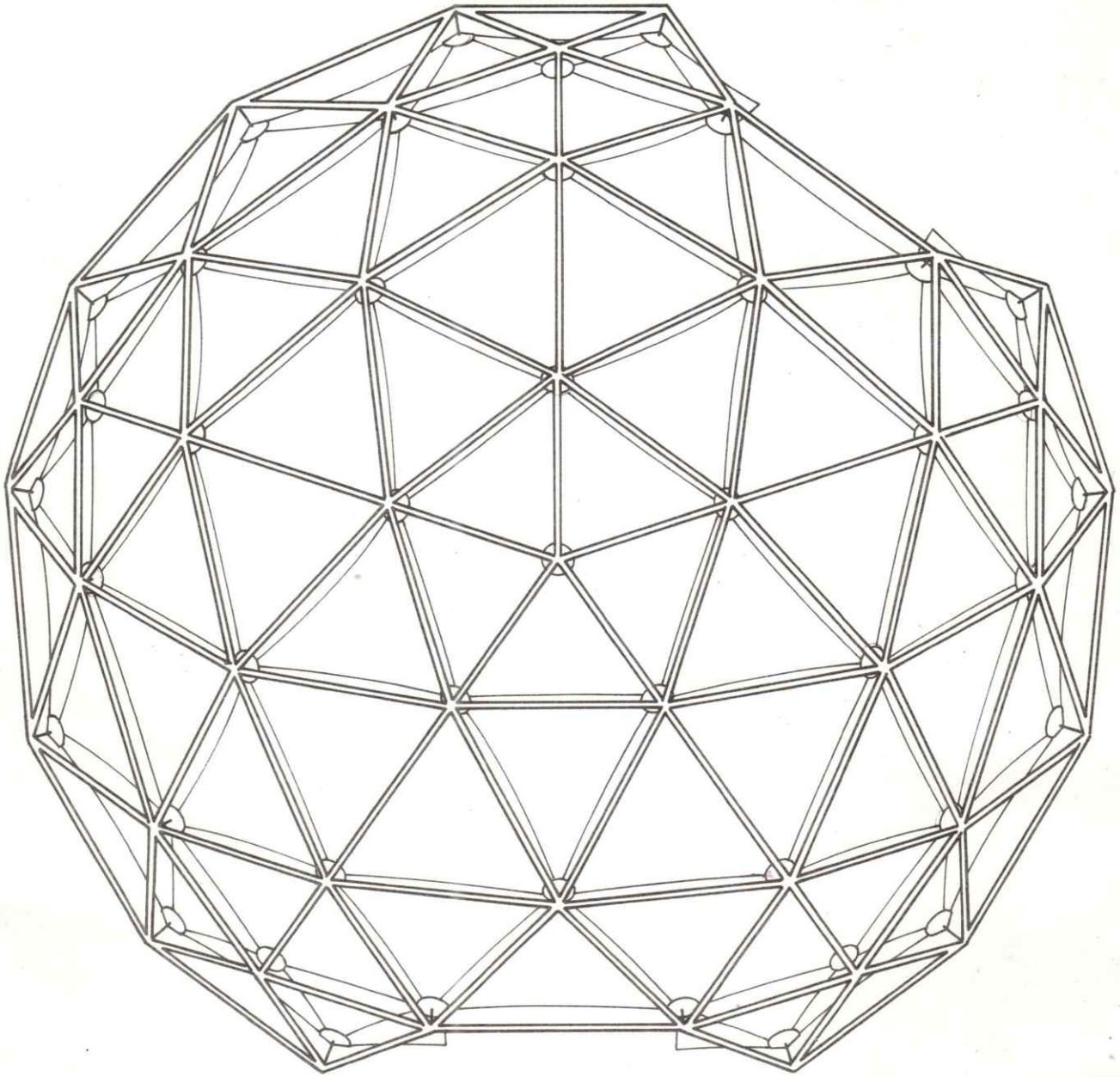

Fig. No. 28 Plan of a 60' diameter exhibition dome. A 3^{V} Alternate, vertex zenith strut and membrane structure, entries between base penagons.

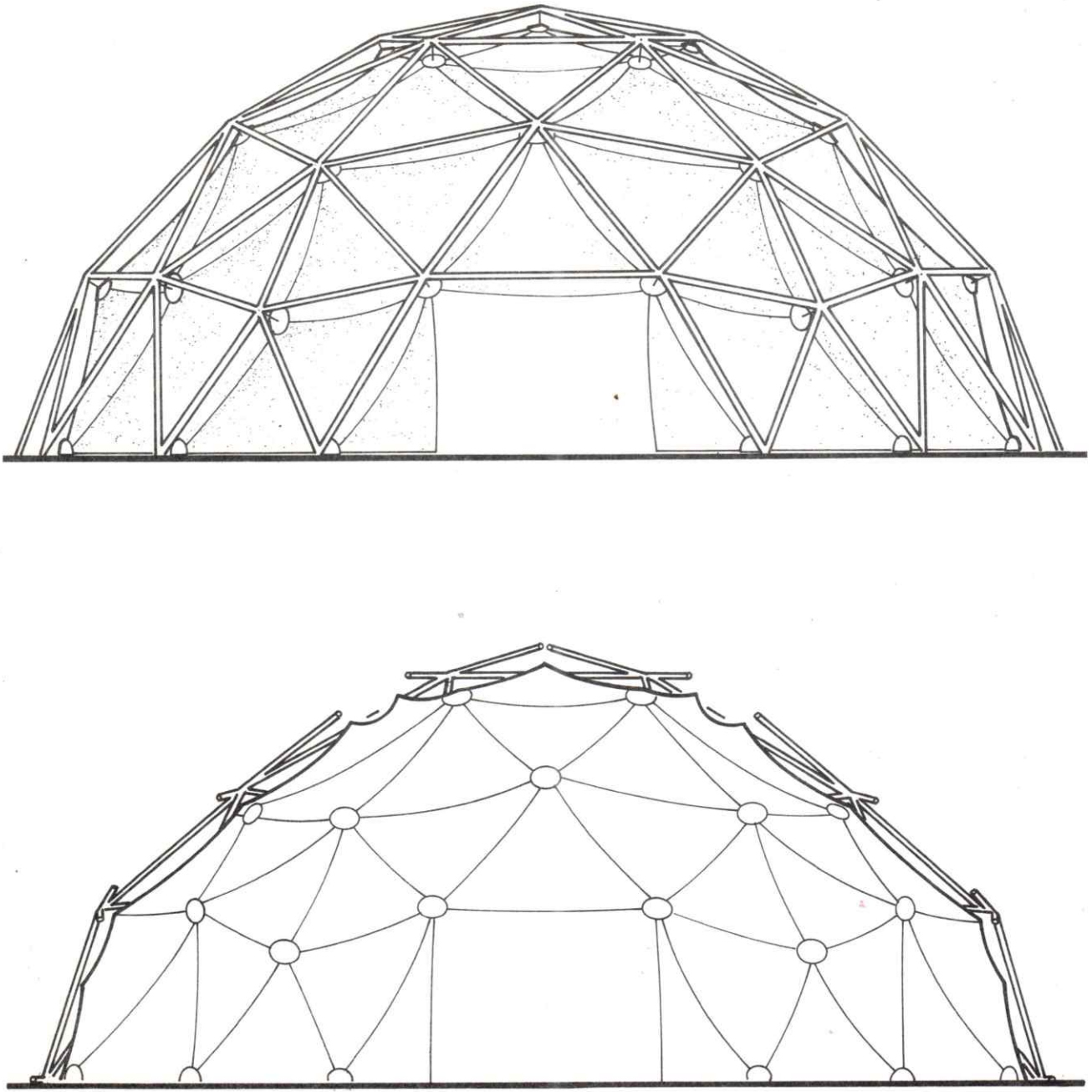

Fig. No. 29 Elevation and section.

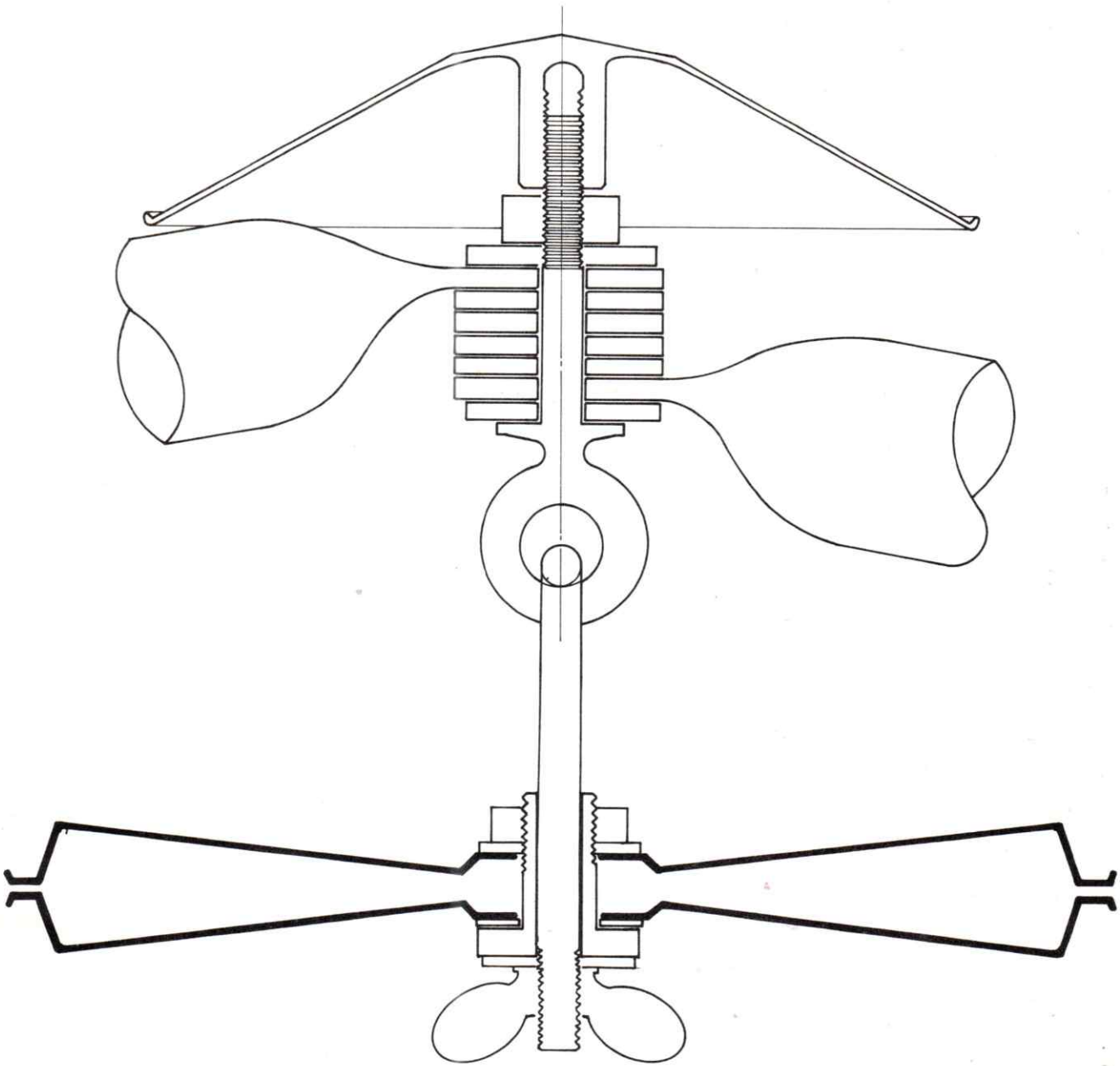

Fig. No. 30 Strut and membrane connector. Struts have flattened and drilled ends, eye bolt pins joint preventing joint rotation. Membrane is clamped between two metal disks and secured to strut eye bolt by hook and wing nut assembly. Bonnet over struts serves no function, joint is rather primitive in light of chain pick up assemblies of previous projects. A Geodesic, Incorporated study.

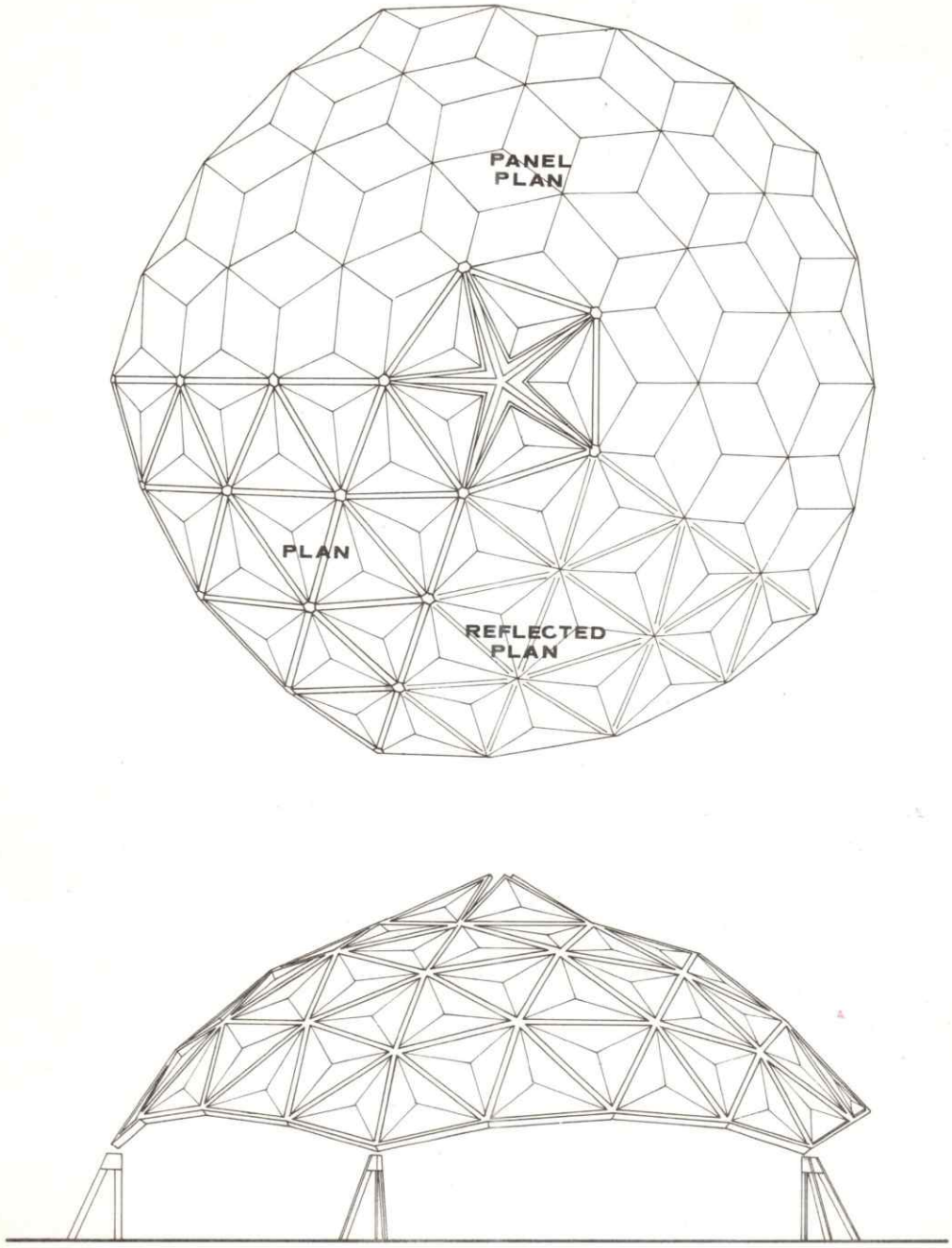

Fig. No. 31 Plan and elevation of 51' diameter Sasaki Dome. The 4^V Alternate dome is point supported at the five icosa-pents.

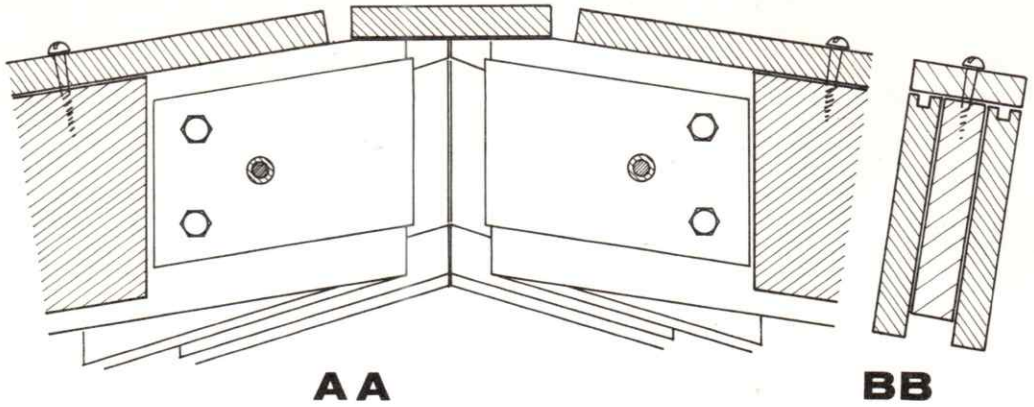

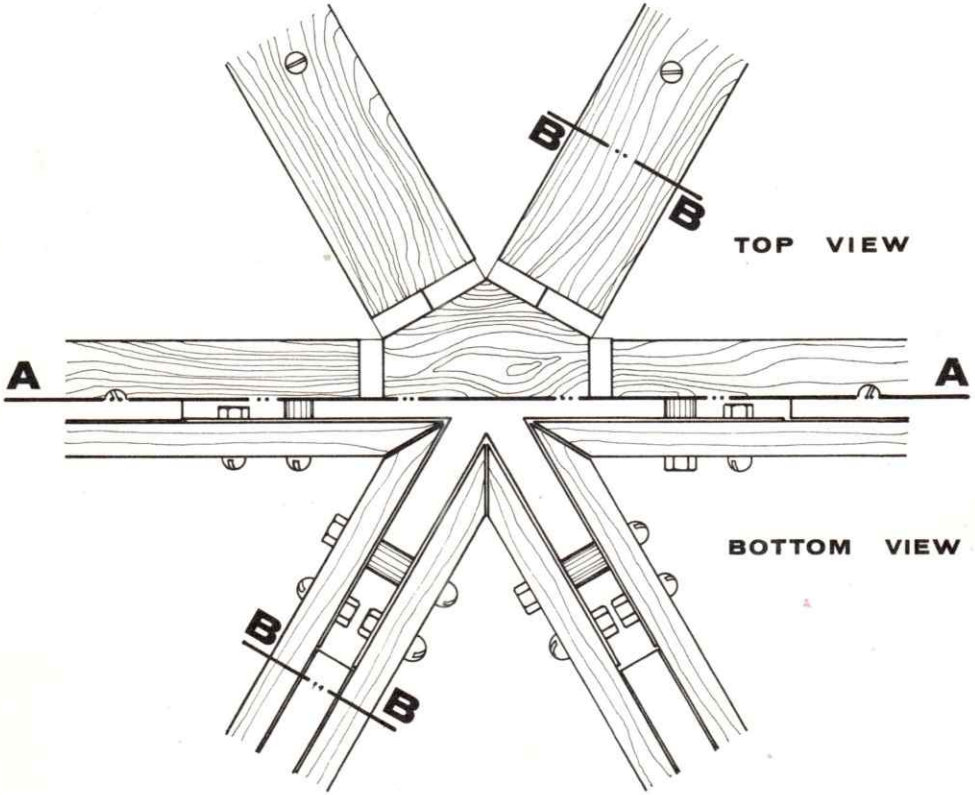

Fig. No. 32 Joint details adjacent struts are joined by a metal angle secured by spacer and screw assemblies. Enclosure was fiberglass panels locked to the strut by flanges fastened in a continuous groove, see Section BB. Dome was not built. Study by Geometrics, Incorporated.

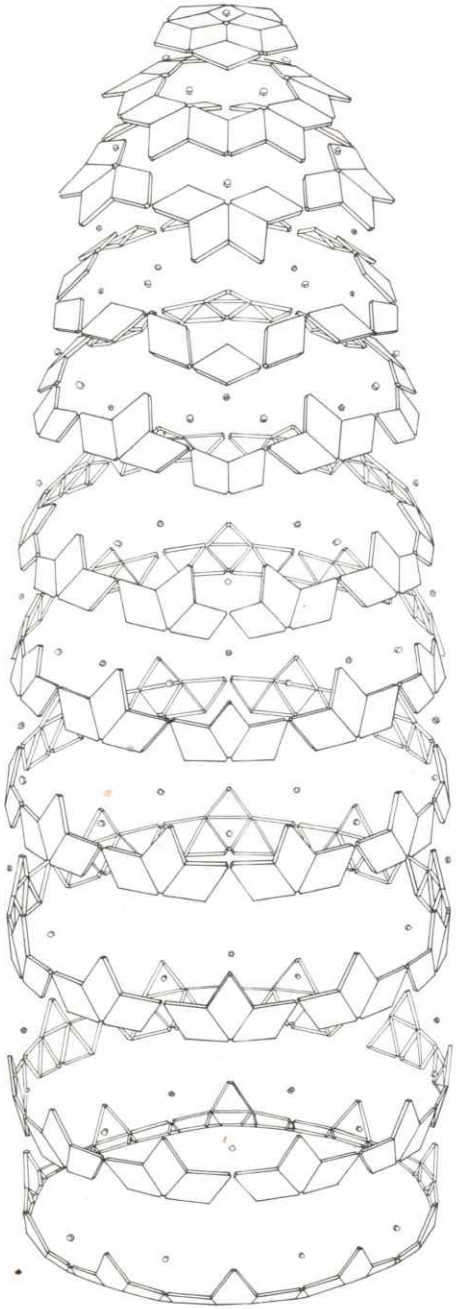

Fig. No. 33 Exploded assembly view of 55' diameter 2/3 sphere polyester fiberglass panel radome. A Geometrics, Incorporated project.

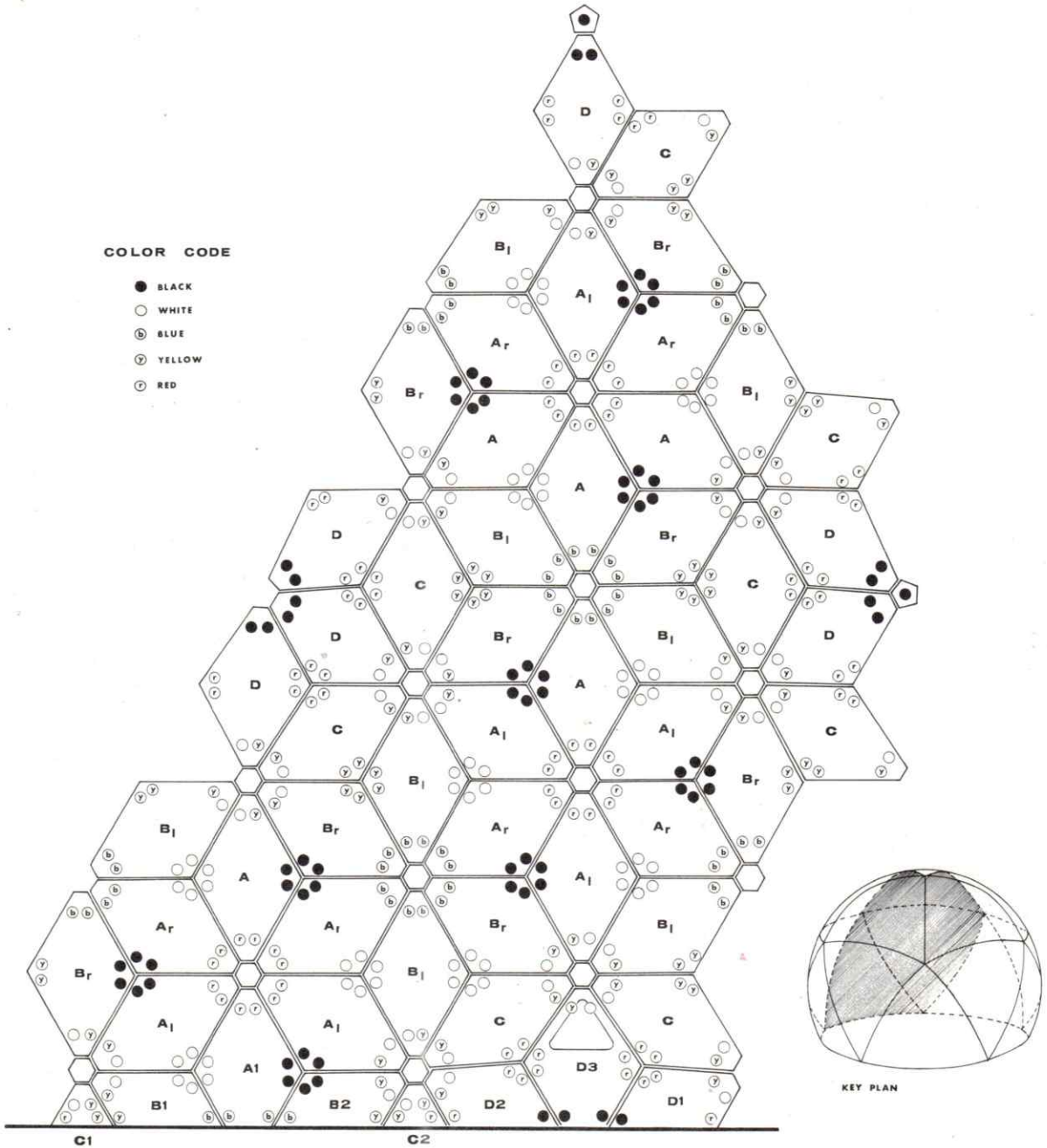

Fig. No. 34 Assembly drawing for 1/5 typical segment of Fig. 33. Key plan indicates portion of sphere covered in drawing. Viewed from inside, panel numbers and color code check are shown. Frequency determined by pentagonal vertex hubs, 6^V Alternate. Triangular hatch door appears on base panel D3. See Figs. 105 and 106 for erection study.

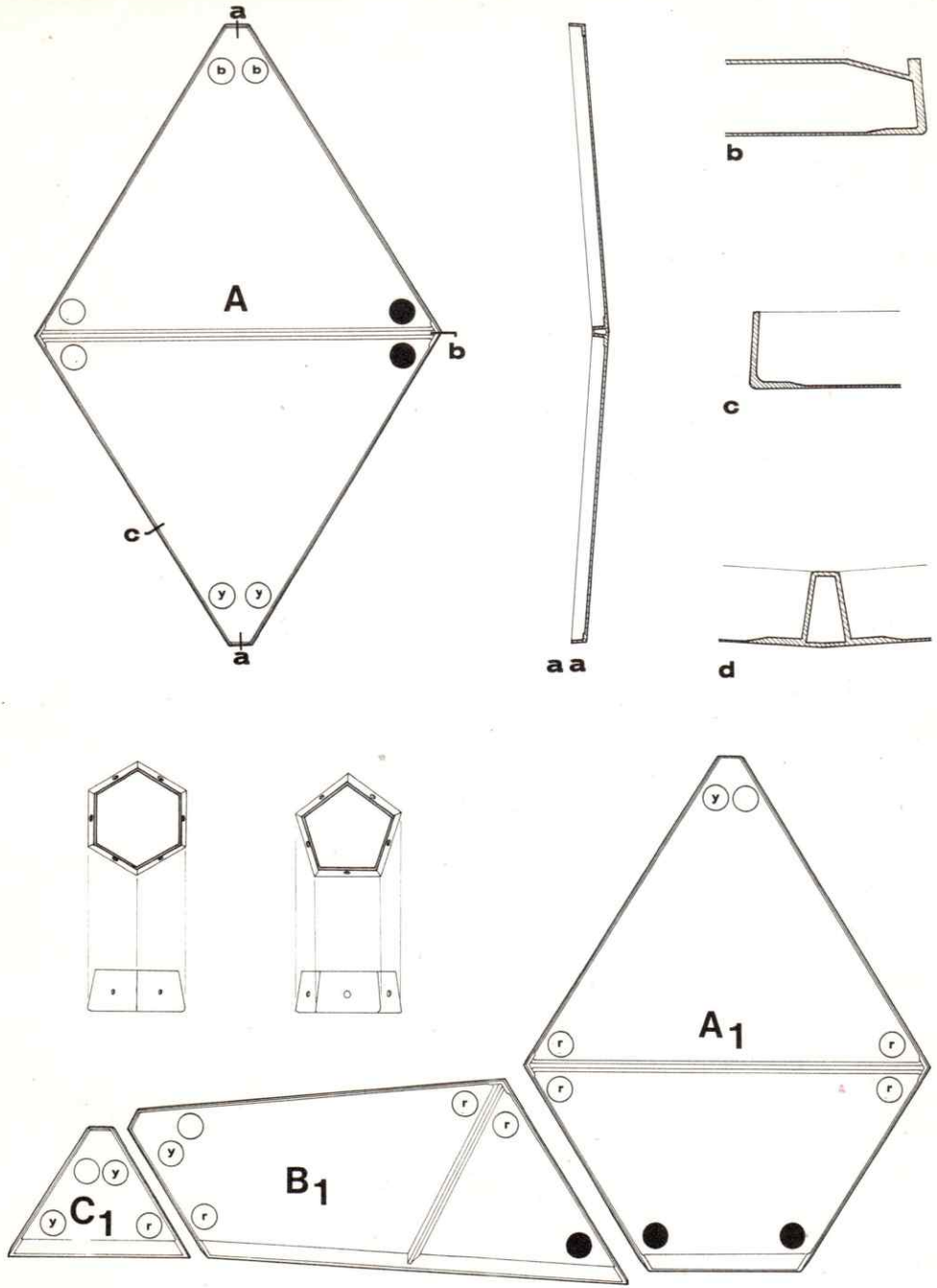

Fig. No. 35 Typical polyester fiberglass panels. Structural "rails" are formed when two adjacent panels are joined by fastners. A built up section such as "d" is achieved by placing a foam plastic piece on the panel and glassing over it with cloth and resen, the foam strip is merely a form. Vertex hubs are usually cast assemblies. Again color codes are indicated.

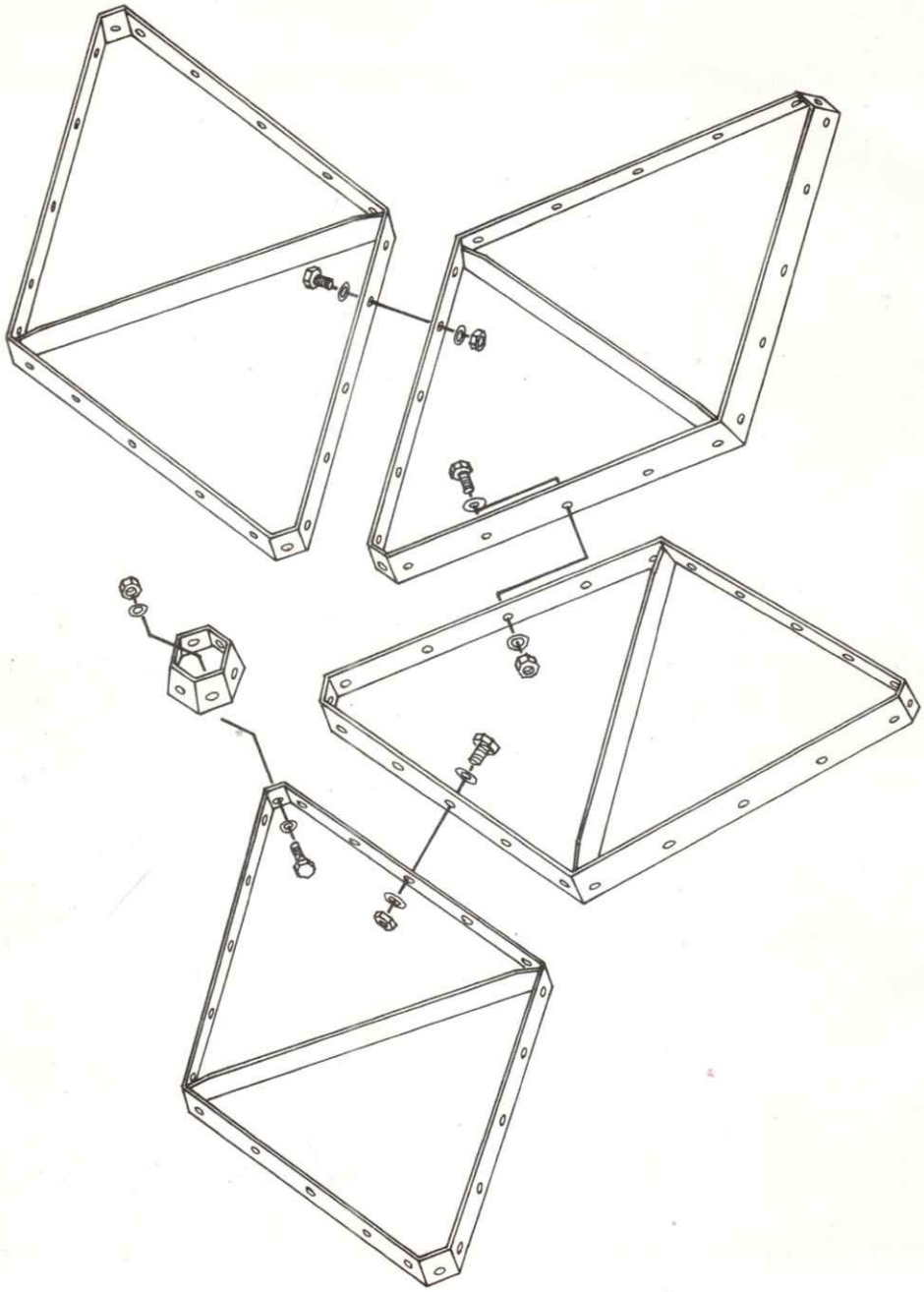

Fig. No. 36 Diagramatic panel assembly.

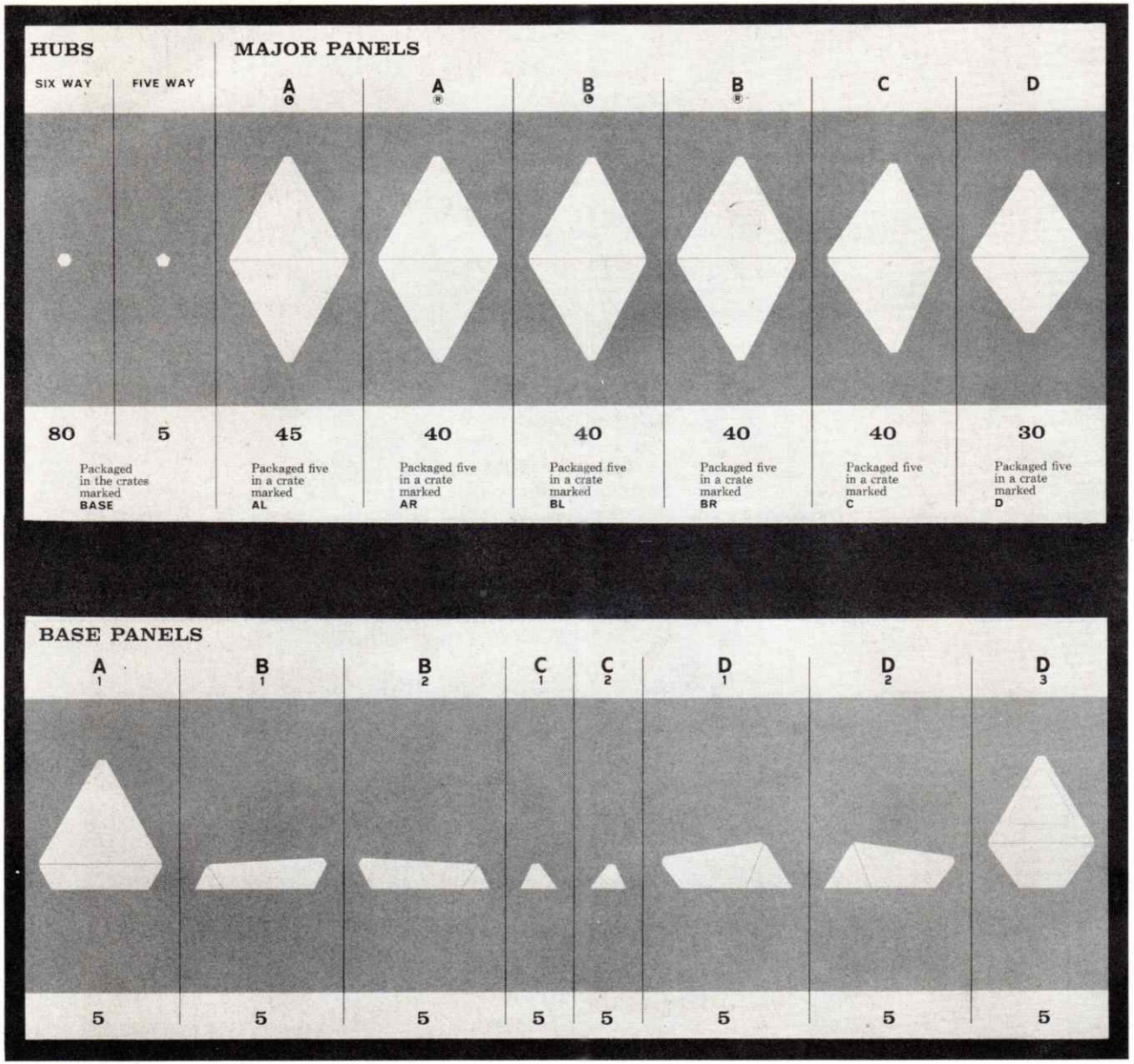

Fig. No. 37 Typical packaging and identification for 55' diameter radome.

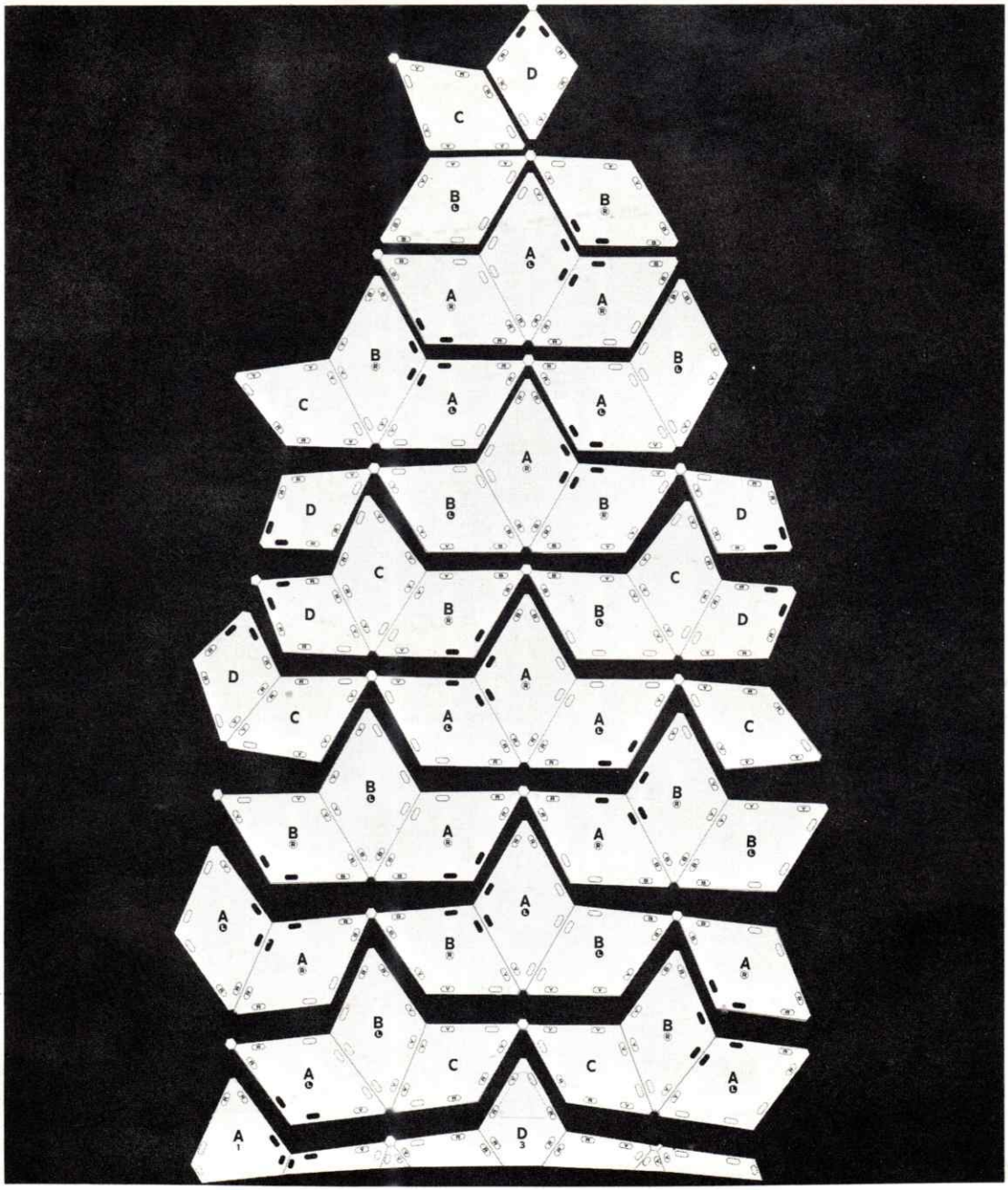

Fig. No. 38 Assembly sequence typical of 1/5 dome. Panels are erected in 11 concentric rings from base to zenith.

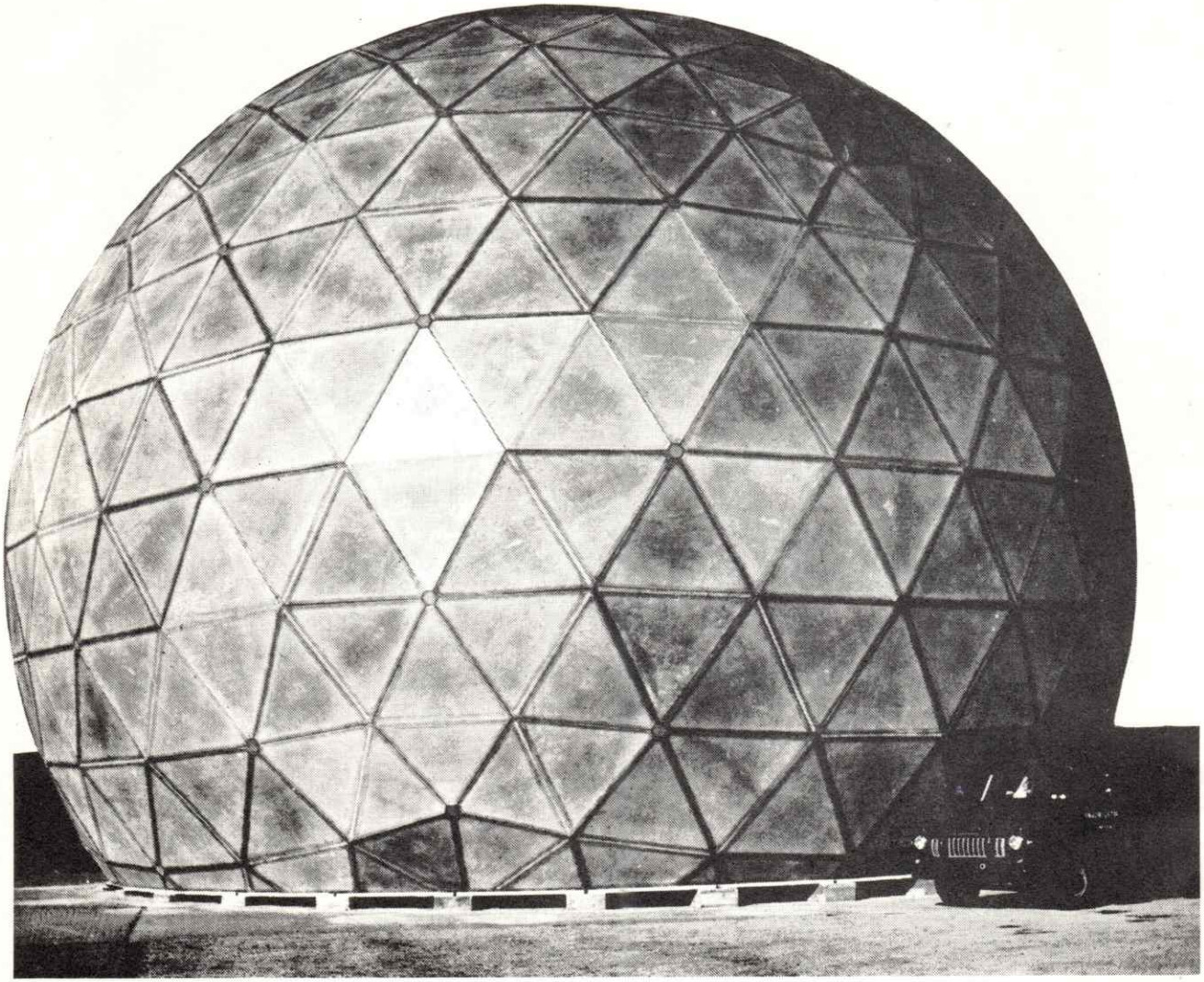

Fig. No. 39 6^{V} Alternate 110 foot diameter radome similar to those described in Figs. 33, 34, 35, 36, 37 and 38. Diamond panels made of fiberglass with triangulating stiffener. Project by English Electric Company, Limited.

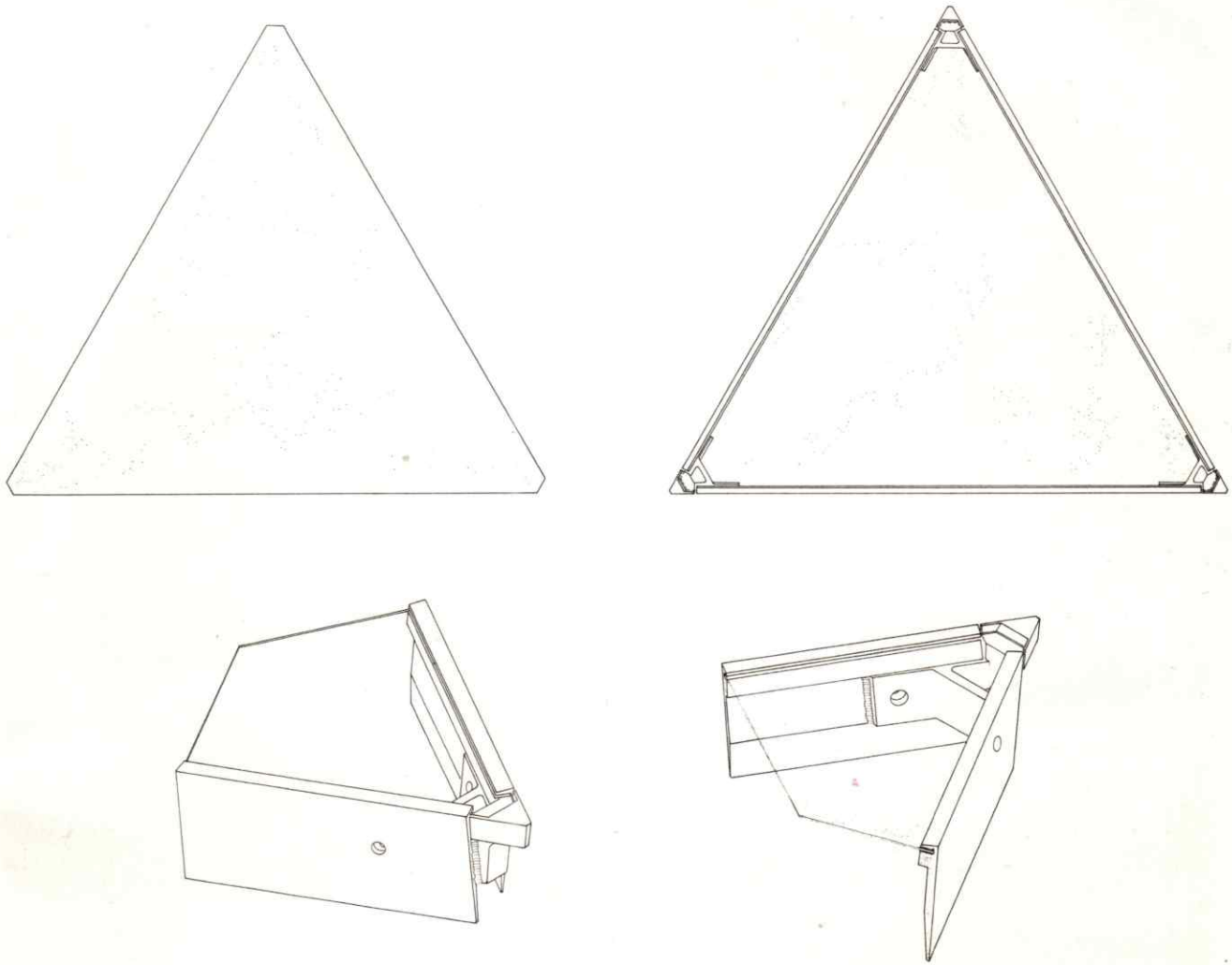

Fig. No. 40 Panel membrane and rail assembly for 110' diameter 10^{V} Triacon dome. Extruded rails receive membrane and become struts when adjacently bolted to another assembly. Casting is welded to rail and transfers high vertex stress, rather narrow proportions of rail cross section were attempts to lessen frontal blockage of the transmitting radar. Project by Geometrics, Incorporated.

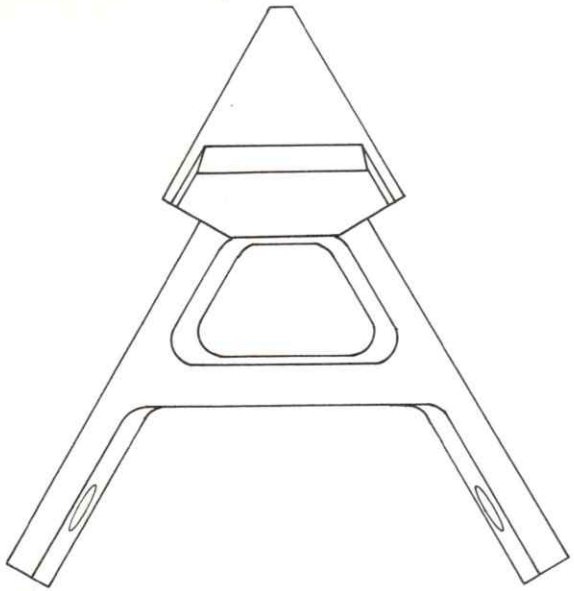

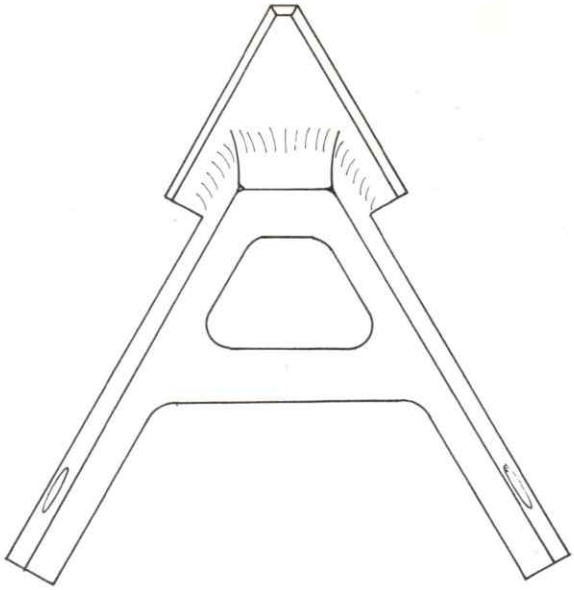

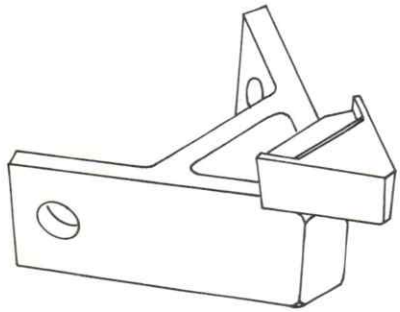

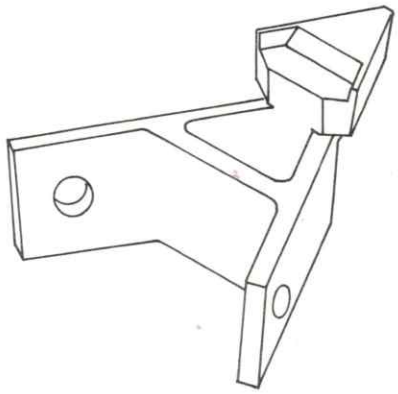

Fig. No. 41 Casting views.

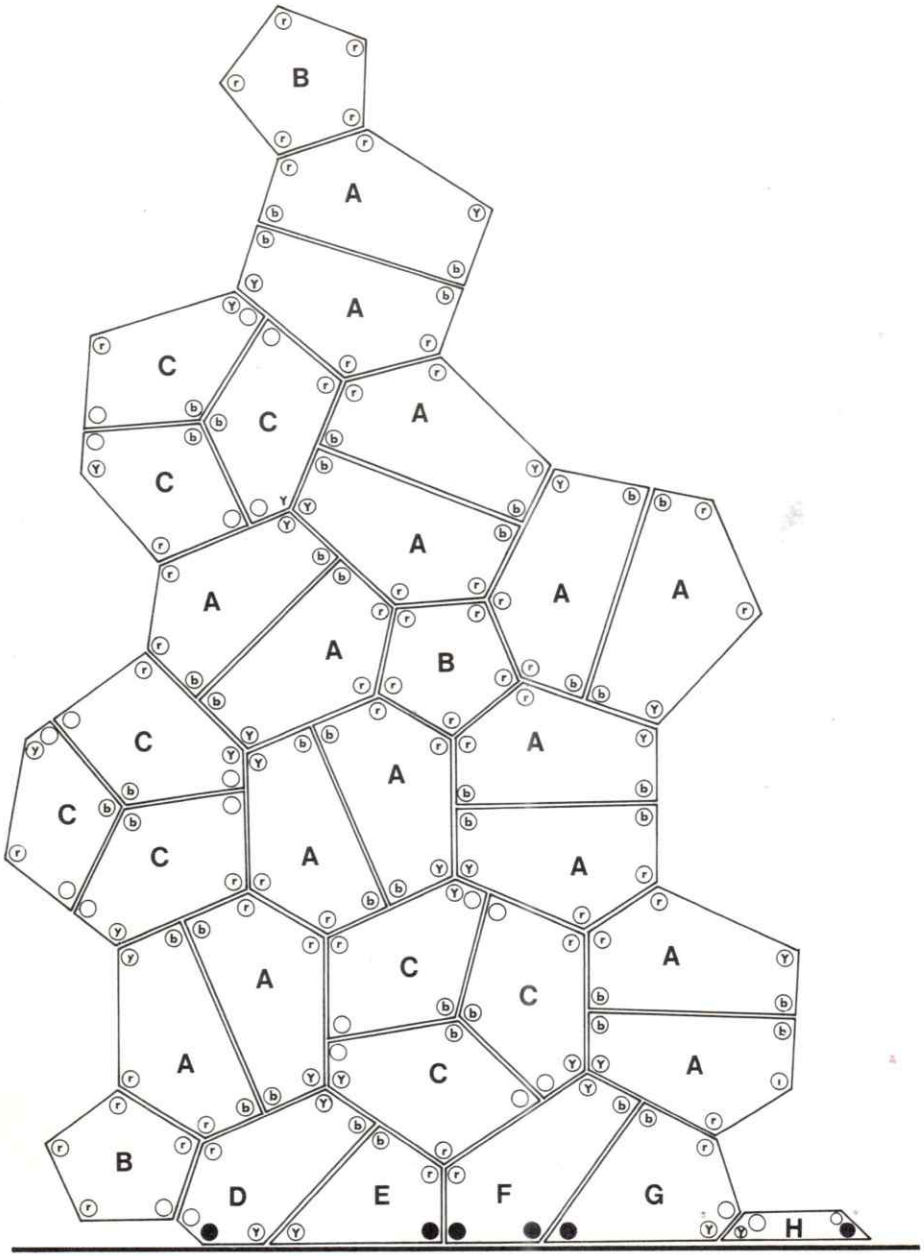

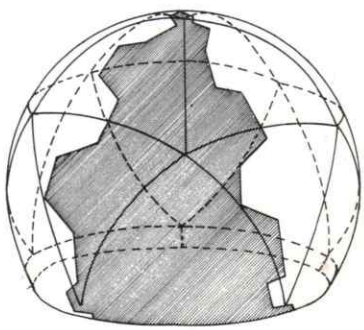

KEY PLAN

Fig. No. 42 Assembly drawing for 60' diameter 3/4 sphere honeycomb panel dome. Of particular interest is the rather awkward appearing breakdown. An attempt was made standardize panels and destroy any continuity established by seams of adjacent panel joinery, it demonstrates that manipulation of the breakdown may follow numerous criterion. Project by Geometrics, Incorporated.

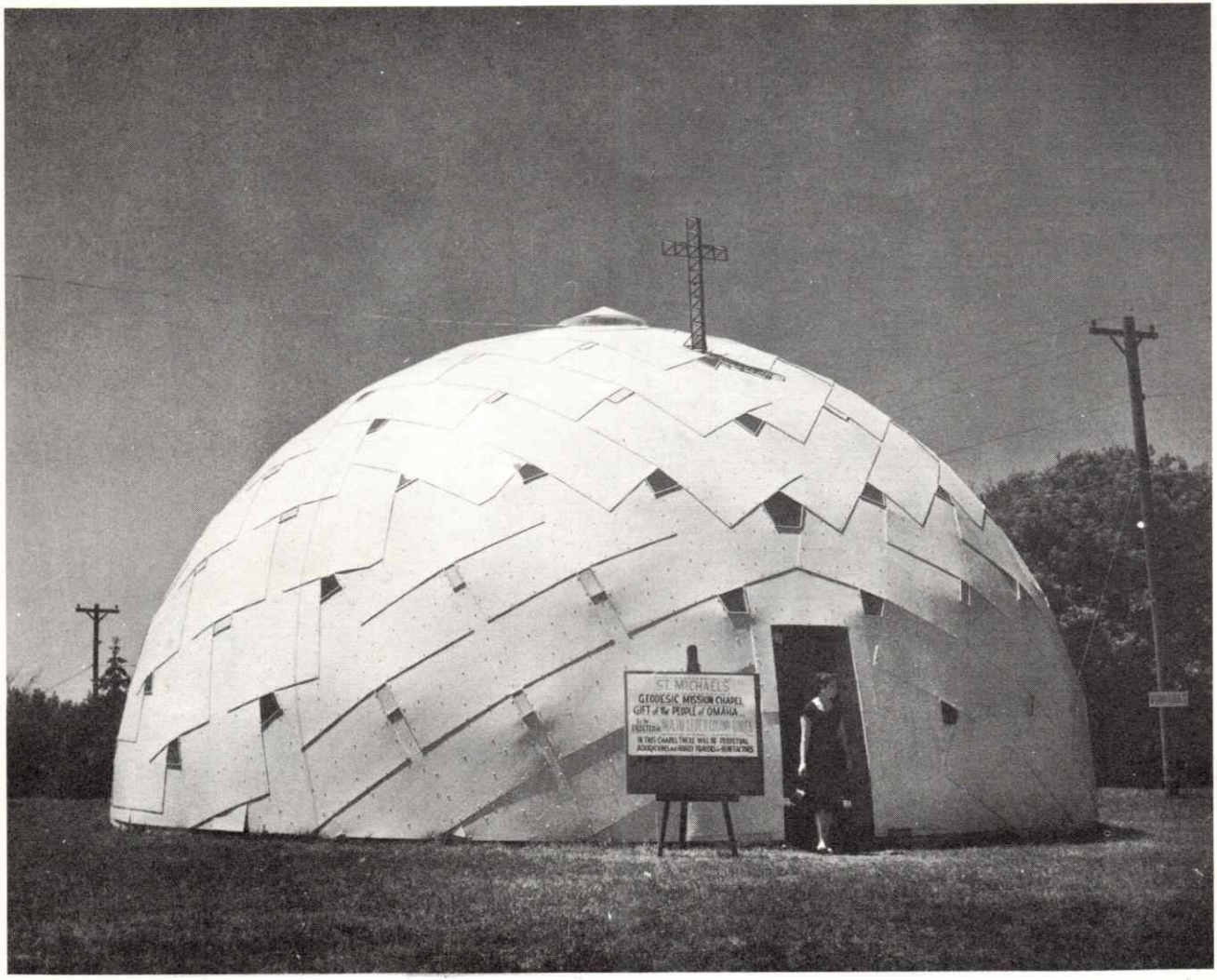

Fig. No. 43 Thirty-nine foot diameter plywood dome. Although not a reticular dome it is interesting to note the use of geodesic geometry and planar sheets of plywood to achieve a dome.

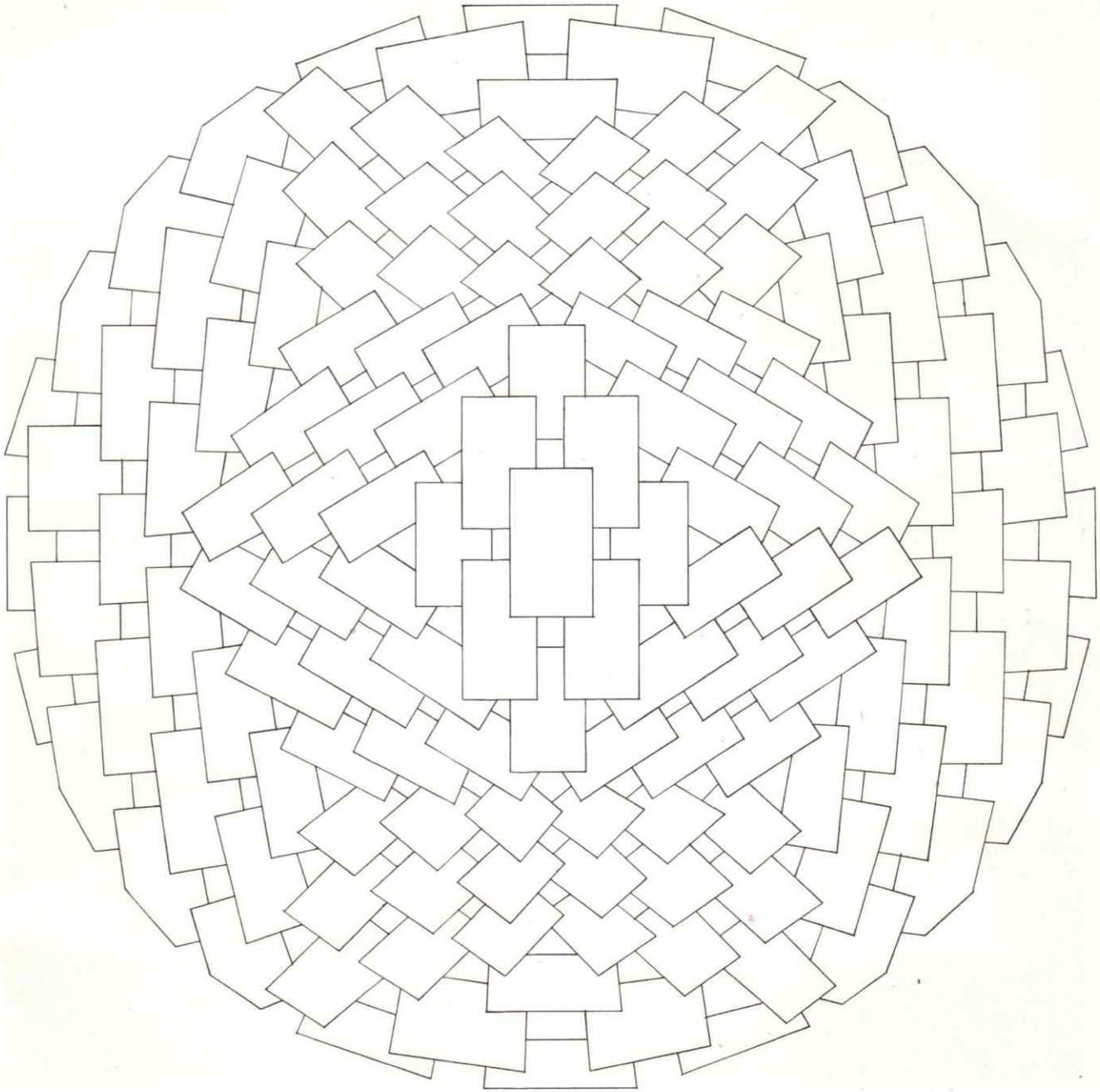

Fig. No. 44 Plan of dome. Plywood, like any semi-flexable planar material can be folder to a degree about an axis. A single sheet could conceivably fold about many axis as long as the creases do not intersect to form compound curves.

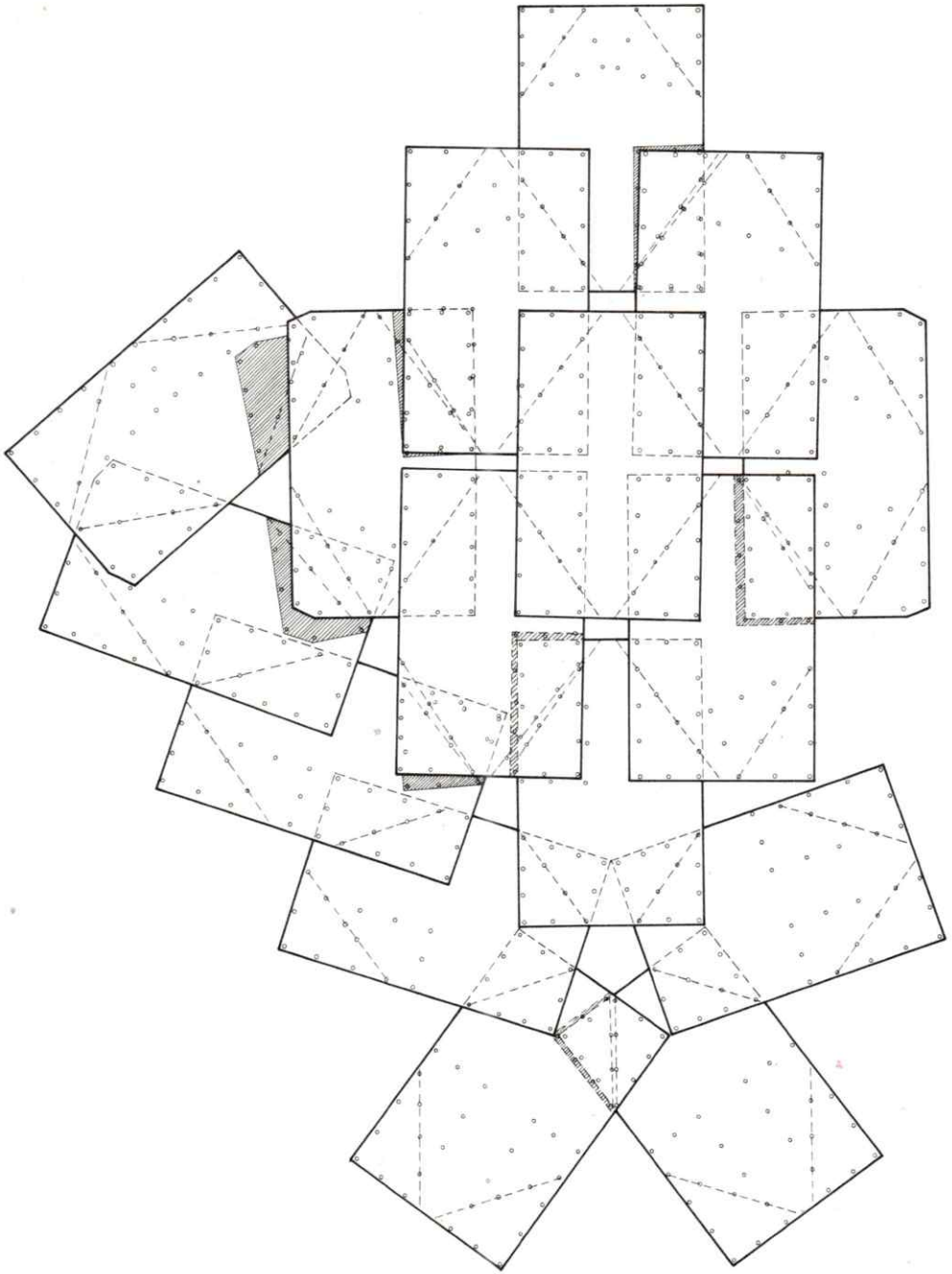

Fig. No. 45 Partial plan of plywood bolt patterns. Sheets are fastened along corner diagonals, when drawn together they pucker out forming a spherical surface. Shaded areas indicate amount sheets must be drawn together.

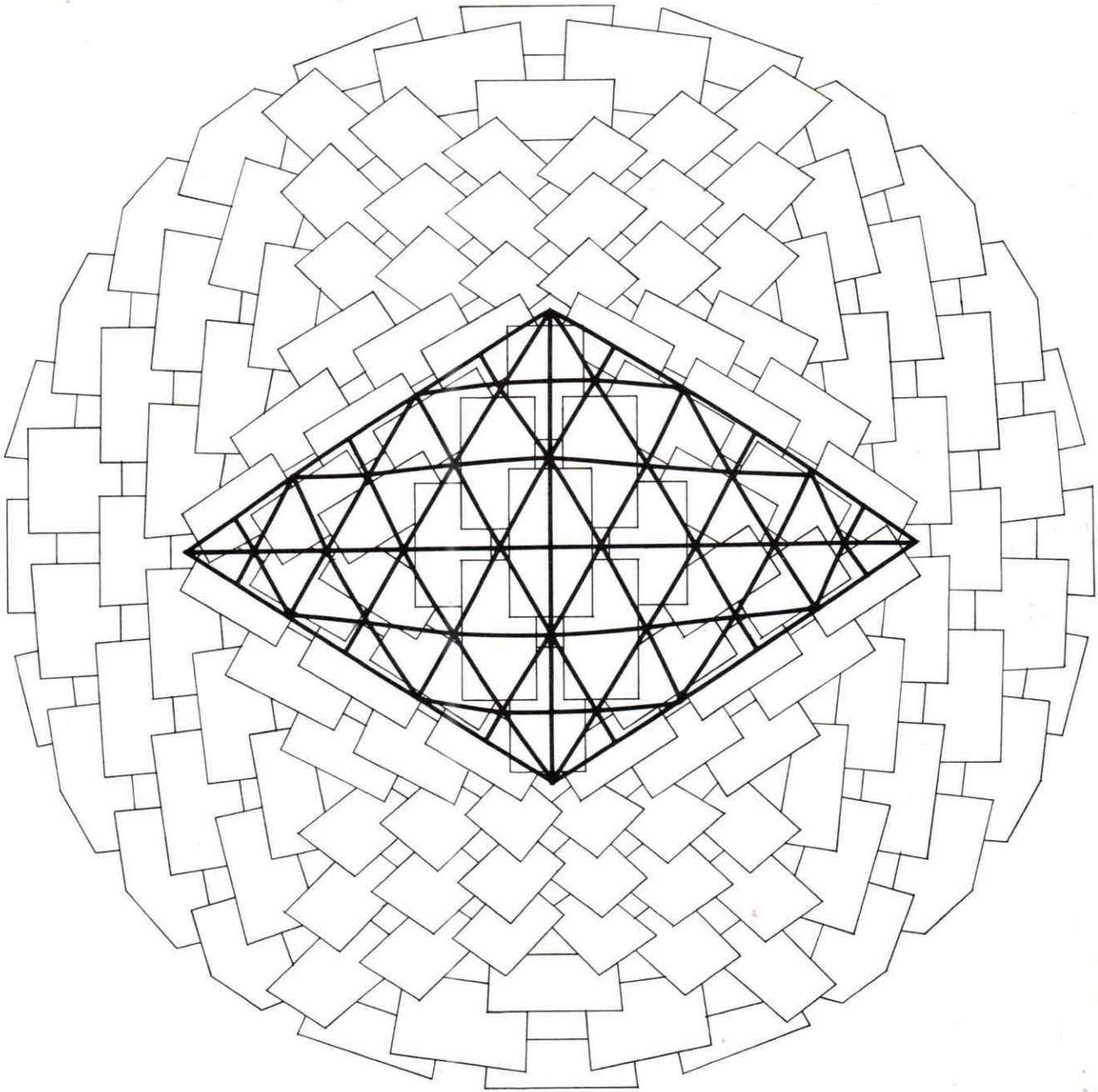

Fig. No. 46 Geometric interpretation of sheet fastener and fold axis. A 6^V Triacon, edge zenith breakdown. Note pentagonal windown remain as cues. Although shingle action aids in water proofing the enormous quantity of fasteners and window variance make this structure questionable. The ingeniousness of the material use for spherical forms however is to be admired. See Fig. 99 for similar erection. Project by Geodesics, Incorporated.

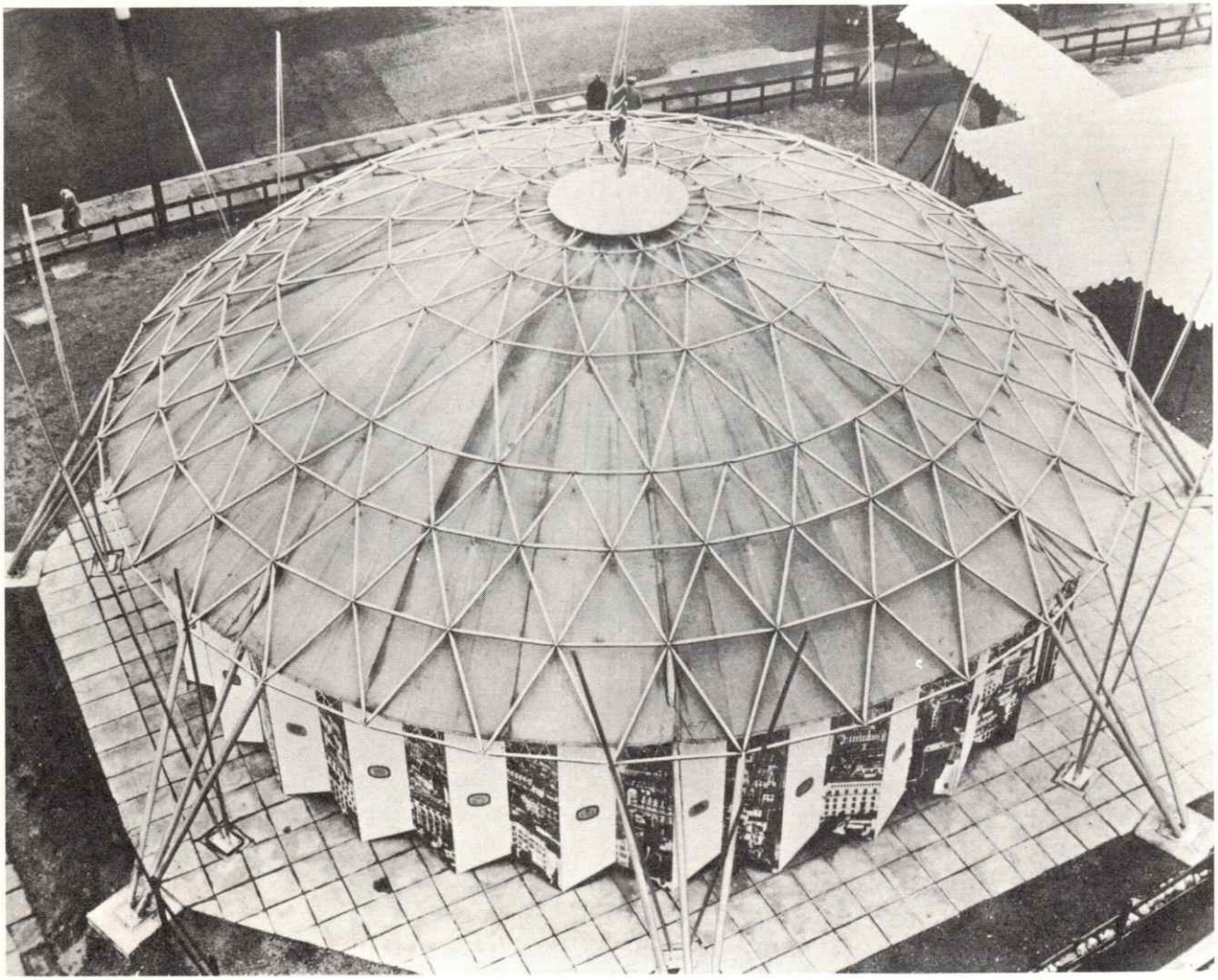

Fig. No. 47 Sixty-six foot diameter lesser circle dome by Triodetic. Geometrically not of the icosahedral family this breakdown resembles the bi-polar subdivision of longitude and latitude.

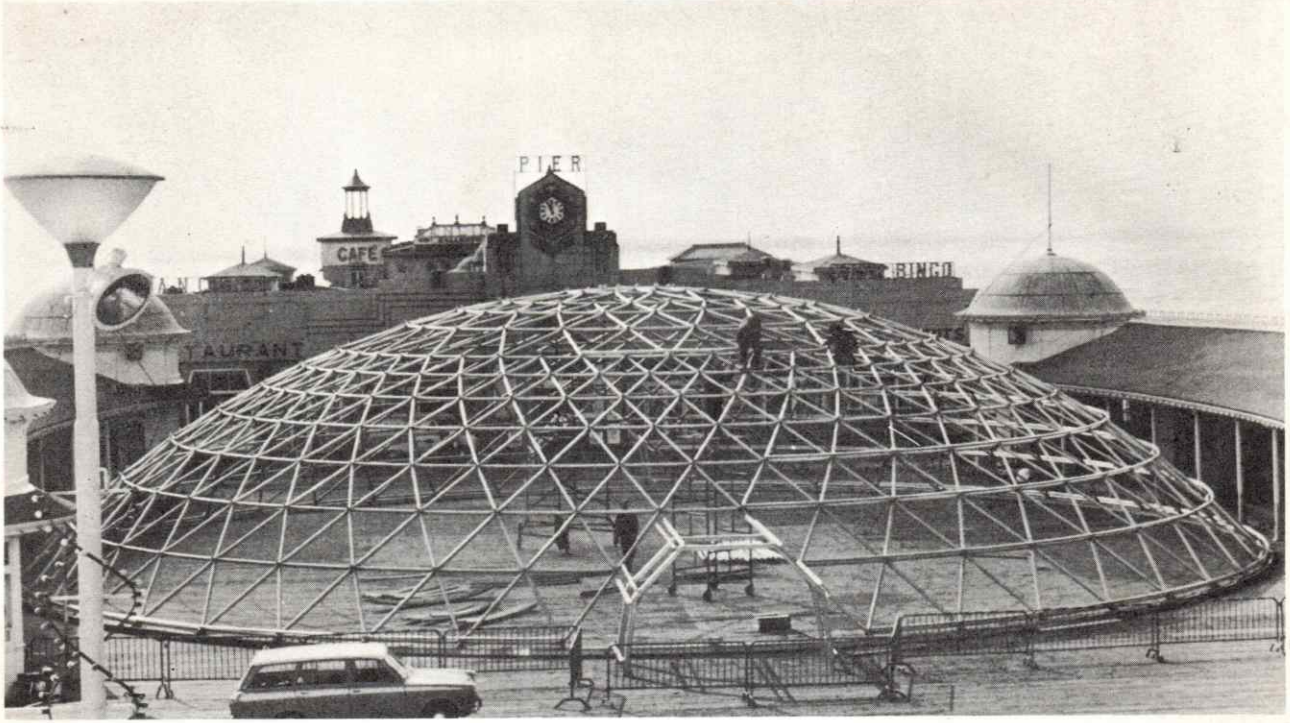

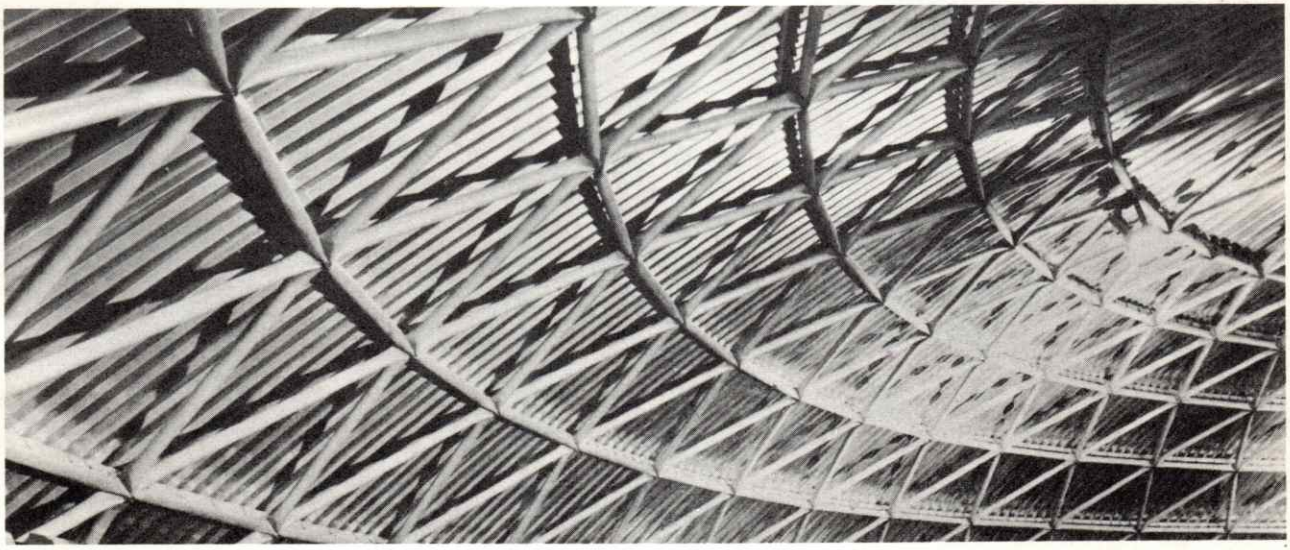

Fig. No. 48 Similar to Fig. 47 this lesser circle geometry permits the accumulation of the most struts where they are least needed, the zenith. The icosahedral forms we have concerned ourselves with do not have this pitfall.

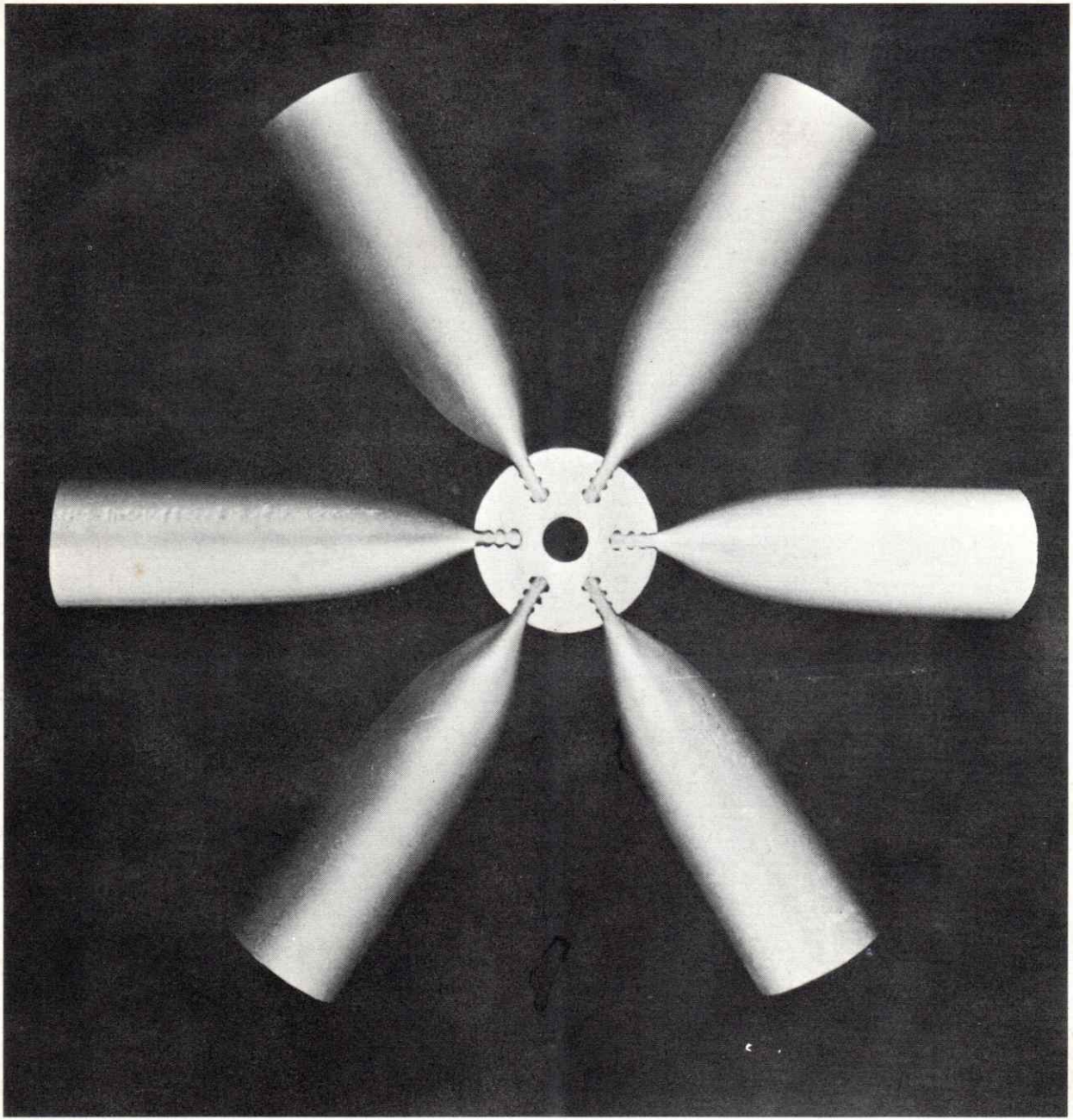

Fig. No. 49 The triodetic connector. This connection device is merely an extruded hub with female ridges to receive strut ends with corresponding male ridges. One operation flattens, ridges, and sets dihedral angle without any loss of material. The extruded hub can receive any number struts as physically possible by merely increasing the ridges. Bolt and washers prevent the tubes from slipping out of ridged groove.

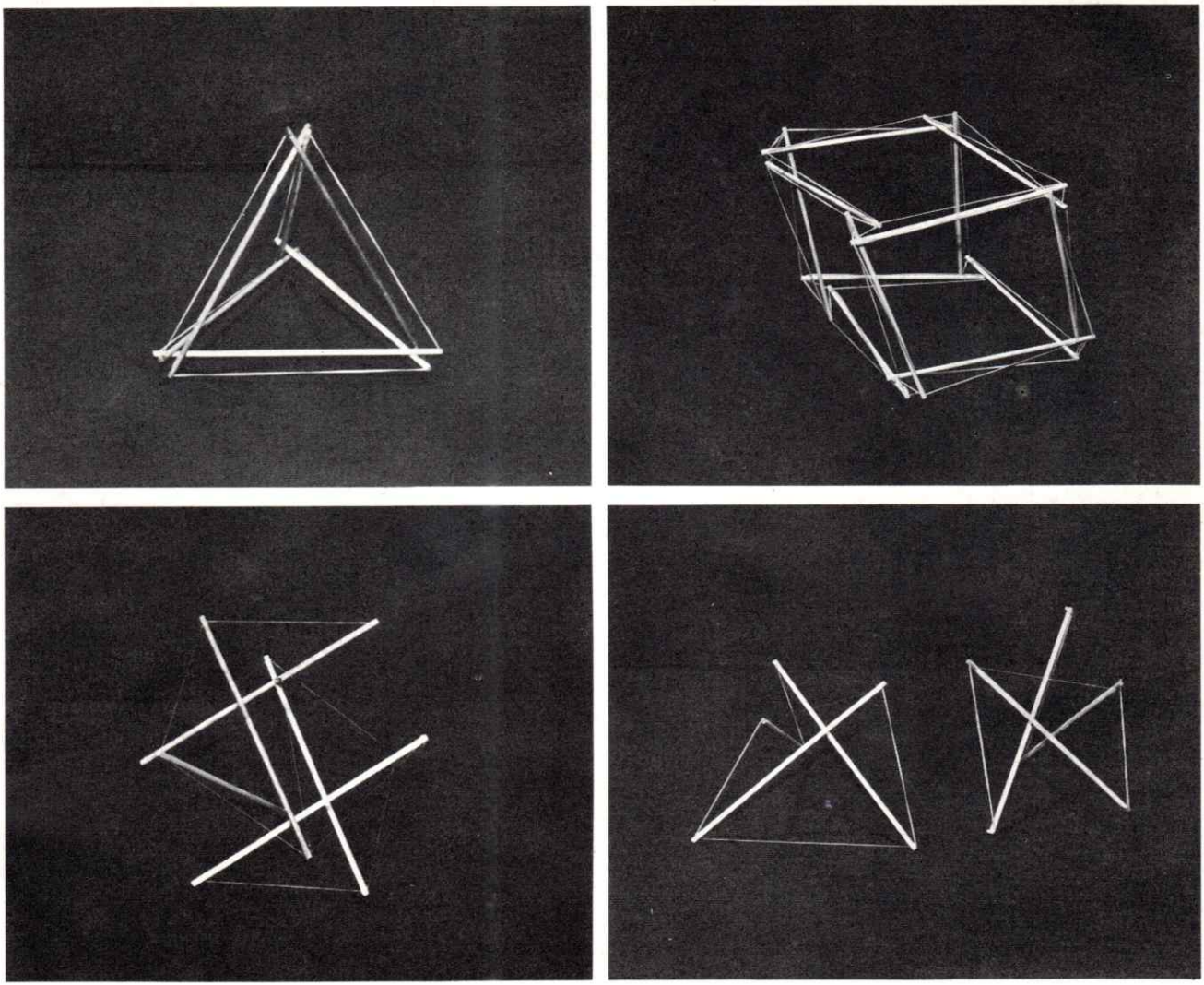

Fig. No. 50 Basic tensegrity polyhedra, discontinuous compression-continuous tension. Row 1 Tetrahedron, Cube. Row 2 Icosahedron. (If any two parallel struts are translated along an axis normal to each, the remaining struts simultaneously react the same, equal in relative direction and magnitude), Octahedron.

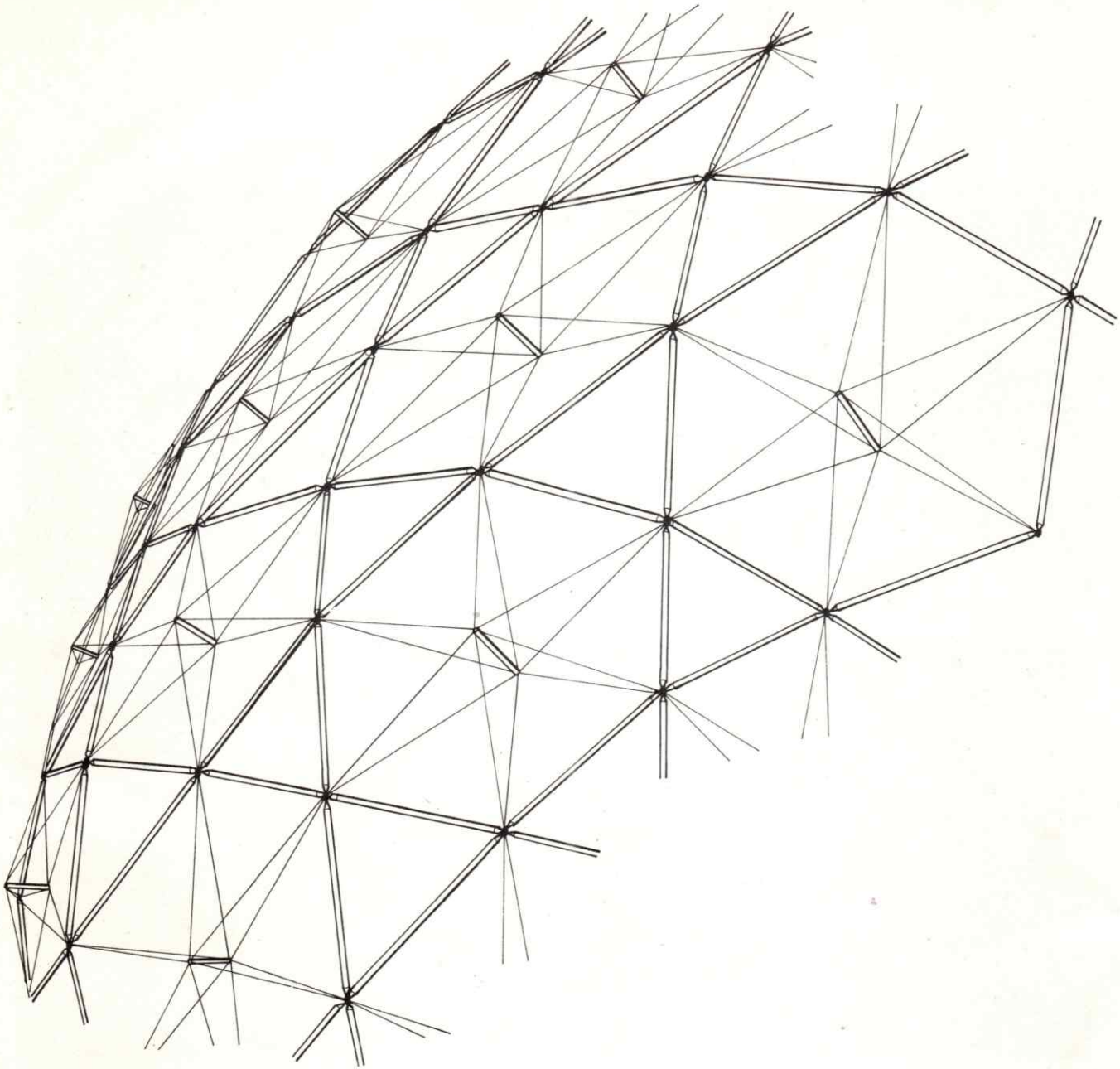

Fig. No. 51 Partial elevation of triangular - hexagonal breakdown. Unstable hexagonal pattern receive triangulated tensegrity sub assembly. Space rather than planar triangulation prevents any translation or racking tendencies the hexagon may have.

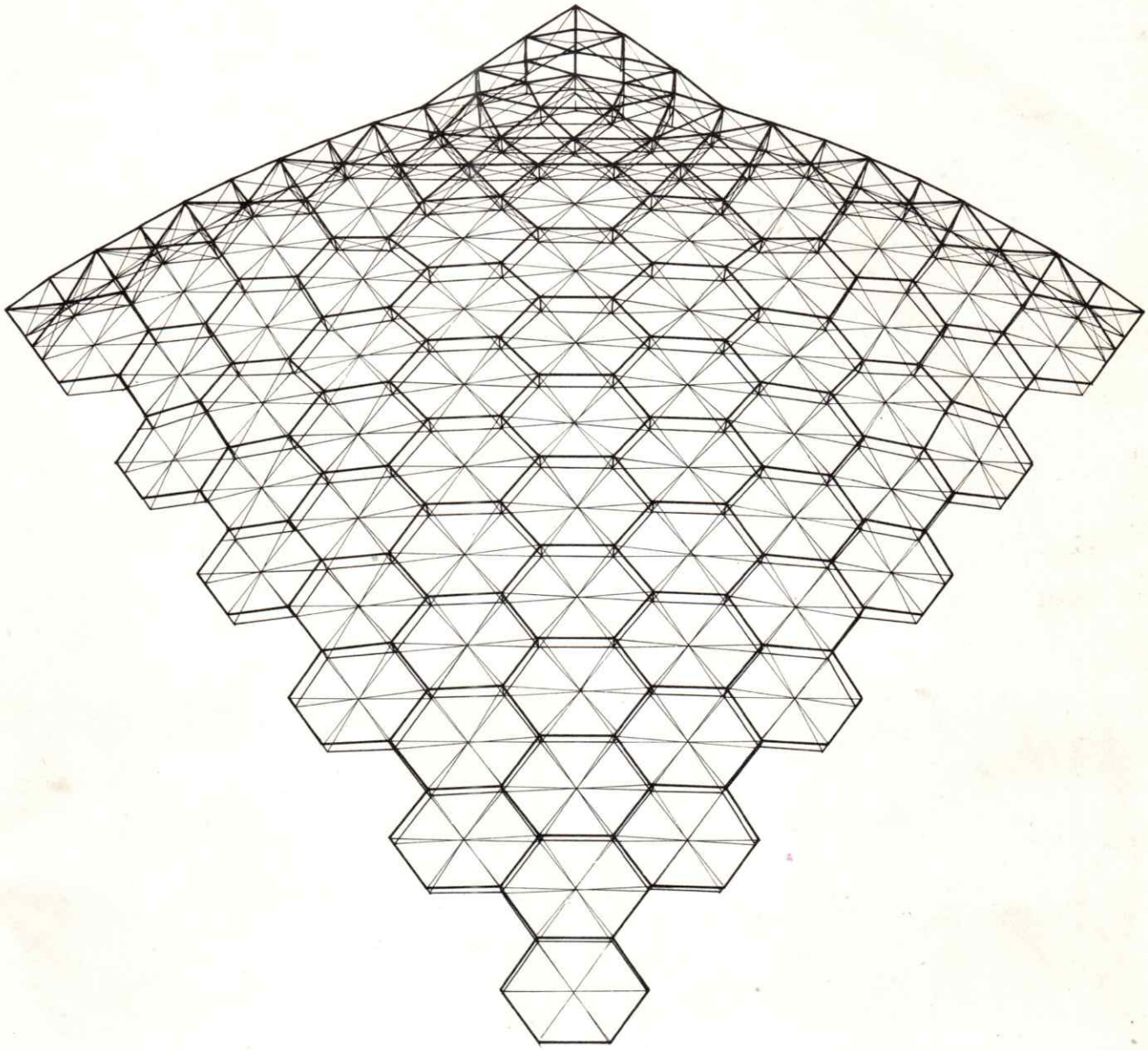

Fig. No. 52 Partial plan of 24^{V} Triacon, hex-pent dome. Double layer hexagonal grid receives stabilization from inner tension assemblies. When two adjacent hexagonal grids are analyzed, the sub assemblies form octahedrons. Assemblies sometimes called wire-wheel truss.

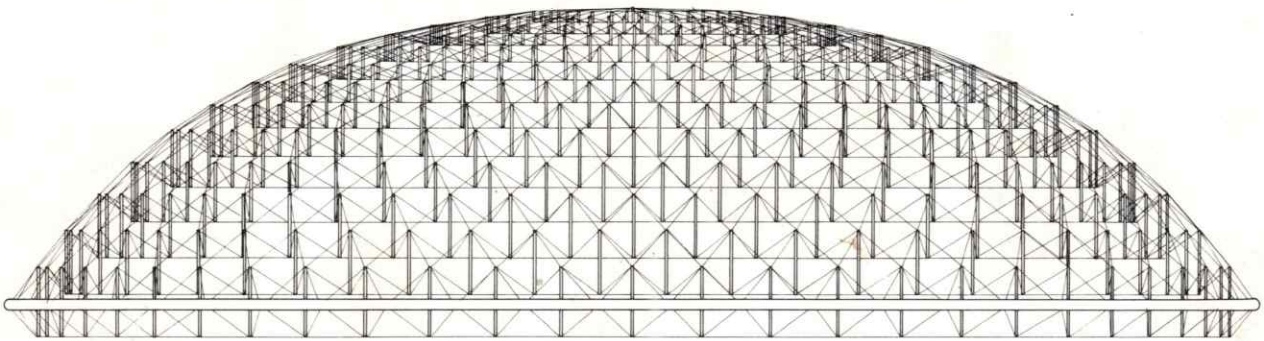

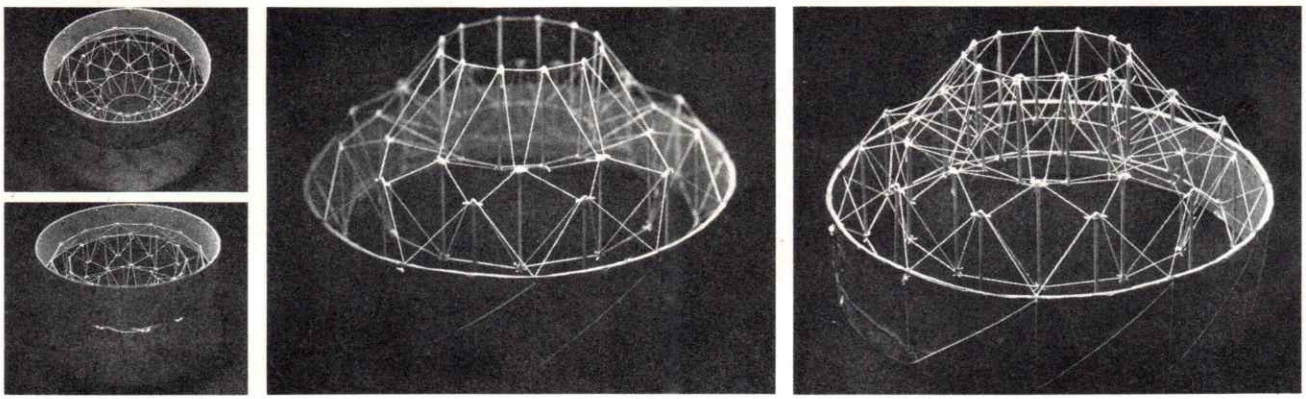

Fig. No. 53 Elevation and erection sequence for 200' diameter tensegrity dome. Although the breakdown is bi-polar or lesser circle the framing technique is applicable in icosahedral forms.

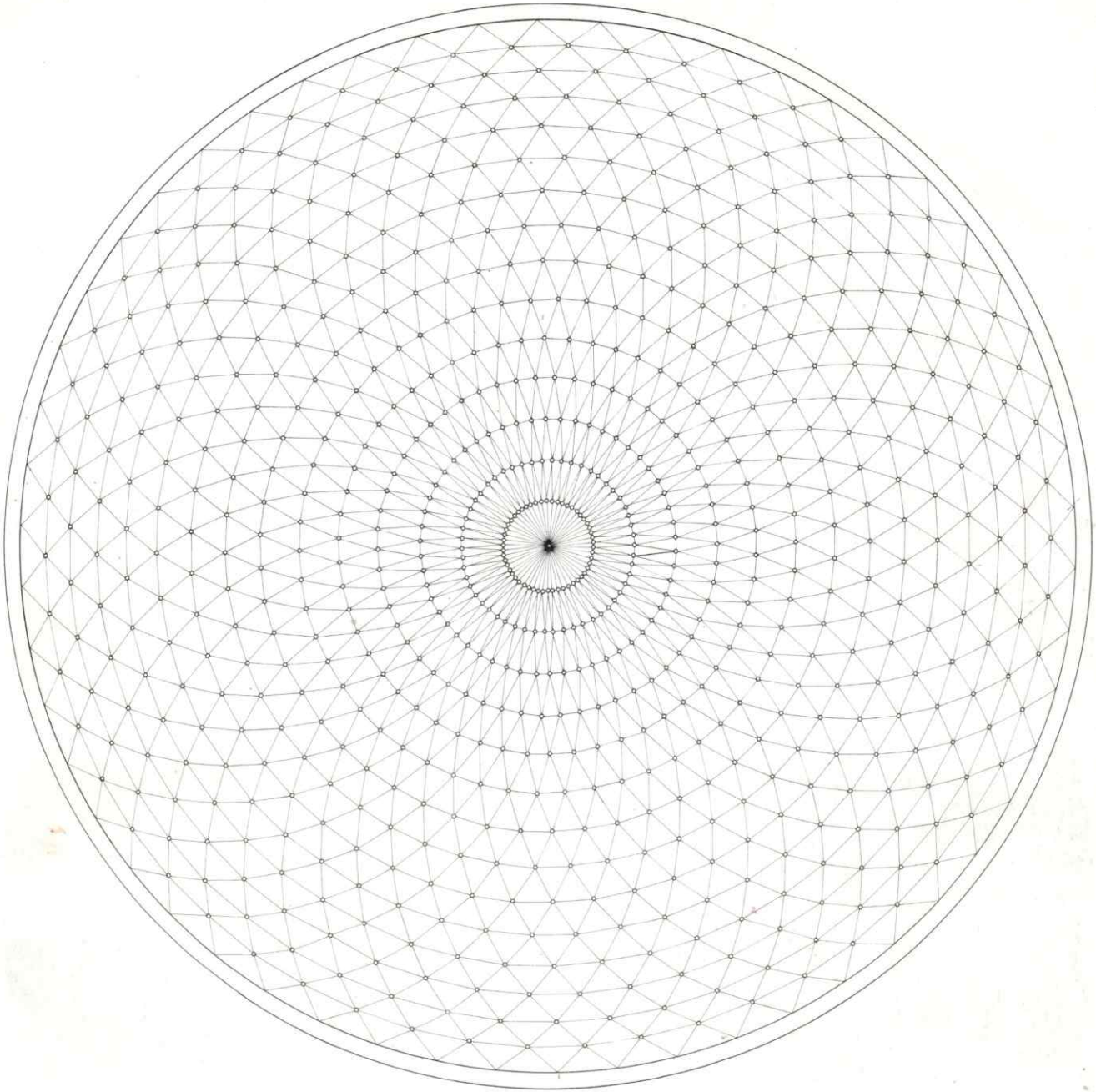

Fig. No. 54 Plan, base ring provides compressive restraint. Rapid accumulation of tensile strees from zenith to equator restrict large diameter use.

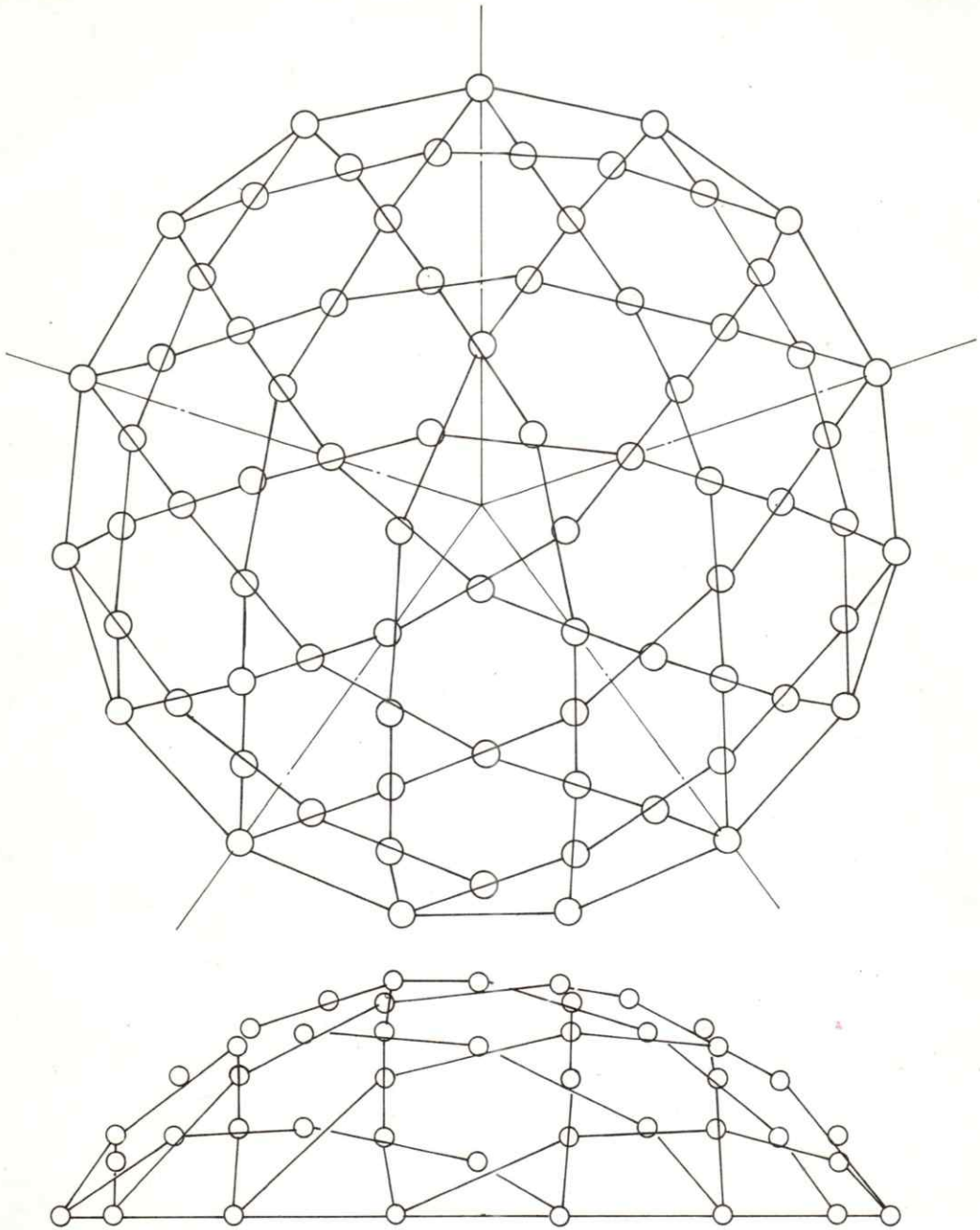

Fig. No. 55 Plan and elevation of 6^V Alternate dome. Diagramtic presentation of strut and connector sequence similar model in Fig. 56.

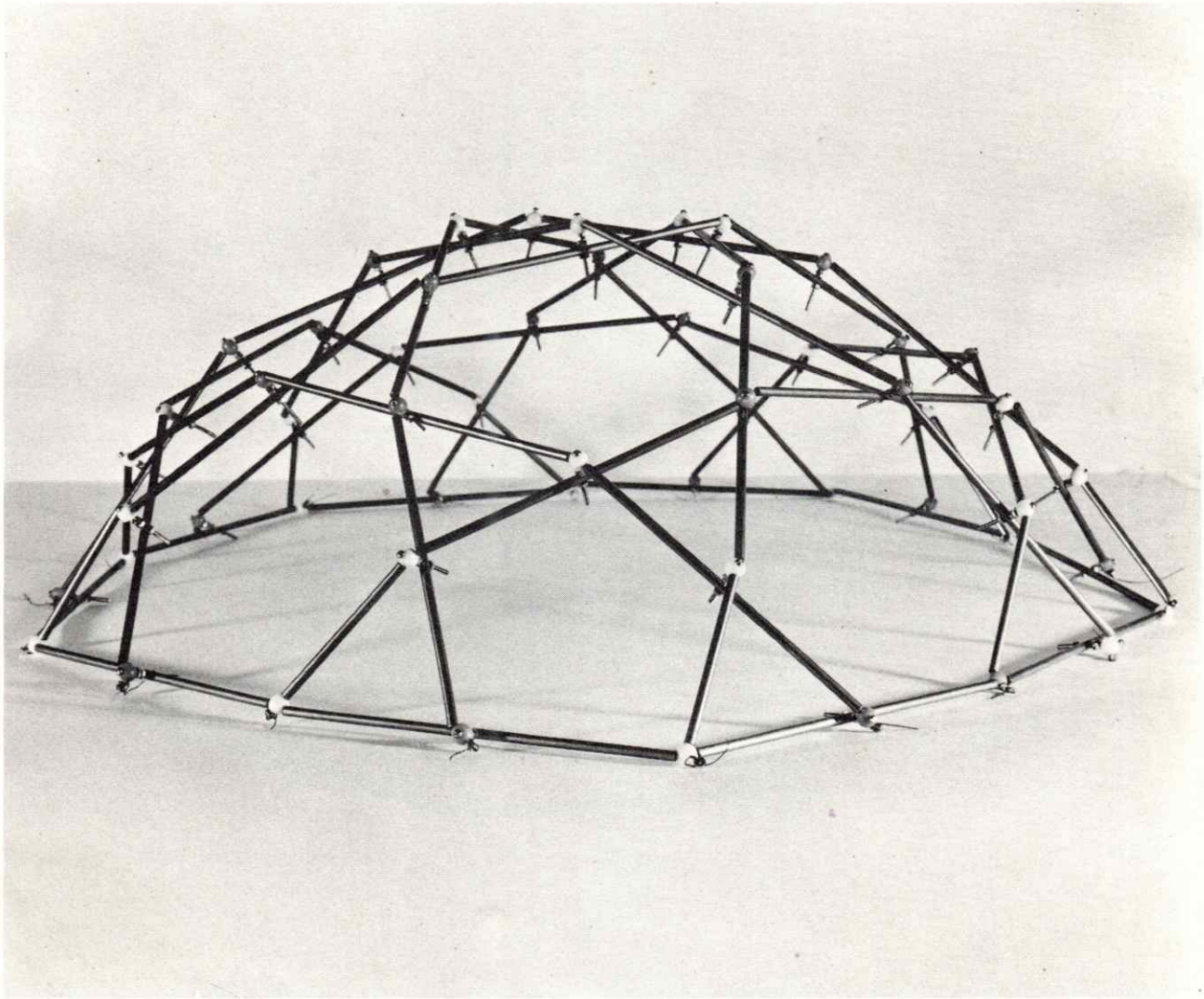

Fig. No. 56 Framing study of 4^V Alternate dome. Hex-pent stability achieved by contineous strut overlaping. However, stable each axialy loaded strut receives induced bending load at mid point reducing greatly over all efficiency. Project by Taisei Construction, Japan.

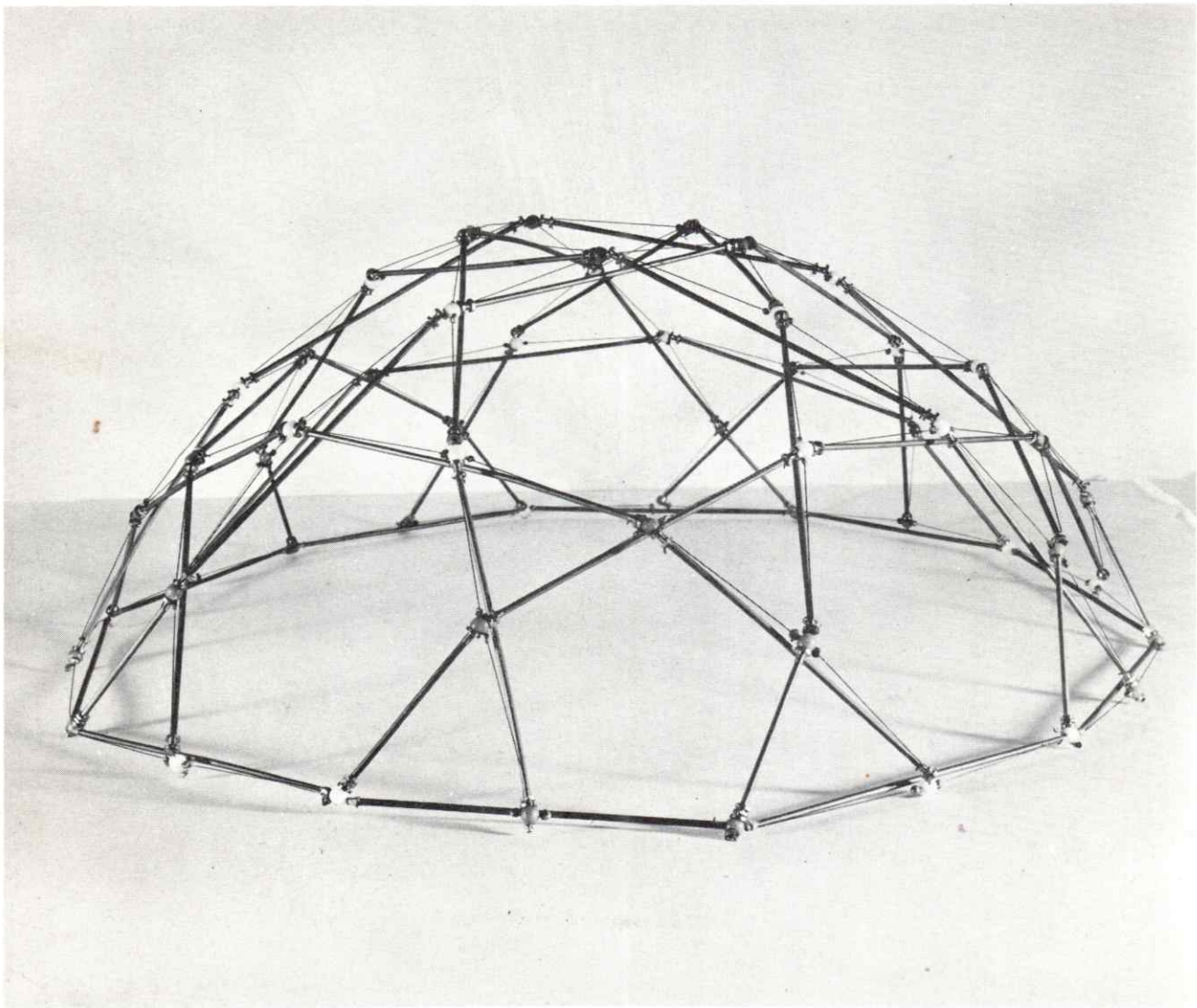

Fig. No. 57 4^V Alternate breakdown. Similar to Fig. 56 in geometry, tension wire eliminates induced bending problem, continuous struts again stabilize hex-pent assemblies. Project by Taisei Construction, Japan.

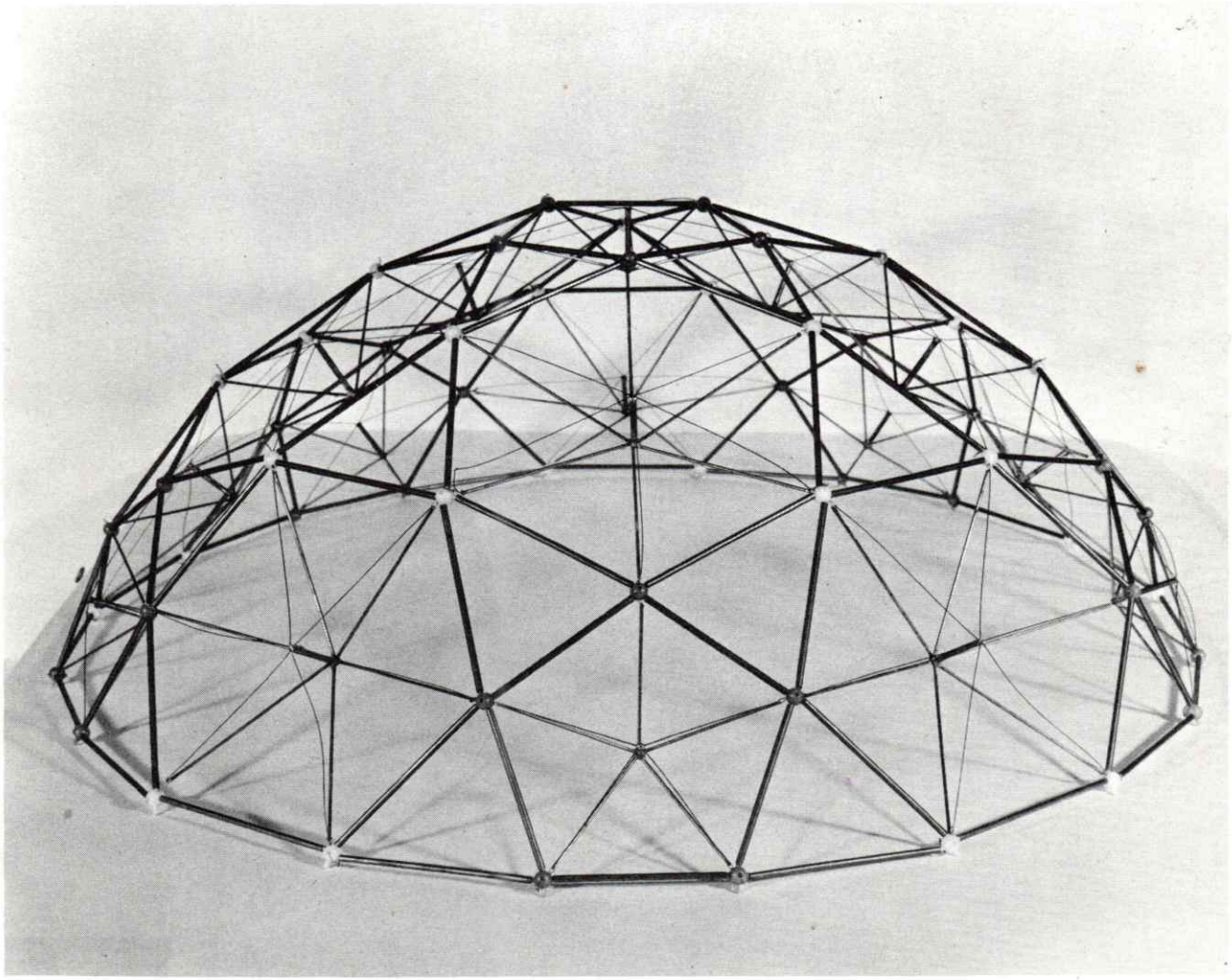

Fig. No. 58 Maintaining previous Figs. 56 and 57 geometry, triangulated sub assemblies now stabilize hex-pent areas. All strut connections are pinned and non continuous. Project by Taisei, Japan.

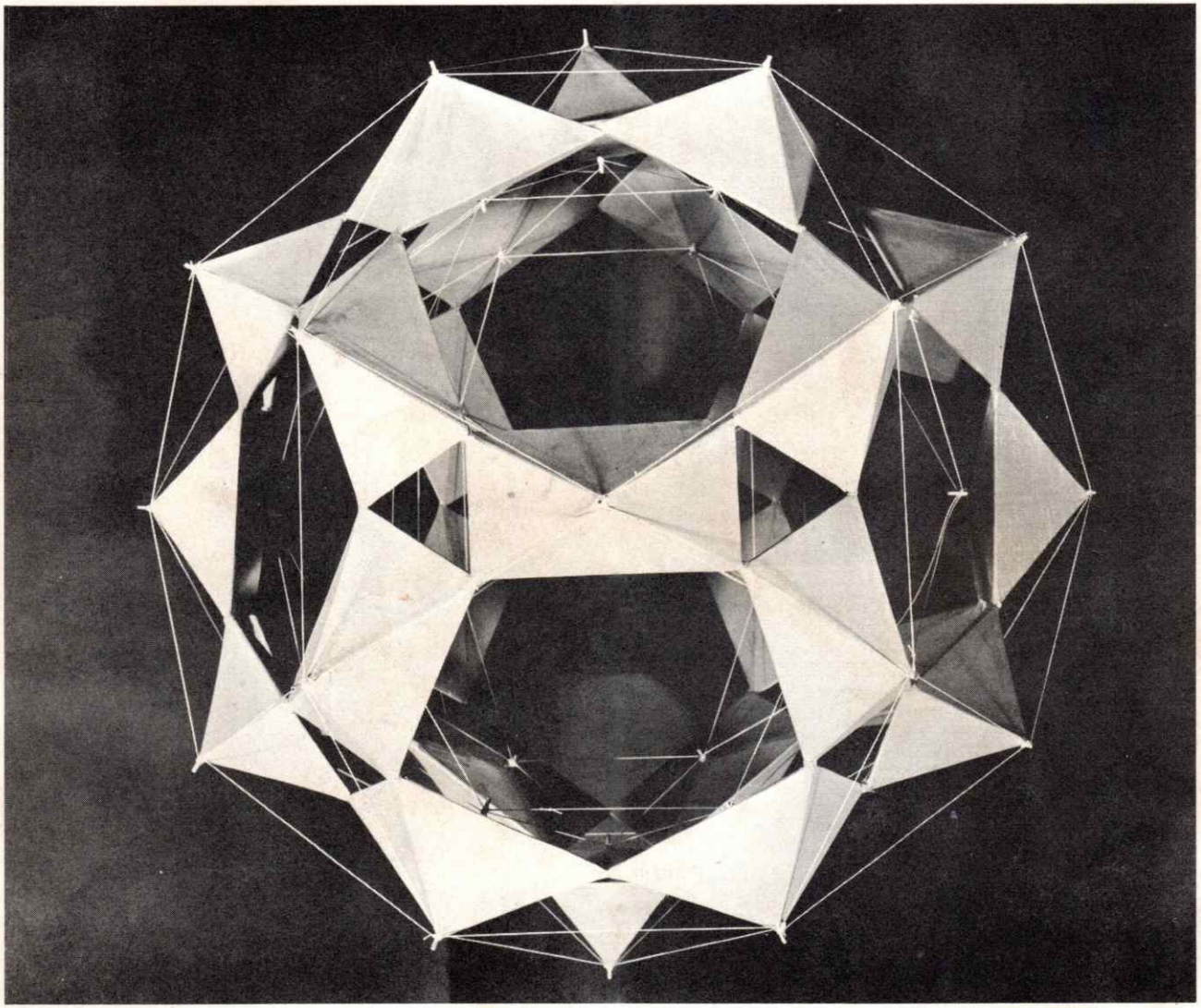

Fig. No. 59 Double grid, 2^V Alternate (edge zenith) post tensioned stress skin dome. Note that both interior and exterior wire grids form the edge geometry of the icosadodecahedron polyhedra (Fig. 1). Inner wire grid tends to pull pyramidal forms inward by way of apex strut. Outer wire grid restrains pyramidal translation. Project by Taisei, Japan.

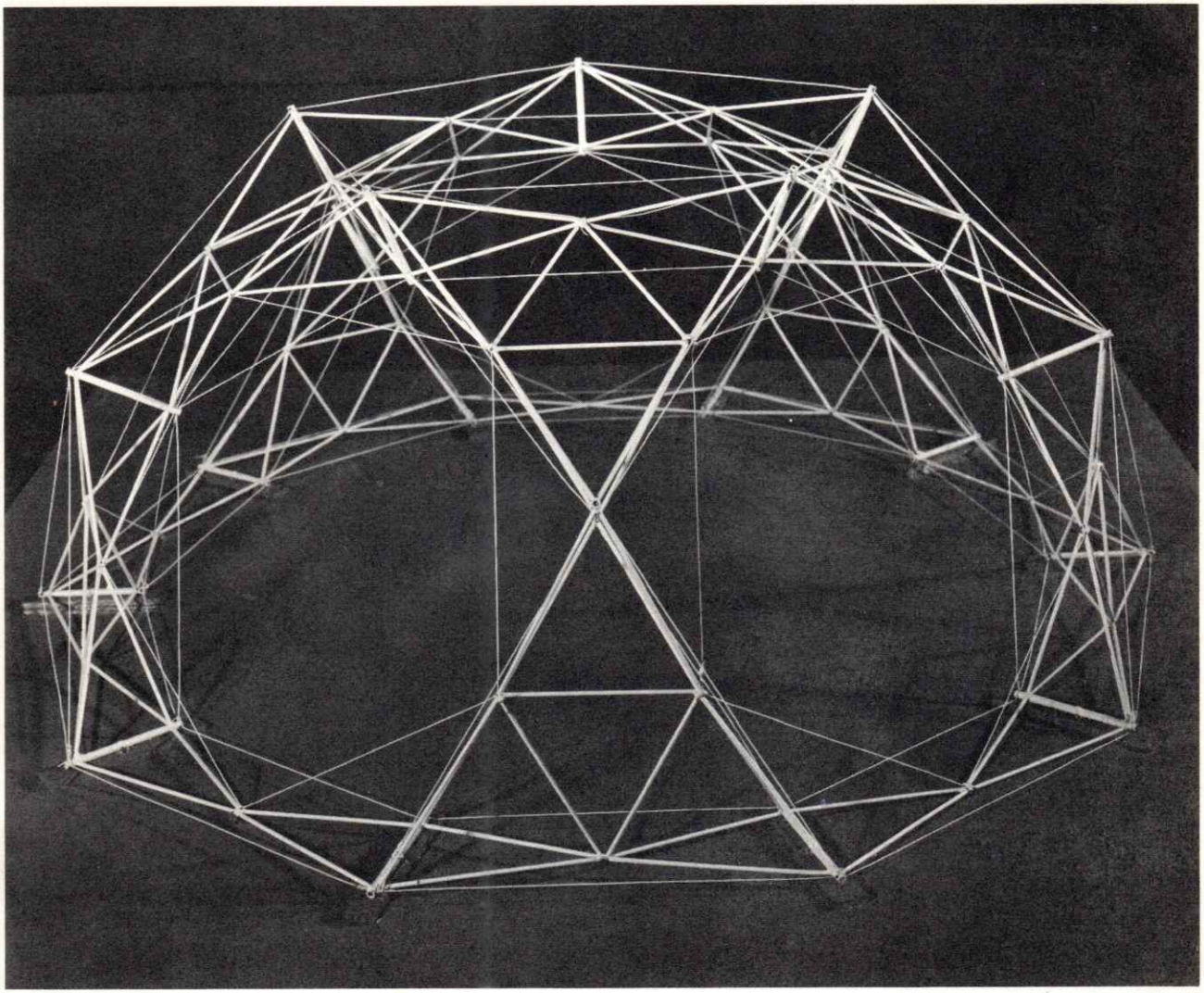

Fig. No. 60 Alternate framings for Fig. 59. Pyramidal form has been replaced by strut assembly. Geometry same as Fig. 59. Project by Taisei, Japan.

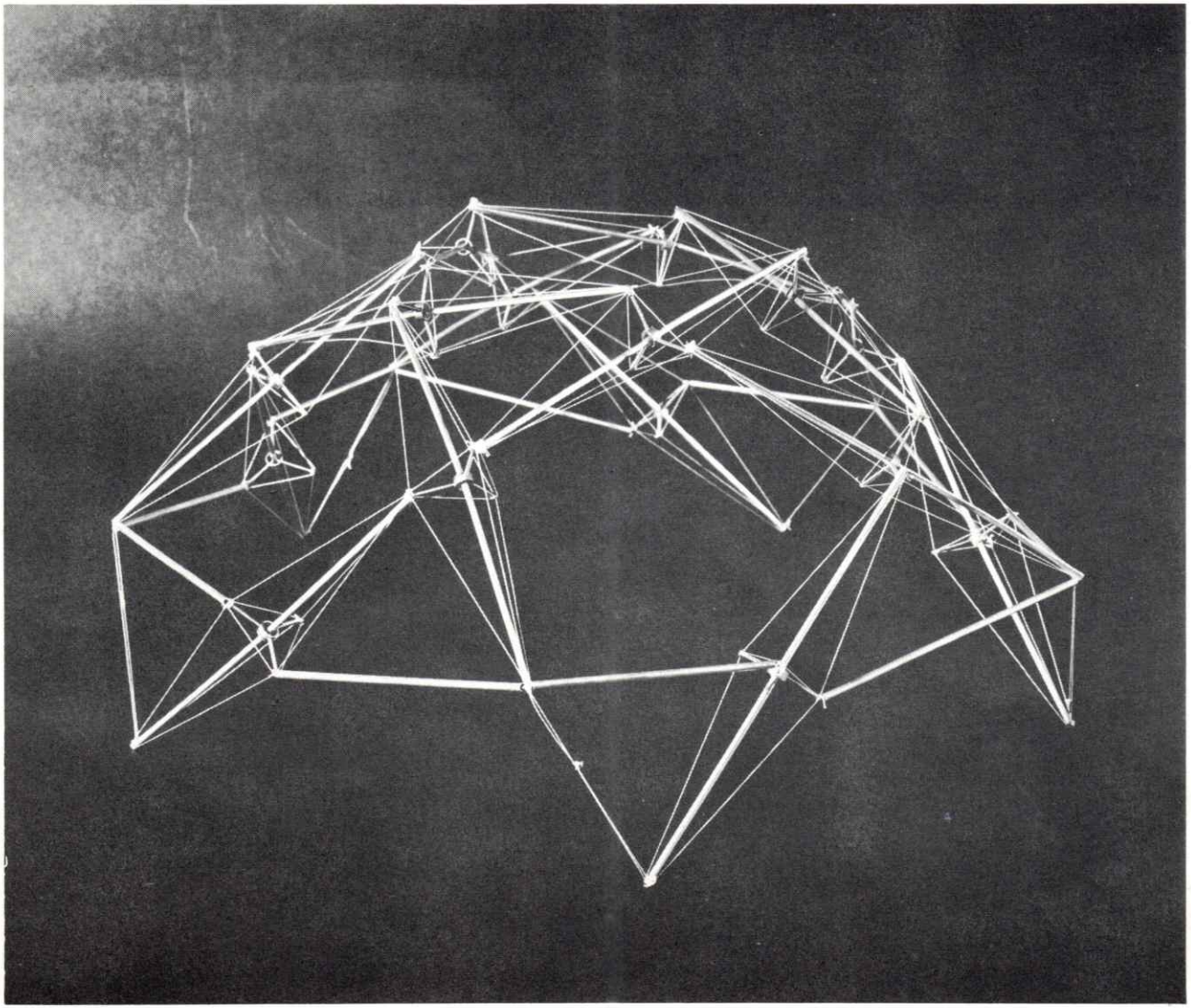

Fig. No. 61 Post tensioned 2^V Alternate, vertex zenith dome. A guy and mid strut star assembly transmit compression from two impenging struts through a tensile force triangle. Same assembly guyed to strut ends provides bracing, regaining column efficiency lost to excessive length in continuous hex-pent bracing. Project by Taisei, Japan.

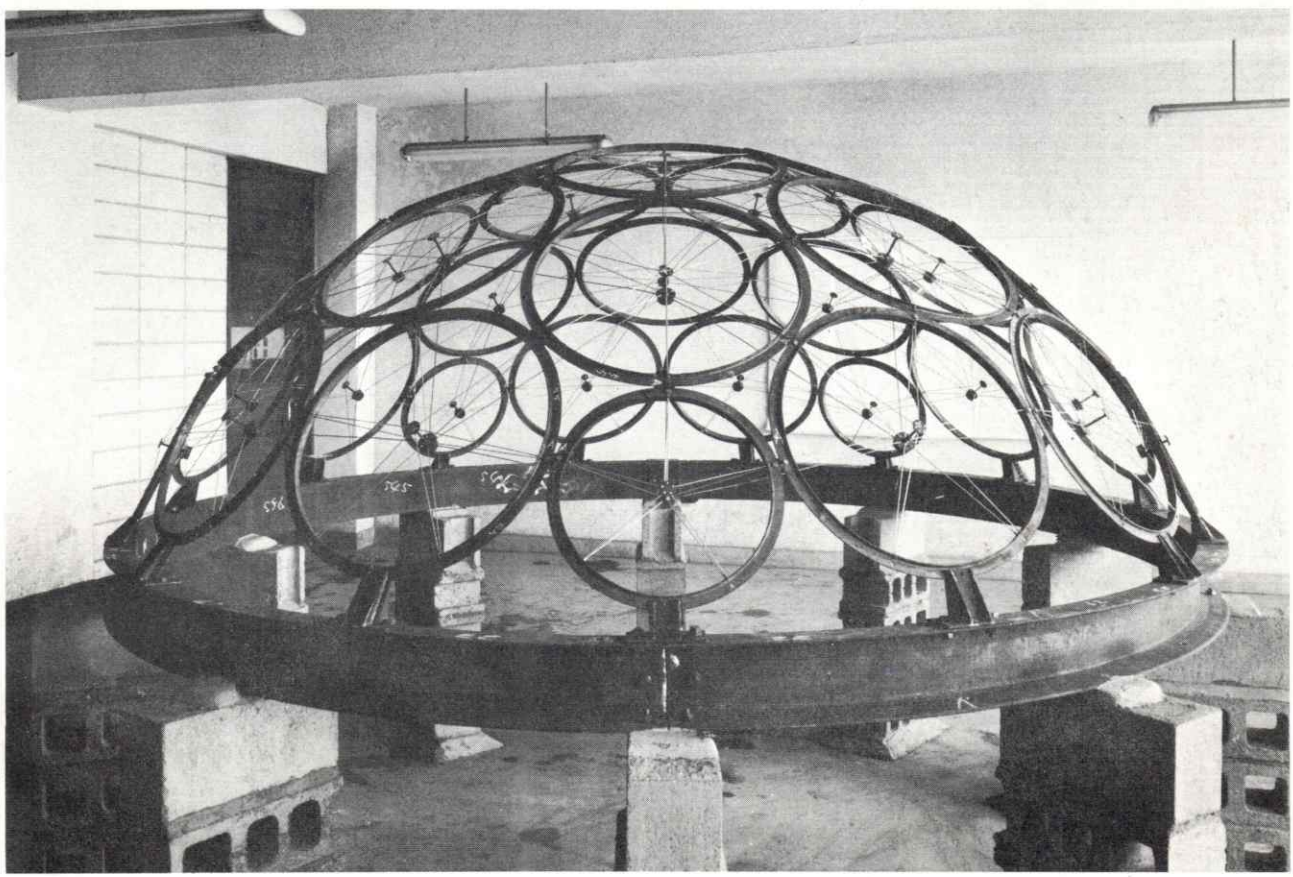

Fig. No. 62 6^V Alternate, vertex zenith, "bicycle wheel" dome. Frequency determined from wheel tangent points and post tentioning sub assemblies. Efficiency greatly reduced for circular wheel rims do not act well as columns between points of tangency, arc induces bending moments. Project by Taisei, Japan.

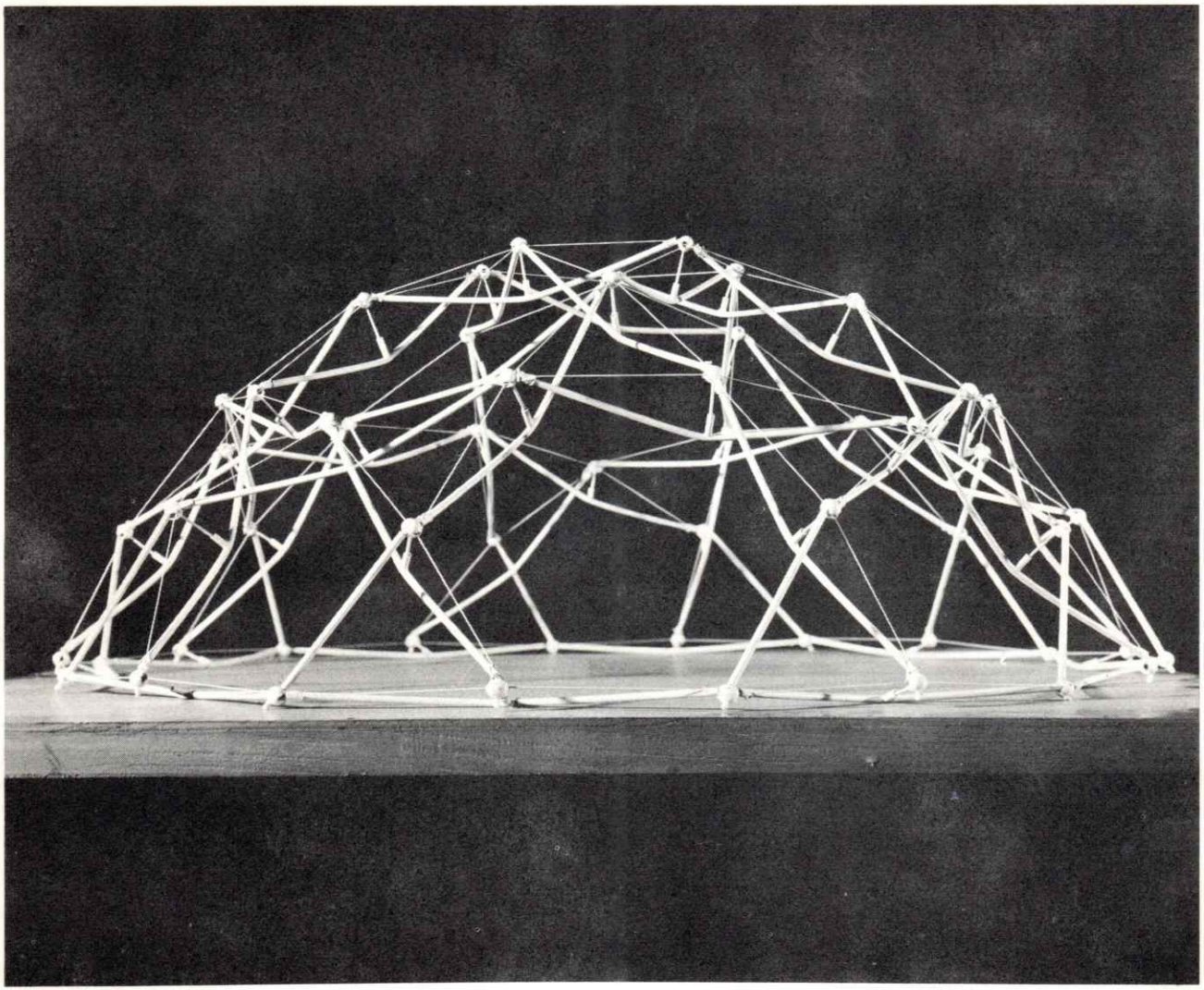

Fig. No. 63 4^{V} Alternate post tensioned dome. Framing diagram similar to 6^{V} Fig. 65. Post tensioned bow units rely on bending resistance of strut to supply ragidity enough for support. Continuous strut bows again stabilize hex-pent assemblies.

Fig. No. 64 Load test of Fig. 63.

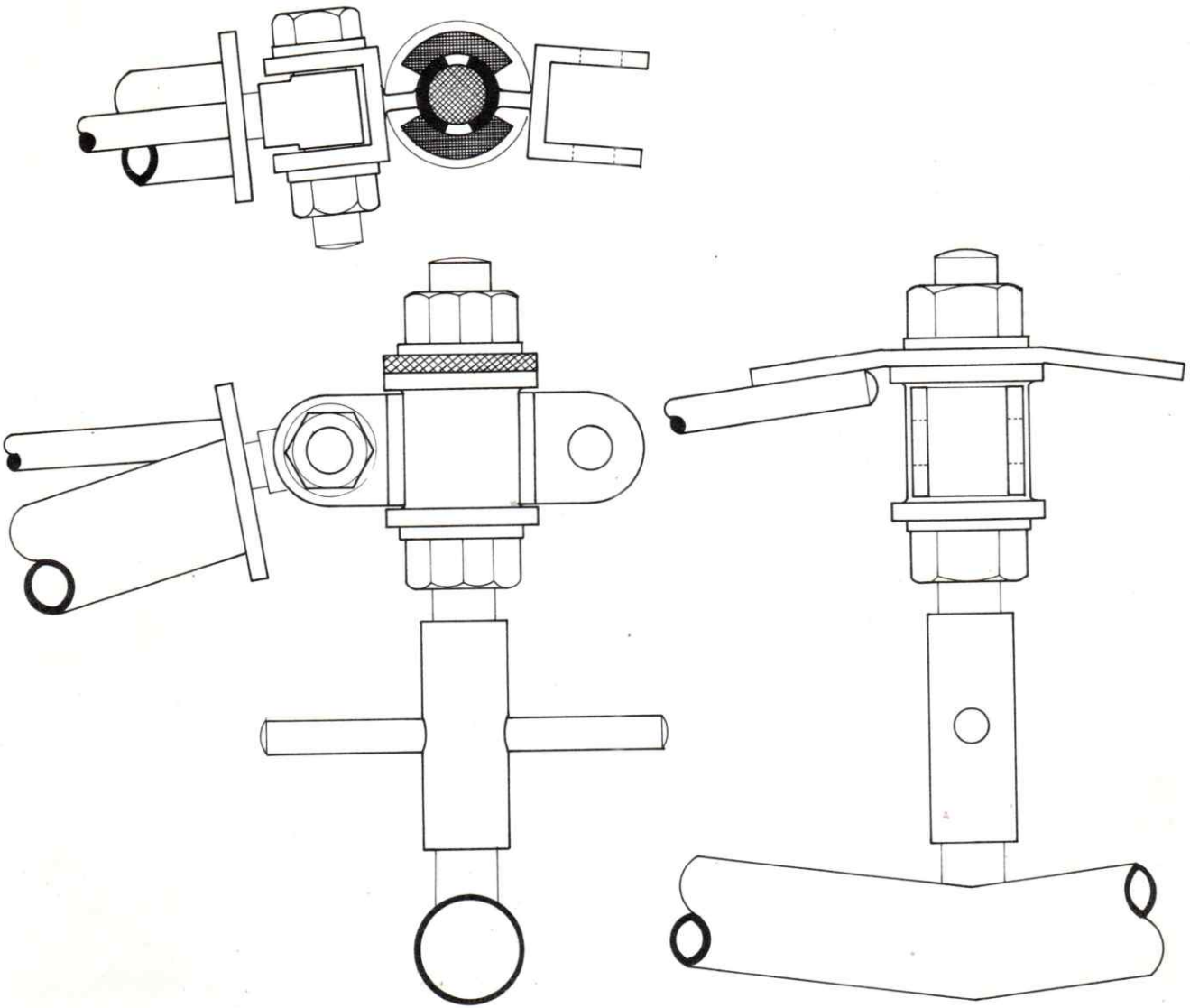

Fig. No. 65 Typical universal pivit joint used throughout test Fig. 64.

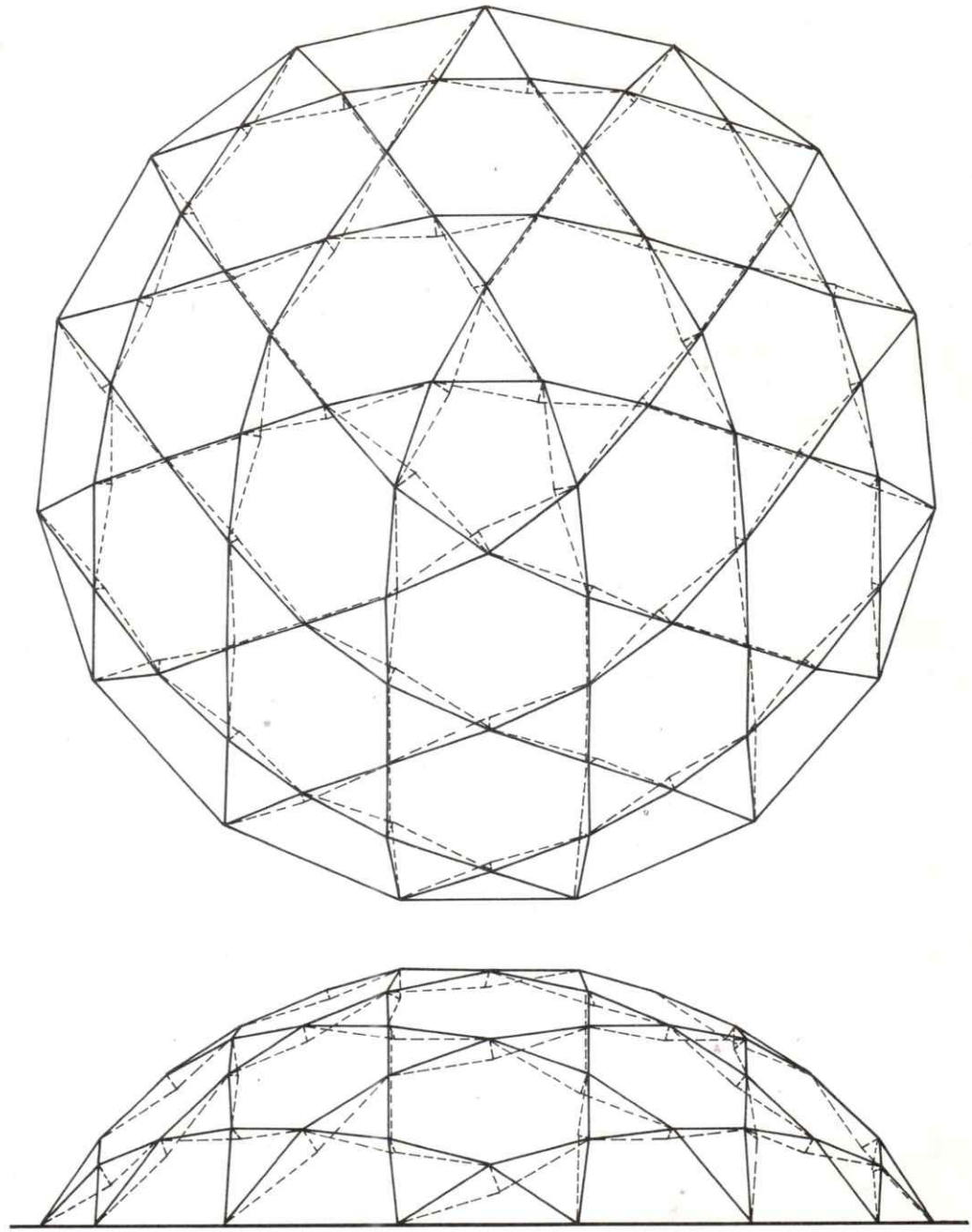

Fig. No. 66 Plan and elevation of 6^V Alternate dome similar to Fig. 63 and 64. Dotted members compression solid are tensile.

Fig. No. 67 Thirty-six foot diameter University of Minnesota dome erected at Aspen, Colorado, 1953. Rhombic triacontahedron diamonds are subdivided by 8^V Alternate truss and wire assemblies. Erection time one hour and a half.

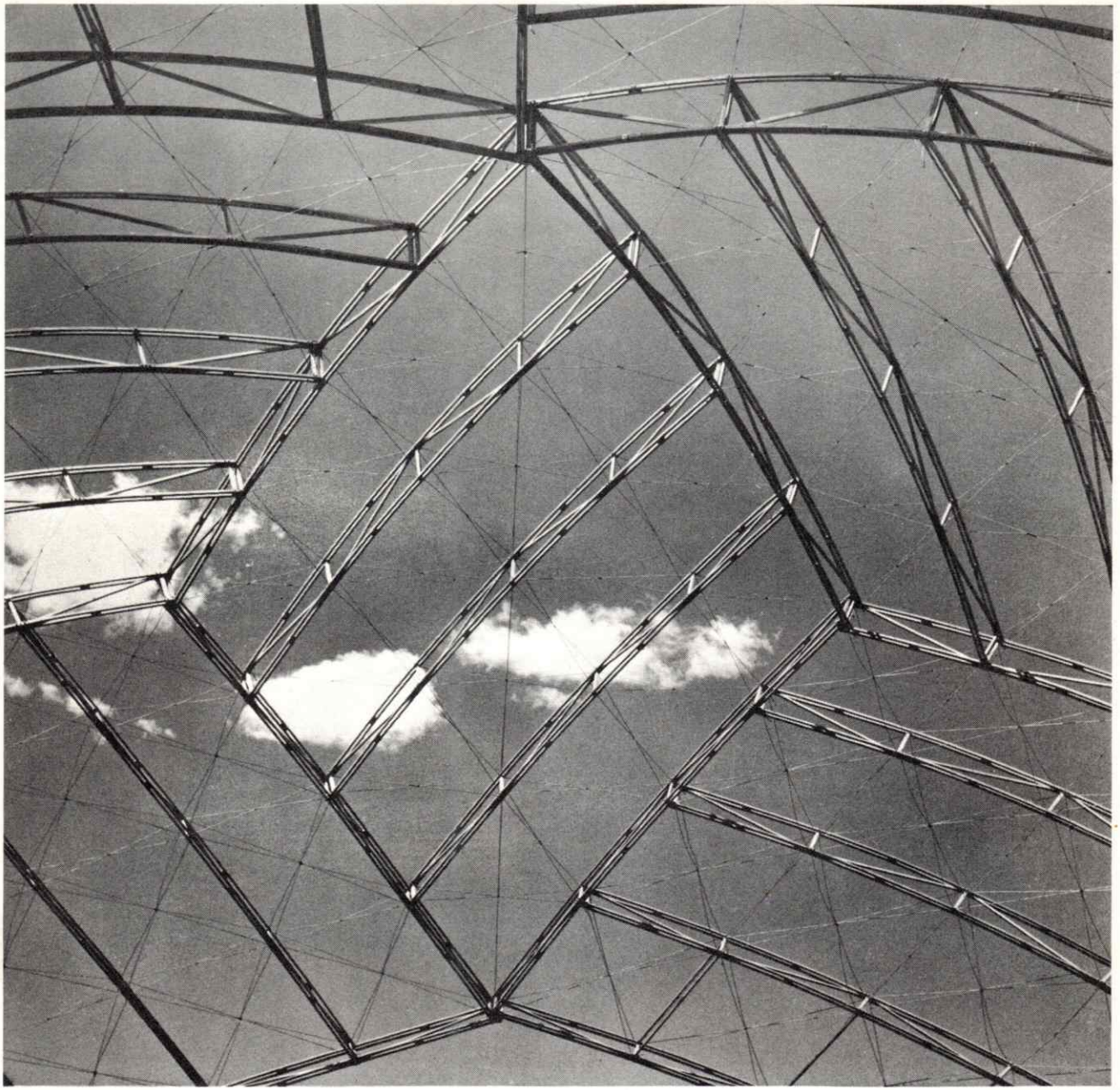

Fig. No. 68 Reflected ceiling view. Diamonds long axis is icosa edge. Rapid assembly achieved by pinning "raft" trusses to rhombic triacontahedral edges. By removing pins "rafts" and sub wires, while remaining attached, collapse accordian like.

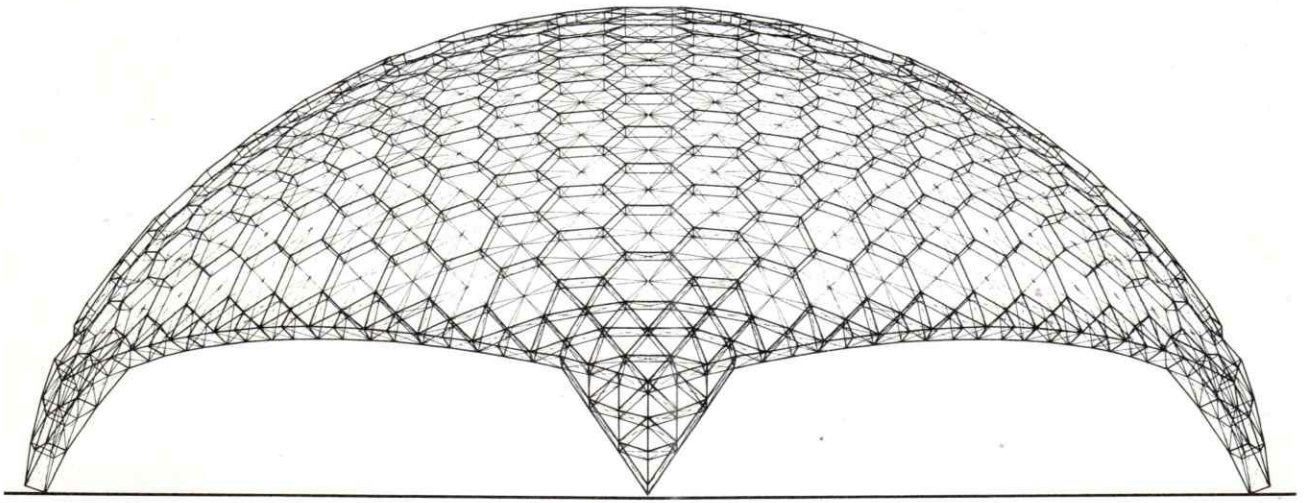

Fig. No. 69 Elevation of American Society for Metals dome, Cleveland, Ohio. Two hundred seventy-seven diameter 102' height, weight/square foot/dome surface 3.2#/square foot. Weight/dome less base truss and pylons - 1.1#/square foot. Project by Synergetics Incorporated.

Fig. No. 70 Plan 24^{V} Triacon hex-pent. Double grid receives stabilization through sub guy assemblies, see Fig. 52. Pents located at zenith and in the middle of each support leg.

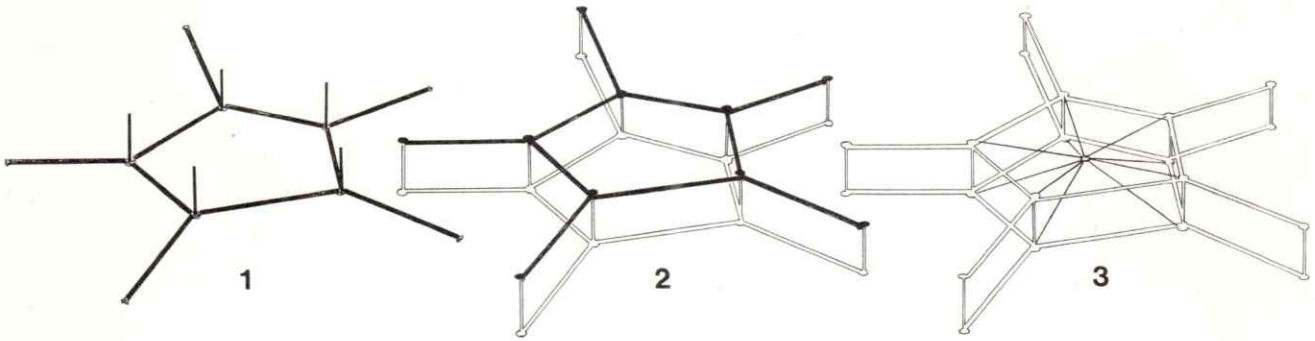

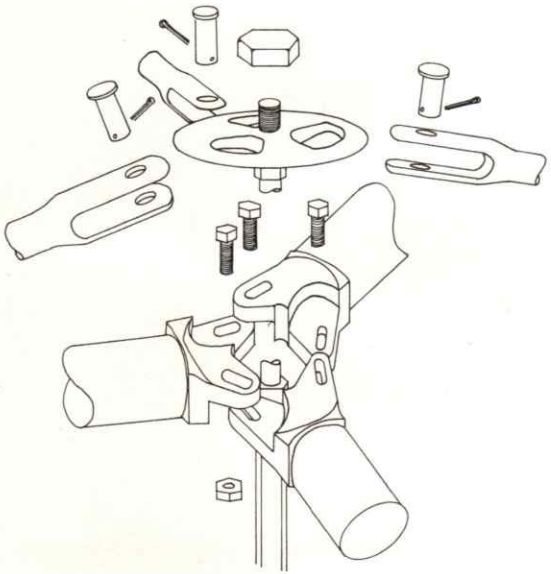

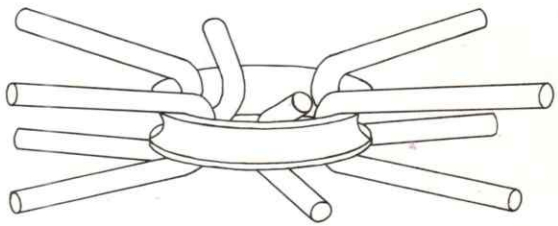

Fig. No. 71 Top: Erection sequence for double grid assemblies. See Fig. 101 for site erection. Bottom: Typical connector. Strut ends receive castings that allow for slight variations in surface angles. Vertex wheel casting joins "hair pin" sub assemblies. Adjustments forces any two wheels located on the same inter grid strut closer or further apart thereby regulating post tensioning of "hair pins." "Hair pins" loop about a mid-hex ring. All members and fasteners - aluminum.

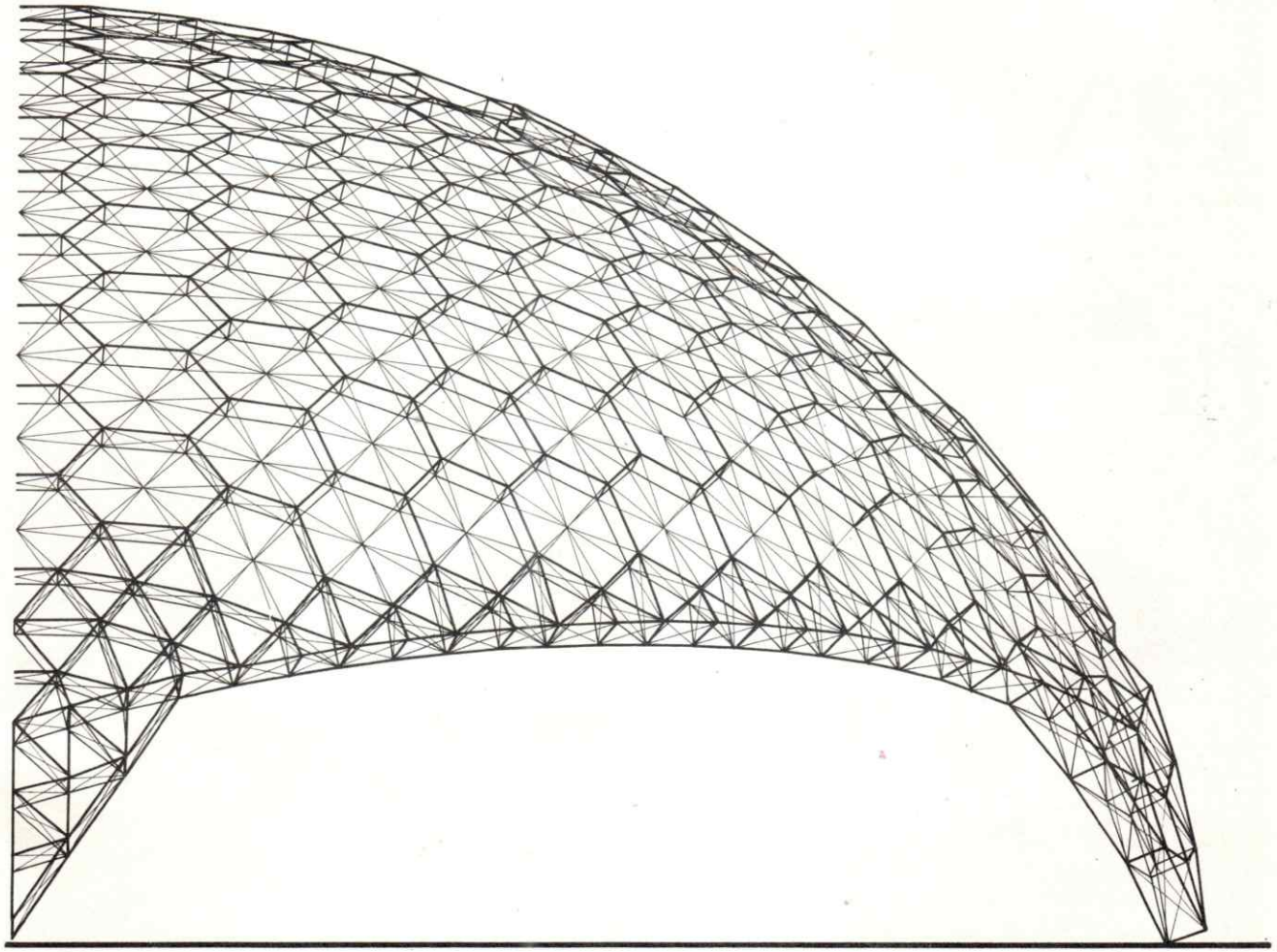

Fig. No. 72 Edge beam of ASM dome. Truss aids in transferring surface stresses to supports, surface truss 30" deep support truss 60' deep.

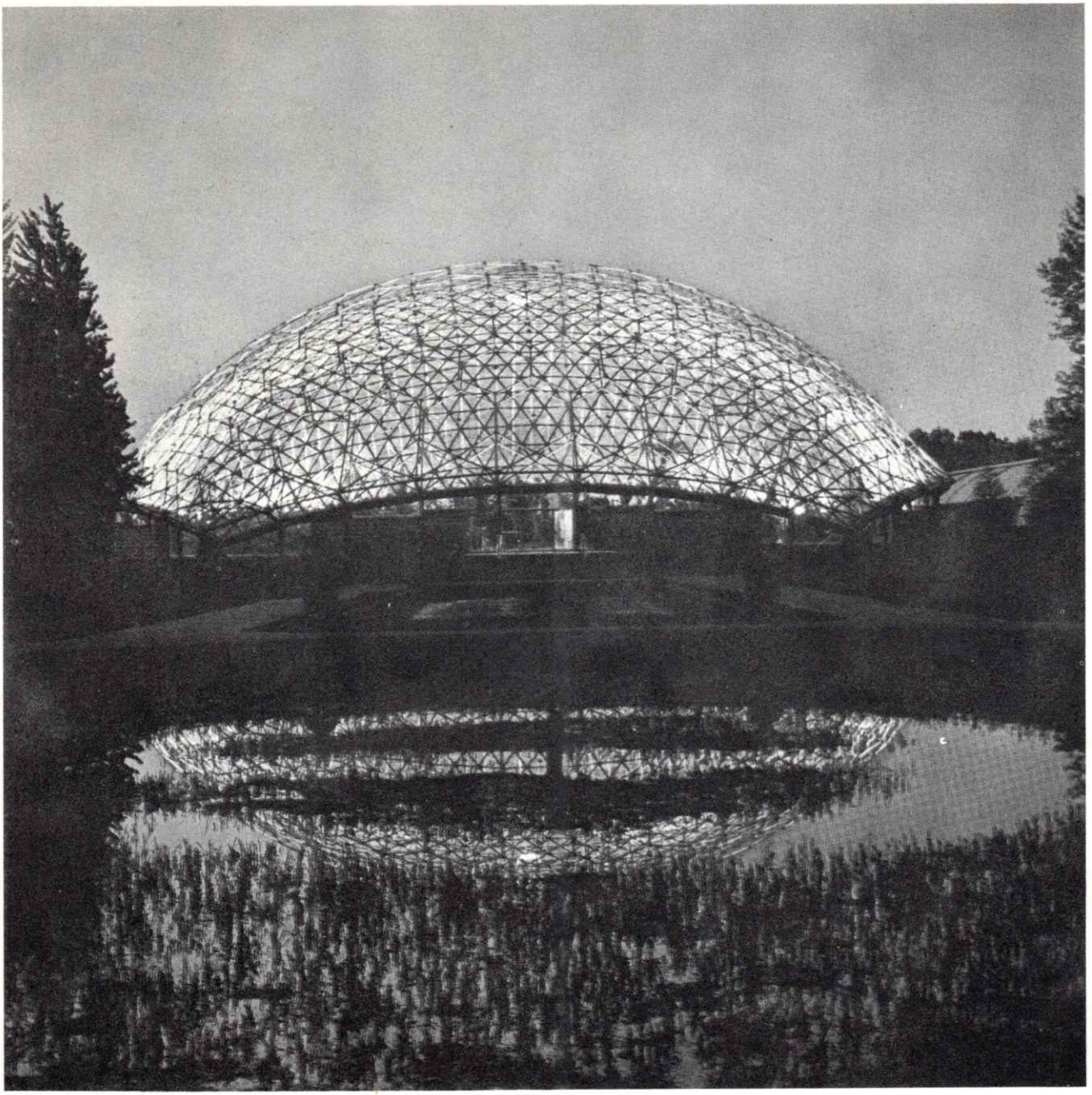

Fig. No. 73 Climatron at the Missouri Botanical Gardens in St. Louis, 175' diameter dome. Similar breakdown and frequency as ASM dome.

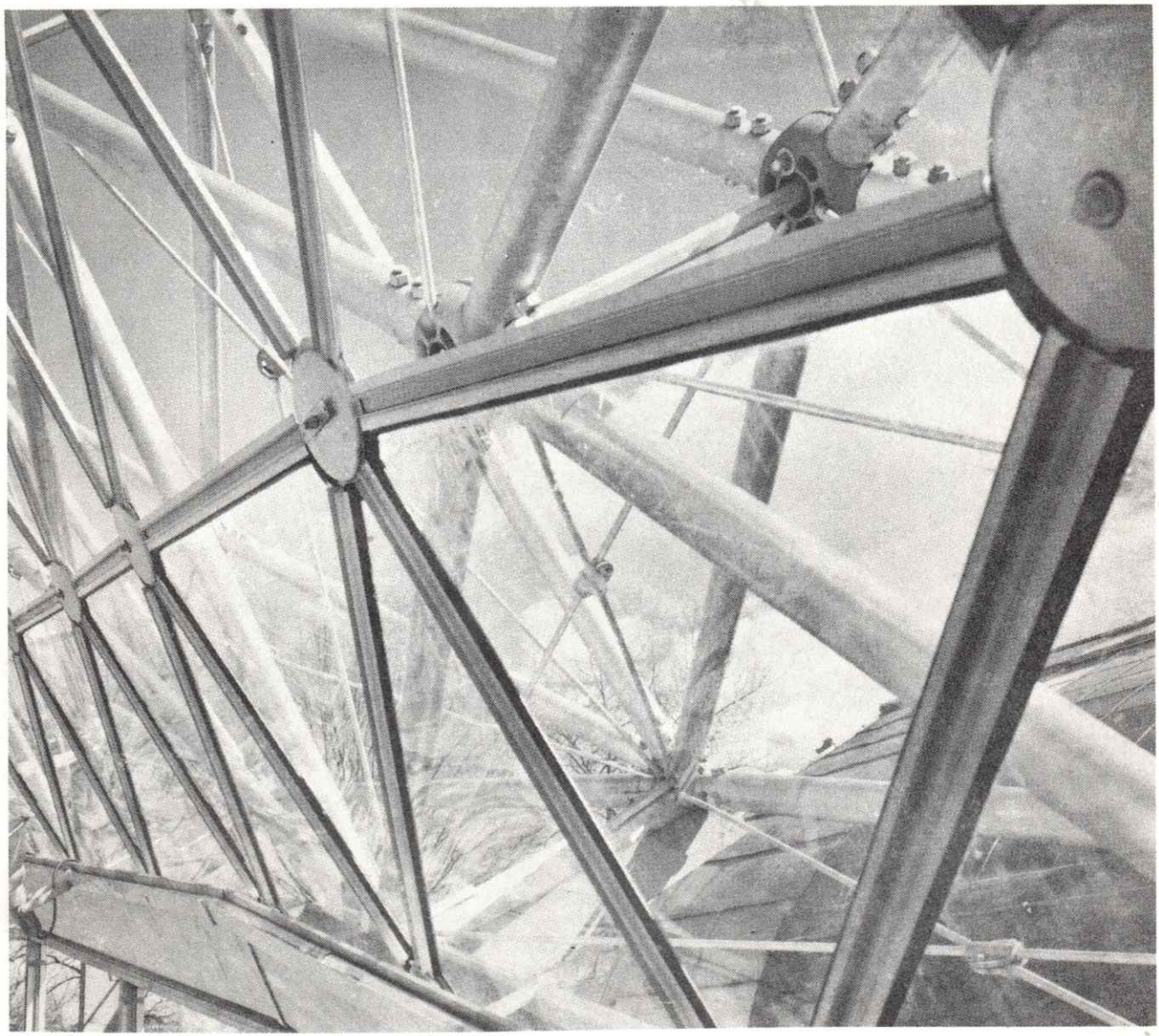

Fig. No. 74 Interior view of Acrylic enclosure. Triangulated mullions receive support intermitently from hex truss work.

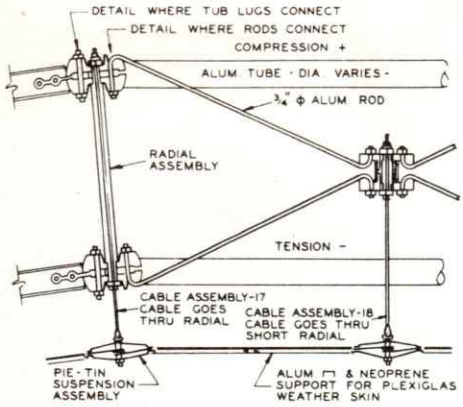

SECTION THRU TYPICAL SUSPENSION ASSEMBLY

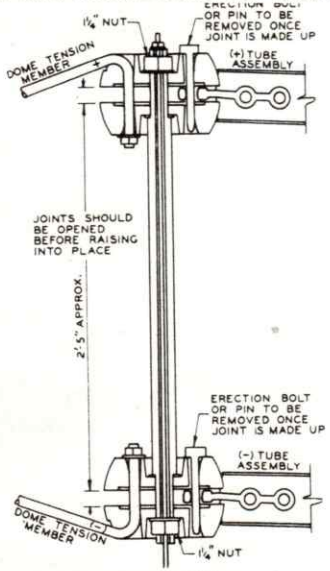

SECTION THRU HALF
OF TYPICAL FRAMING UNIT
TUBE DIAMETERS 3, 4, AND 5 IN.

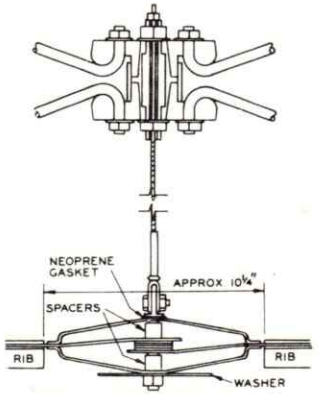

SECTION THRU RADIAL ASSEMBLY
1, 2, OR 3 SHOWING (+) AND (-)
TUBE ASSEMBLIES DURING INSTALLATION

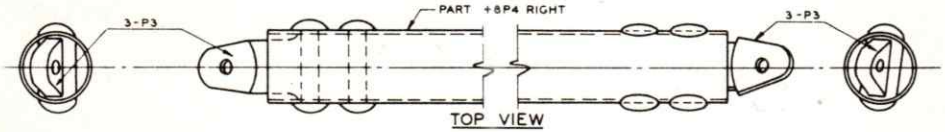

TOP VIEW

TUBE ASSEMBLY +8, RIGHT

Fig. No. 75 Sections of double grid, sub assemblies, and glazing details. Note the degree of refinement inherent in all joinery.

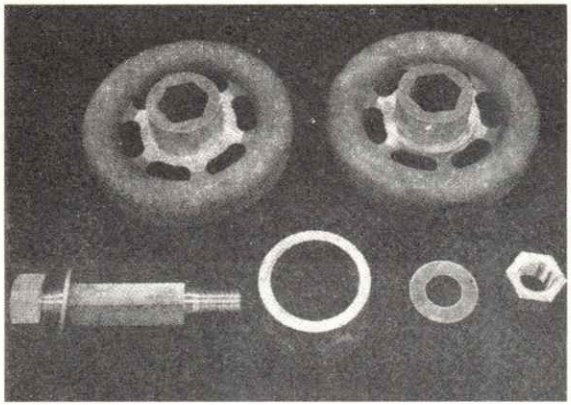

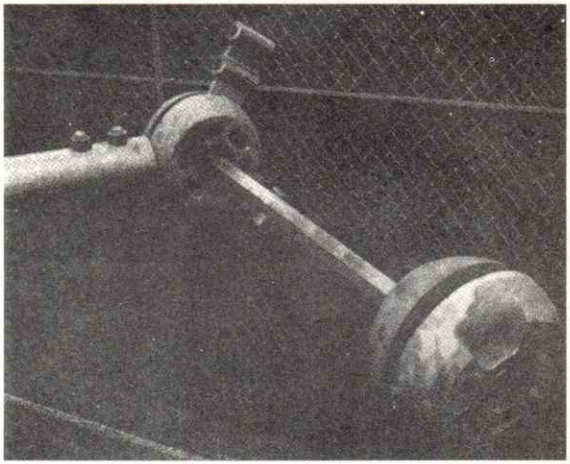

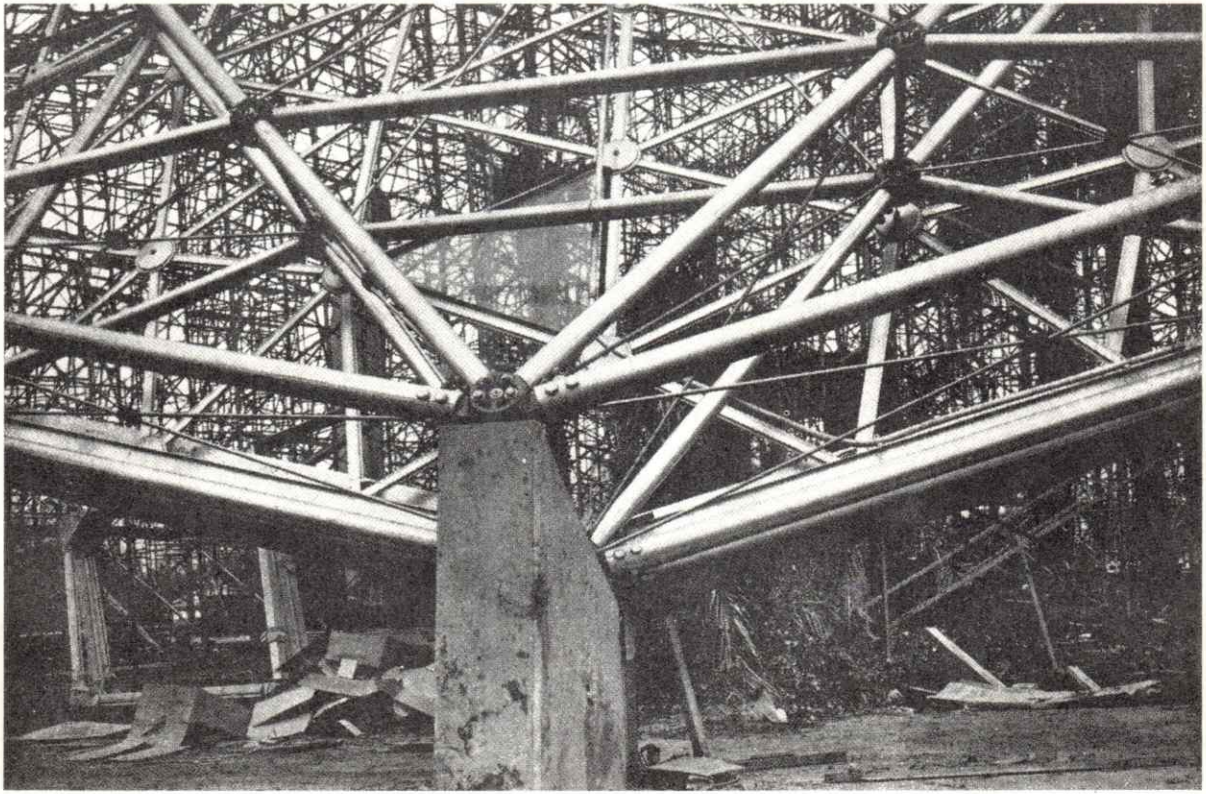

Fig. No. 76 Sub assembly and grid vertex castings. The Climatron is point supported at the five pent points, bents with roller tracks support dome edge in leu of edge beam. Project by Synergetics Incorporated.

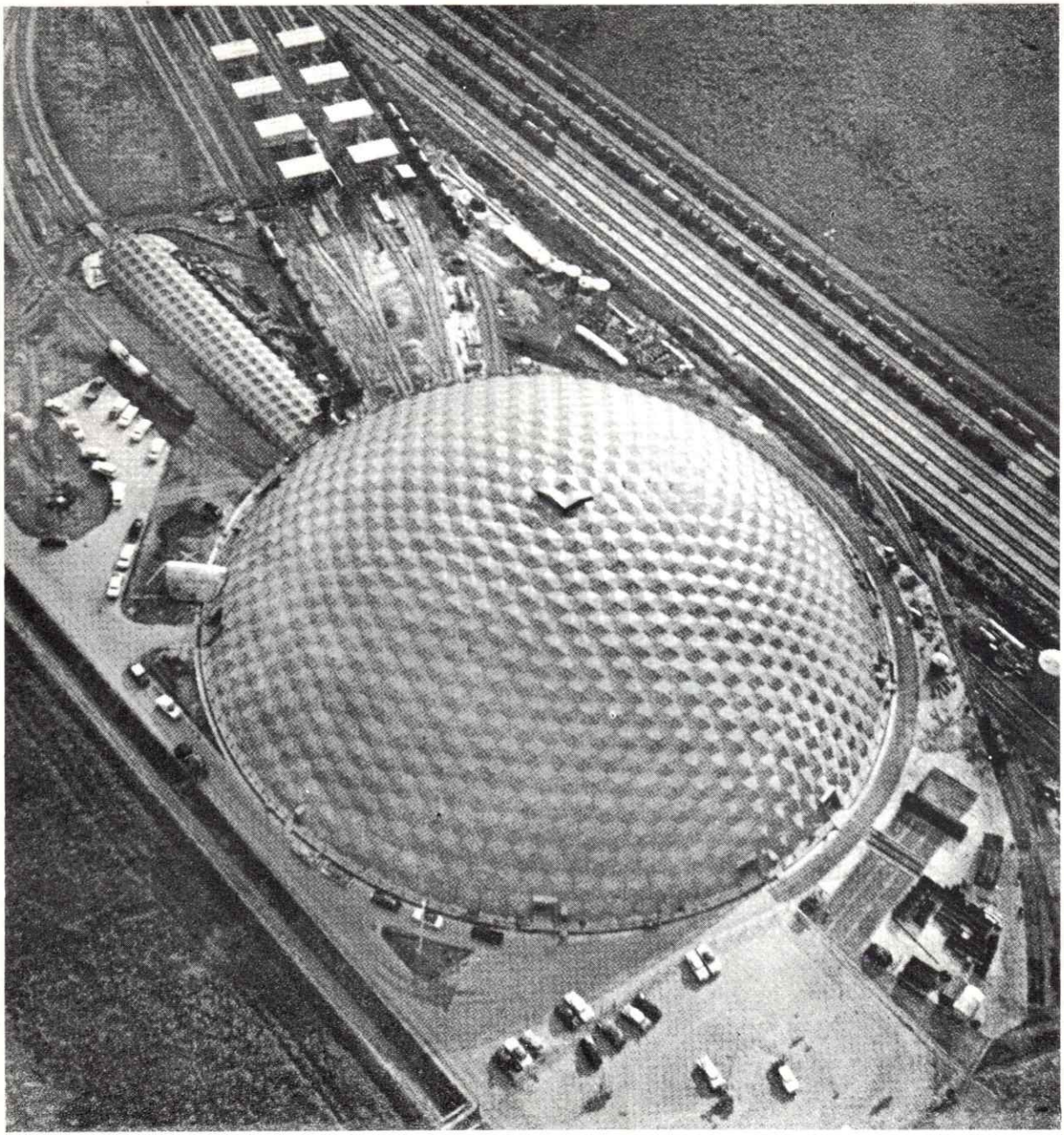

Fig. No. 77 36^{V} Triacon hex pent Baton Rouge dome. Three hundred eighty-four foot diameter, 120' height, the Union Tank Car Company dome with paint tunnel contains 154, 900 square feet of panels. Eleven gage sheet steel provides enclosures.

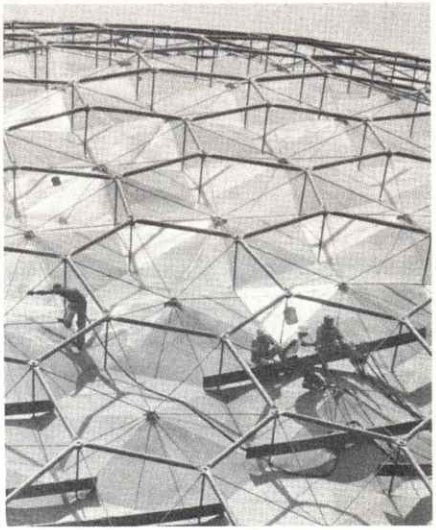

Fig. No. 78 Top: Hexagonal double grid units await installation. Units are basically same as ASM and Climatron domes substituting sheet material for inner grid and sub assembly guys. All seams are continuously welded, upper grid of sub assembly guys perform same post tensioning task as before. Four-inch tension rods make up four feet deep truss. See Fig. 102 for erection. Bottom: Frames in foreground are jigs to pre-assemble hexagonal units. Project by Synergetics Incorporated.

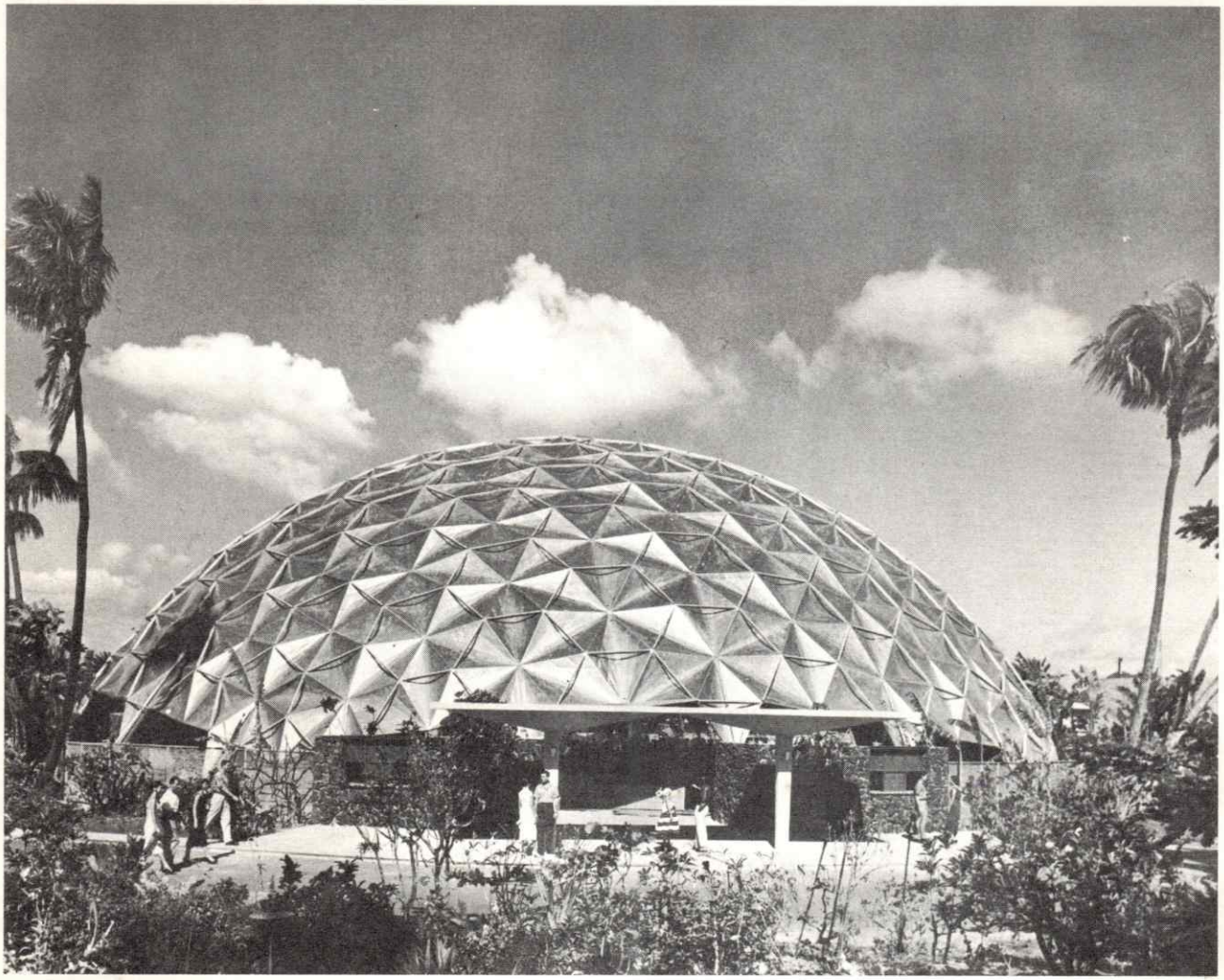

Fig. No. 79 Elevation Kaiser 145' diameter dome. Double grid consists of outer hex-pent grid and inner hyperbolic-paraboloid sheet metal diamonds.

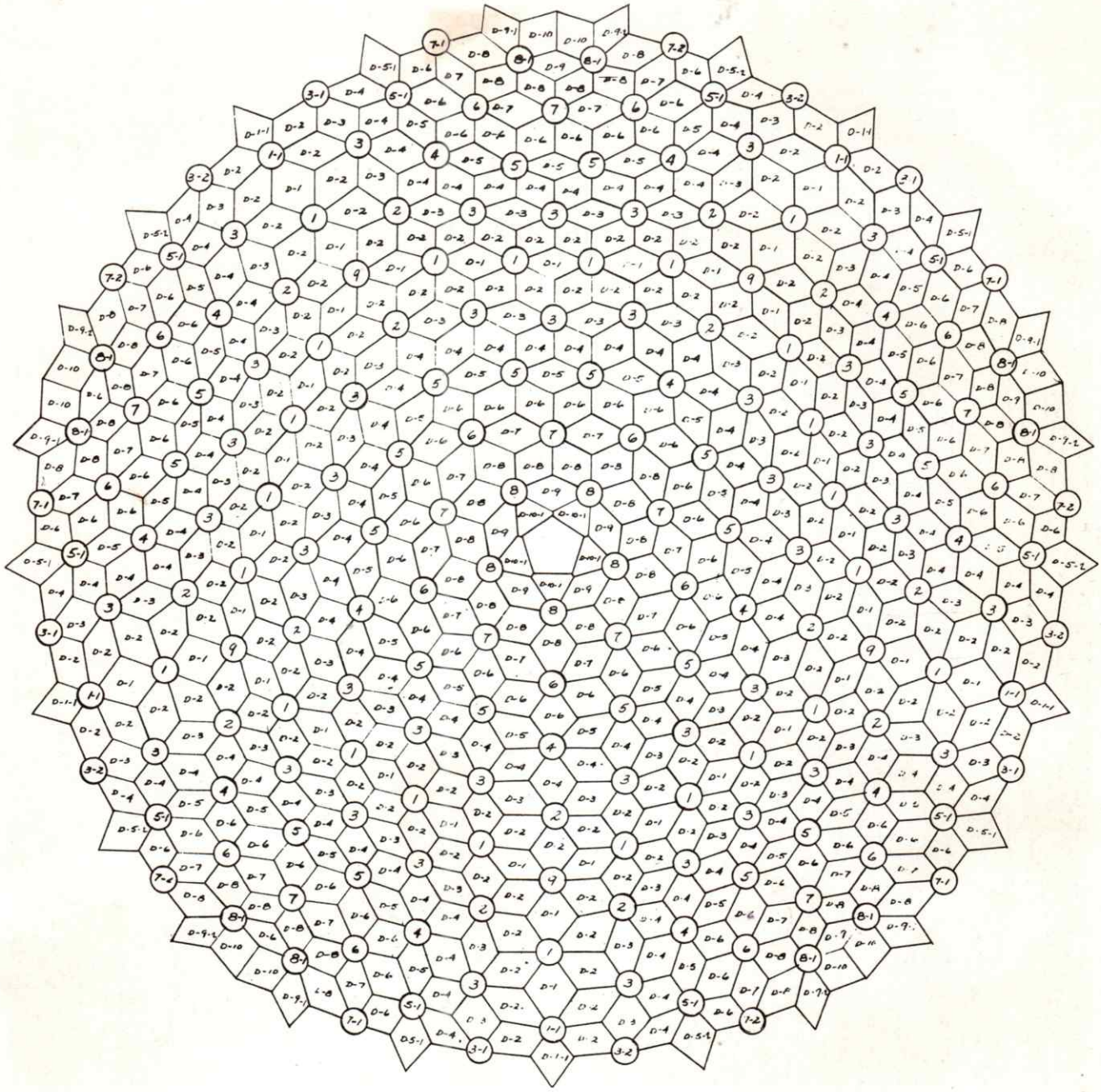

Fig. No. 80 Plan. Location plan for 575 basic diamonds. Forty-nine foot high dome covers floor area of 16, 500 square feet. Assembly time 588 man hours, see Fig. 100 for sequence. Although appearing upon first inspection to be a 15^{V} Alternate a special Triacon application where the dodecahedron edge is evenly segmented into 10 units was used.

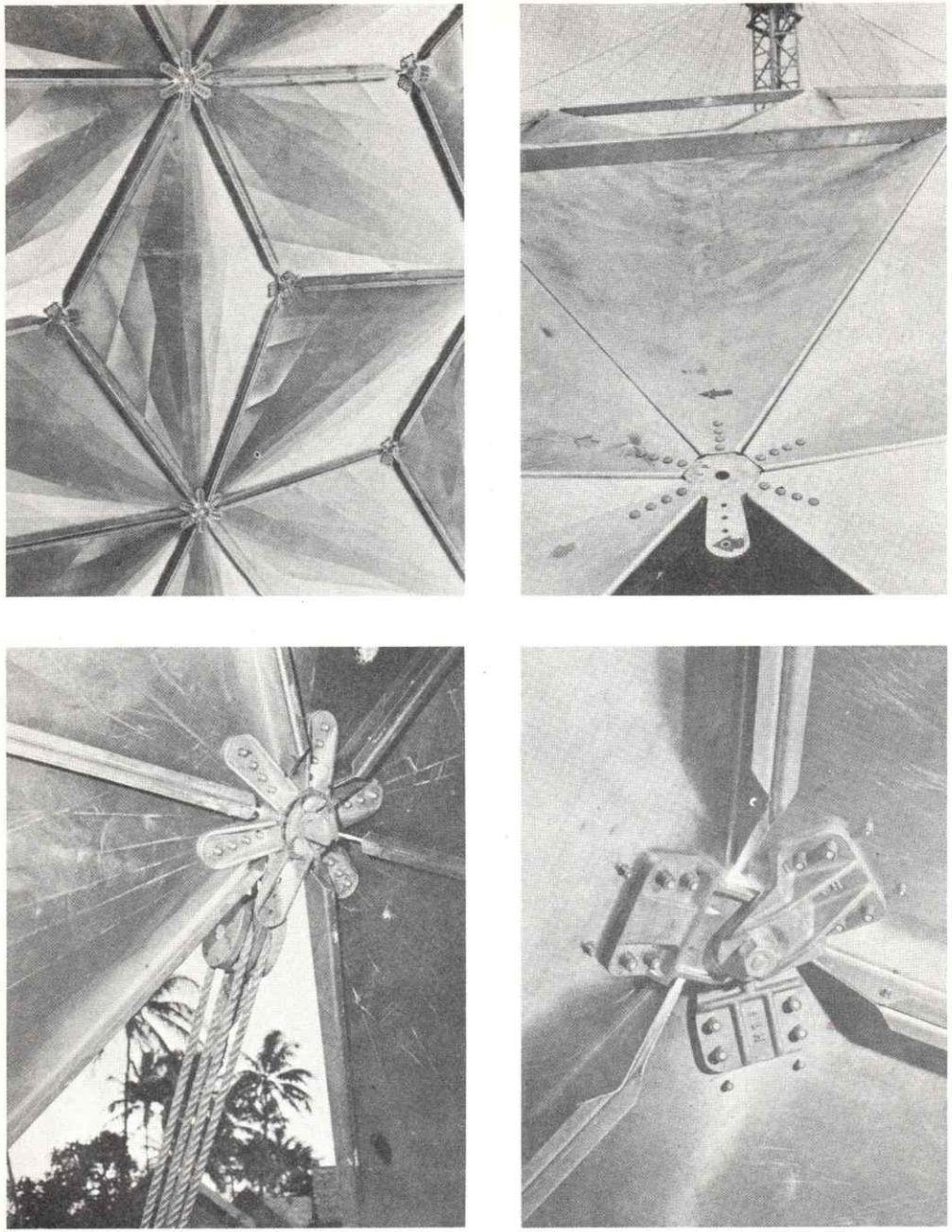

Fig. No. 81 Top: Interior view of diamond panels. Note brake creases do not generate a ruled hyperbolic surface but tend to radiate or fan out from long diamond axis vertexes. Diamonds approximately 9' x 11', 156" thick. Long axes connector from exterior. Bottom: Interior view of long axis casting. Block and tackel used to prevent dome rotation during mast erection, see Fig. 99. Narrow axis casting joins three adjacent diamonds and upper grid struts. A Synergetics Incorporated project.

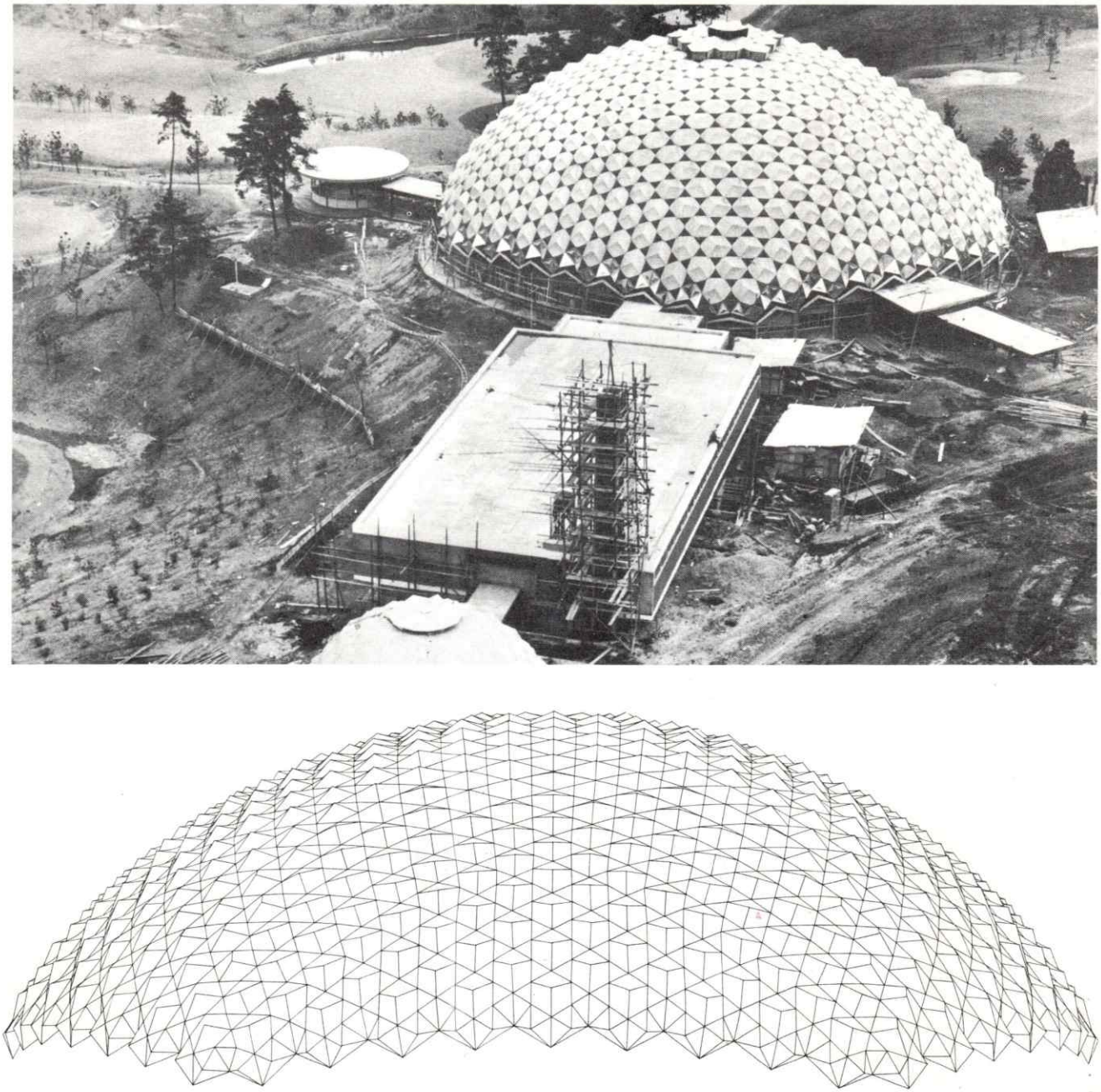

Fig. No. 82 Yomuiuri dome, Tokyo, Japan.

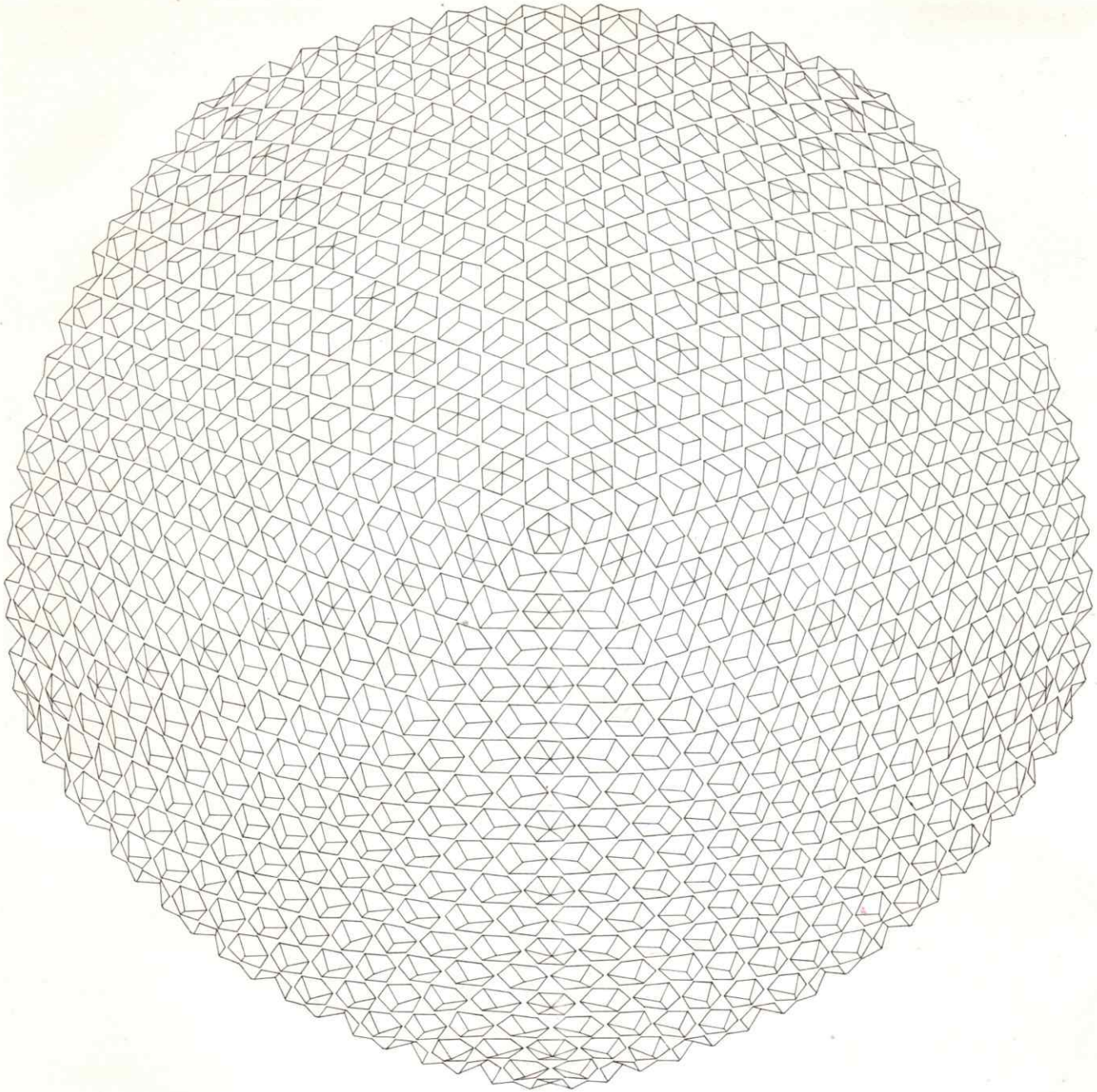

Fig. No. 83 Plan a double grid 36^V Triacon breakdown. Hexagonal grids receive three hyperbolic diamond sky light panels. Intermittent triangles are opaque.

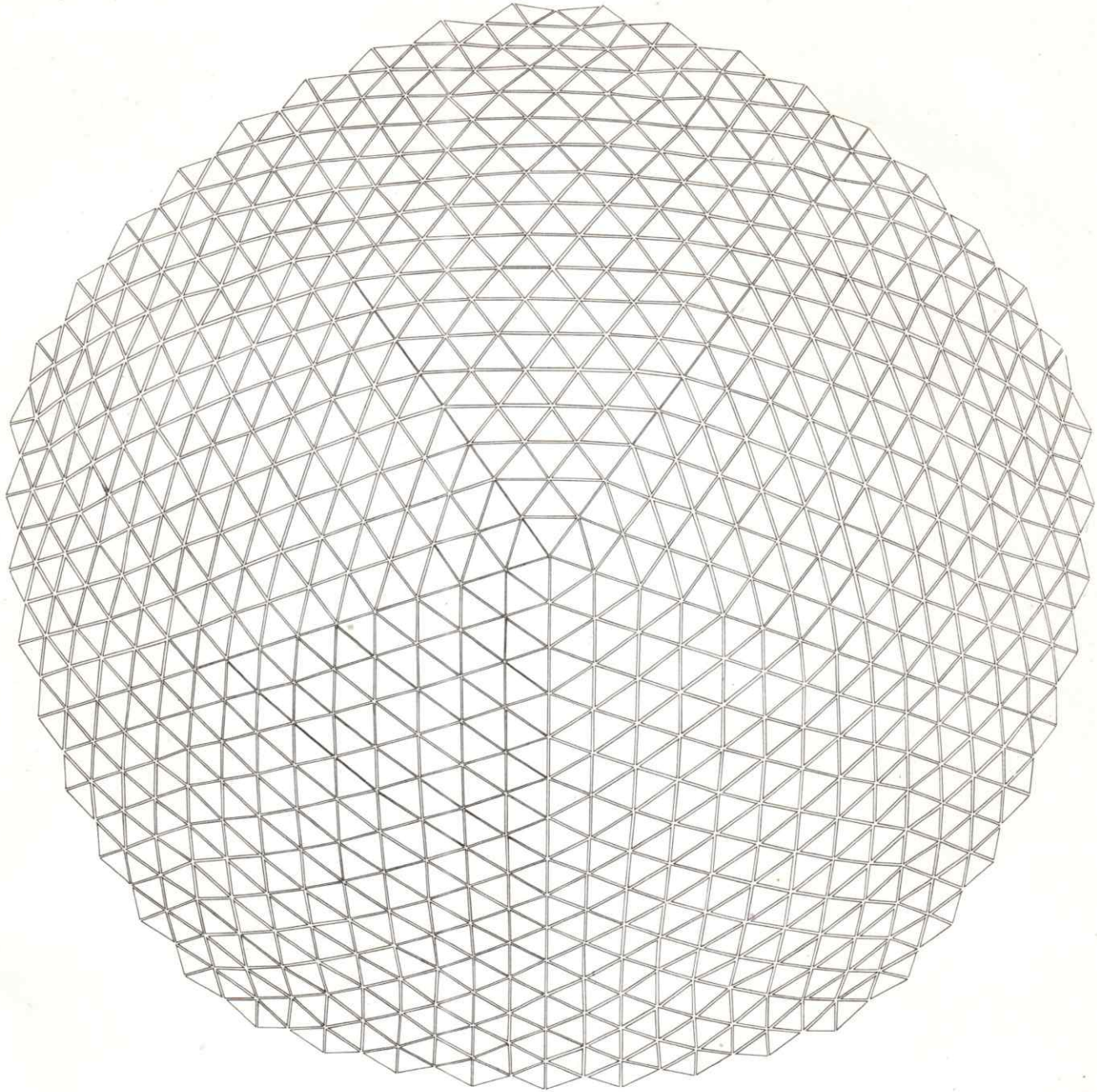

Fig. No. 84 Plan inner grid of sub assemblies 18^{V} Triacon breakdown.

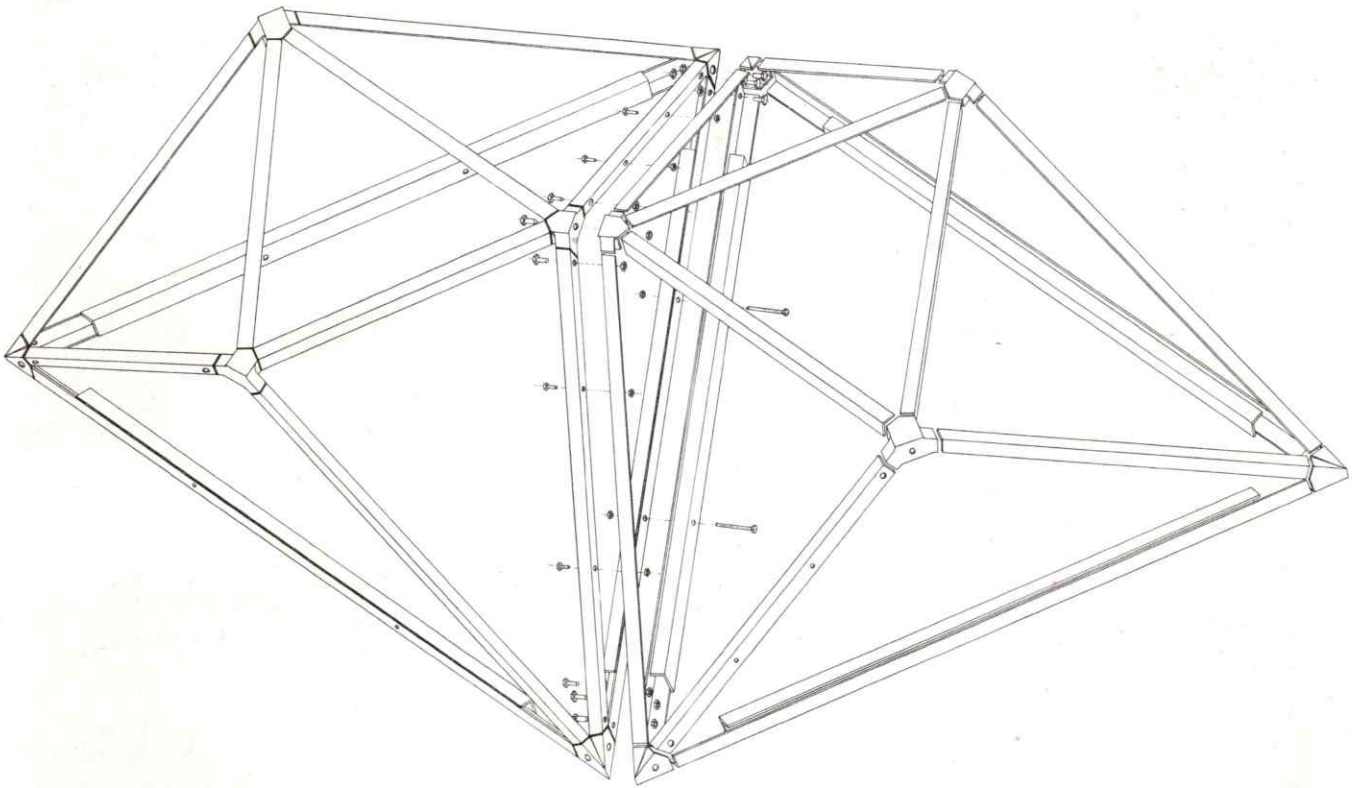

Fig. No. 85 Double grid basic components. Grid components consist of angle iron frames adjacently bolted. Two such units appear here.

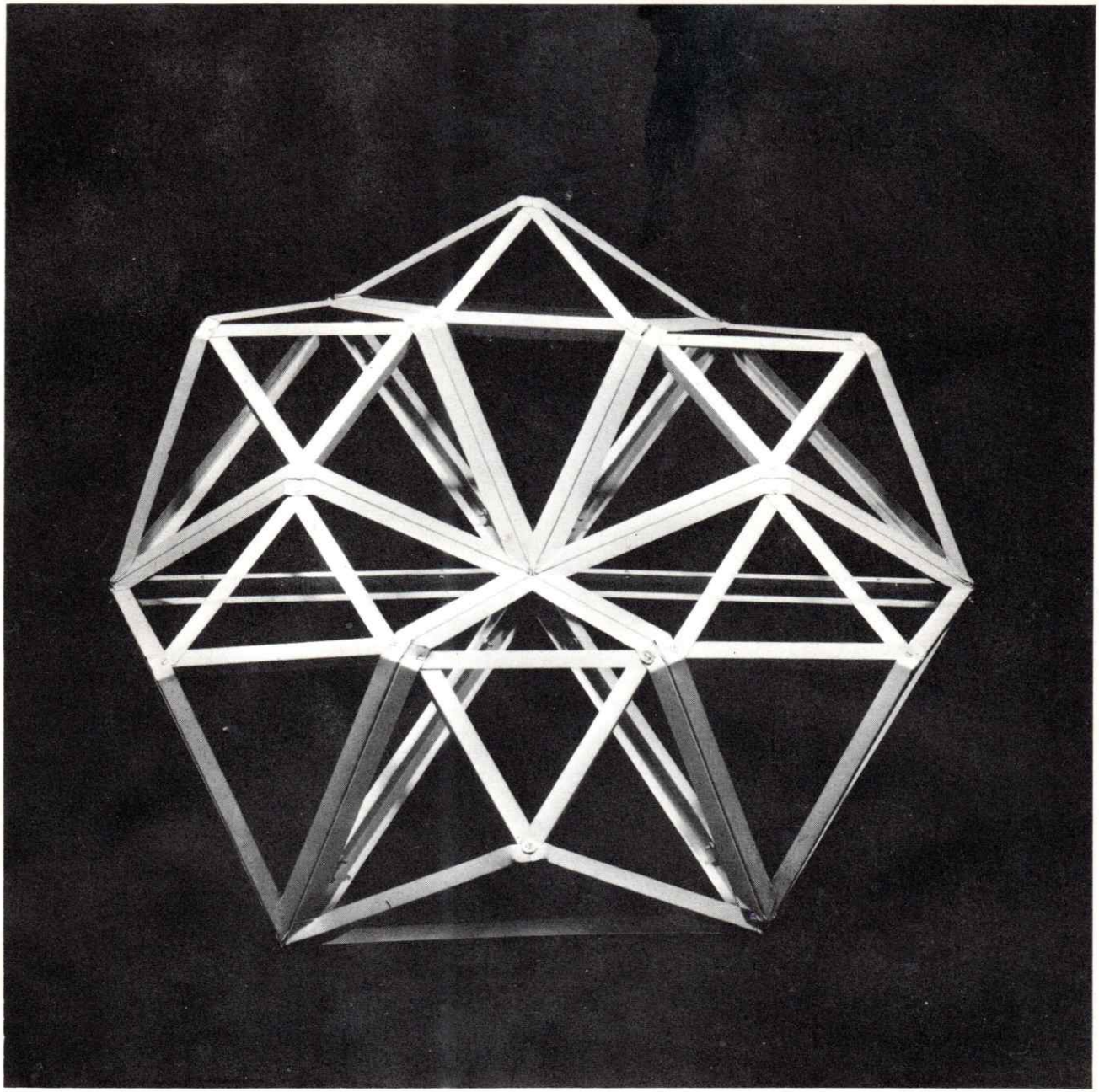

Fig. No. 86 A grouping of six double grid components delineate one surface hexagon and surrounding triangles. View from outside dome. Hexagon receives three hyperbolic diamonds to form sky light. Note why frequency count varies for inner and outter grid.

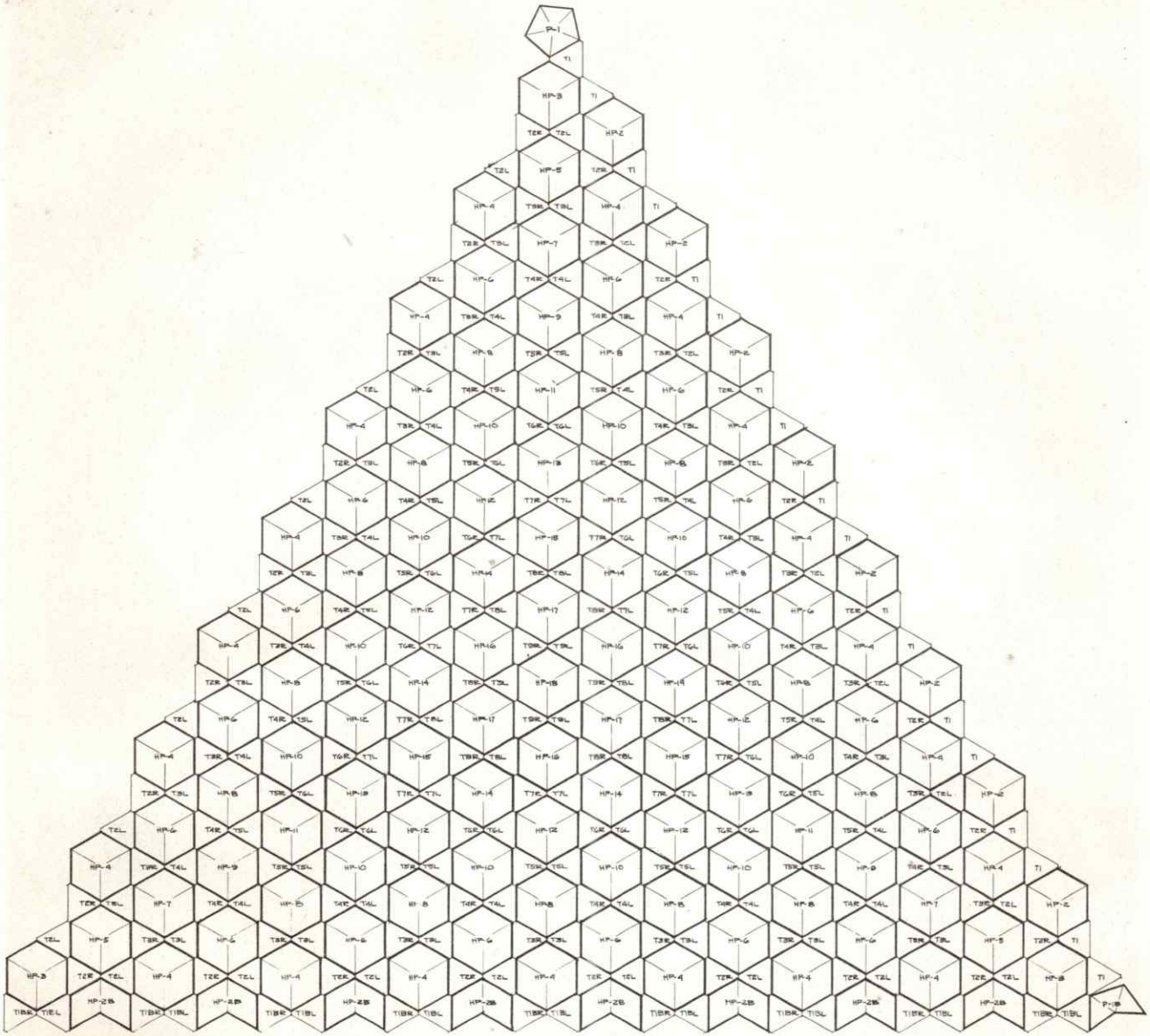

Fig. No. 87 Development of one-fifth dome showing hyperbolicparaboloid sky lights and grid components. Fifth shown is basic icosahedron face with 36^V breakdown. Note pents at zenith and right hand corner. Project by Geometrics, Incorporated.

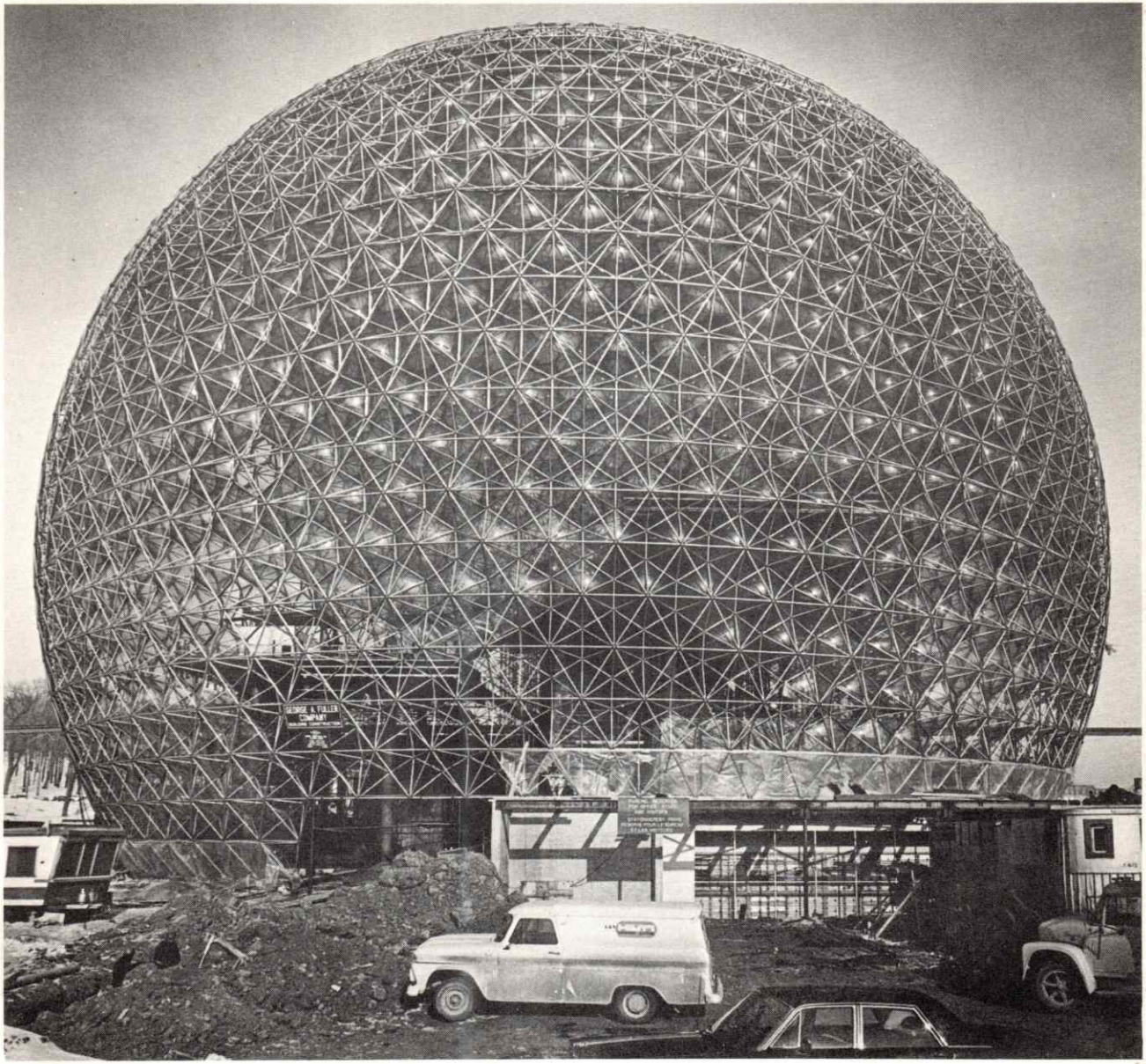

Fig. No. 88 Elevation U.S. Pavilion, Expo '67, Montreal, Canada. Three-quarter double grid geodesic dome, 200' high, 250' diameter and 141,000 square feet. Double layer space frame consists of hexagonal inner layer and triangulated outer layer, a web network joins the two layers.

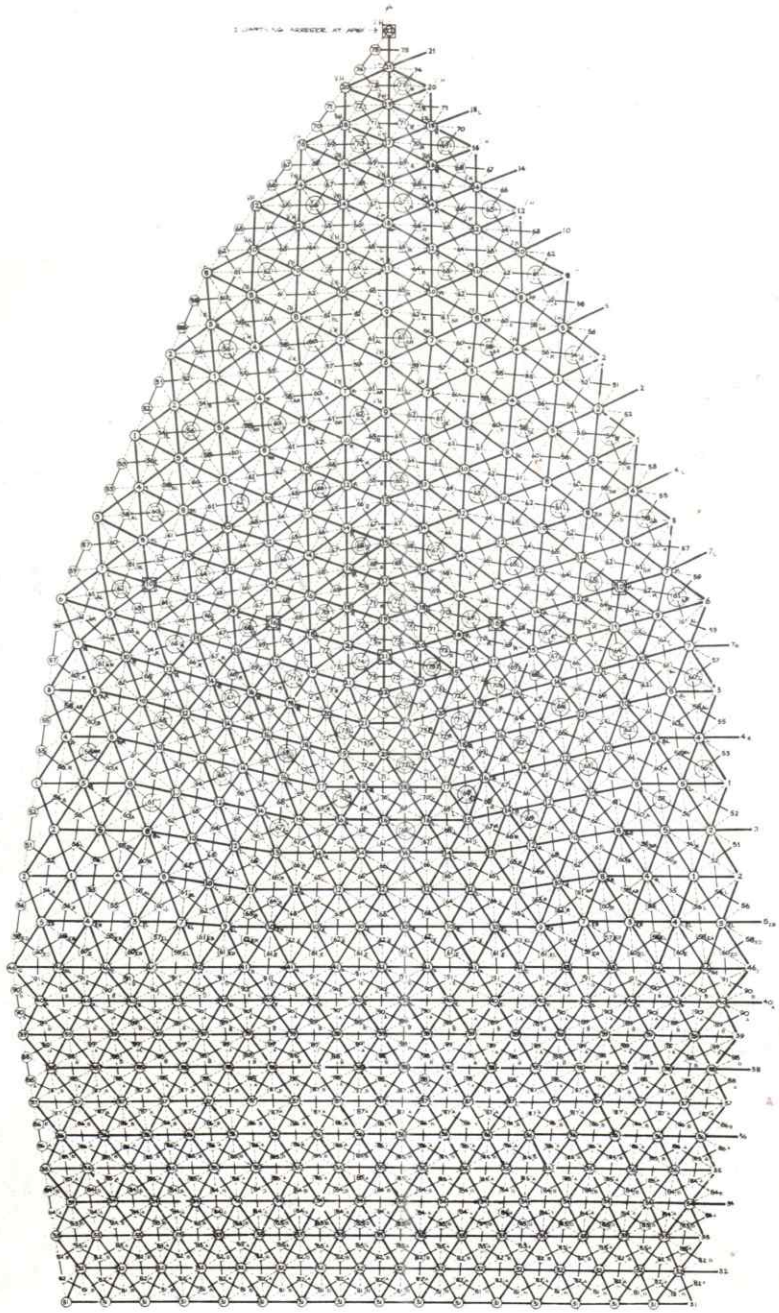

Fig. 89 Development of one-fifth typical assembly net showing orientation of double grids. Dotted diagonal web members connect the inner hexagonal and outer triangular grids. Breakdown consists of a 32^{V} Triacon inner grid with a 16^{V} alternate outer grid. Vertex numbers indicate hub castings.

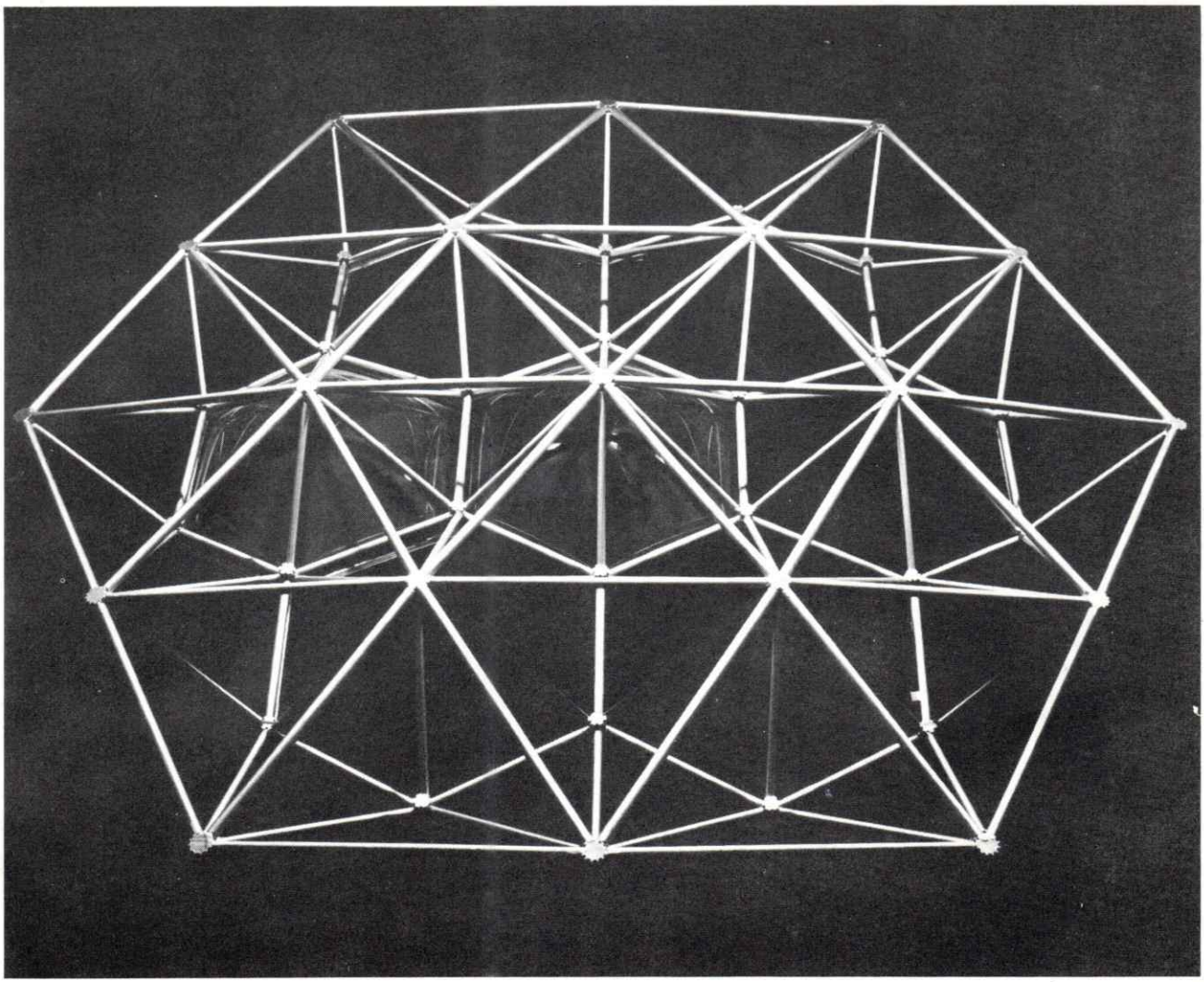

Fig. No. 90 Partial space frame model indicating acrylic dome orientation. Acrylic domes vary from 8' to 10' across the flat. Dome built from 600 tons of 2 7/8" diameter inner grid and 3 1/2" diameter outer grid tubing for a total of 27 miles linear material.

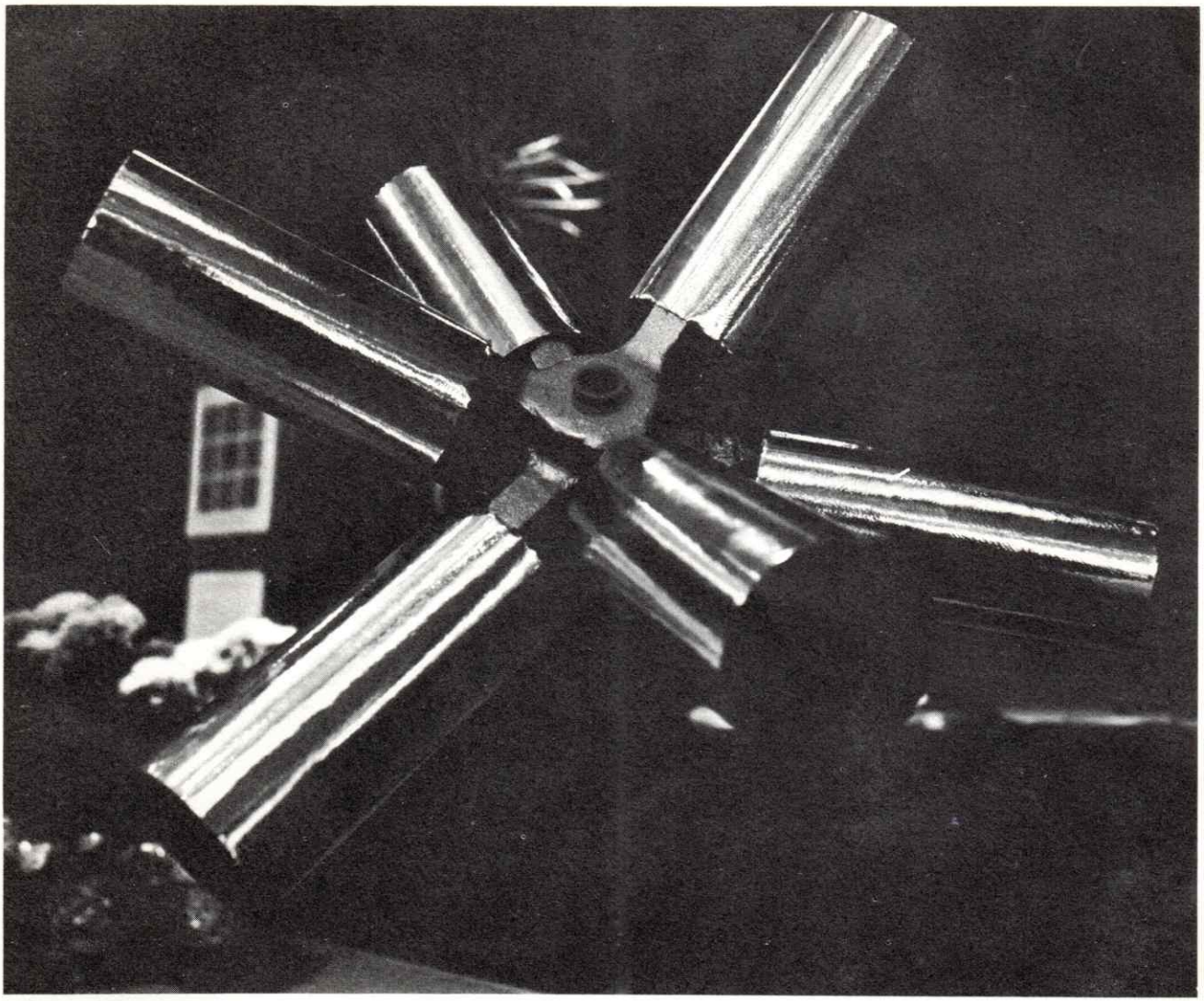

Fig. No. 91 Exterior view of inner grid vertex hub. Slotted pipes (polished portions) are plugged into hub's cast steel tabs, a fillit weld perminantly bonds joint. Each hub consists of a solid steel center with rectangular tabs for each member joined. Inner layer hubs have three tabs for inner grid members. There are two inner hubs for each exterior hub.

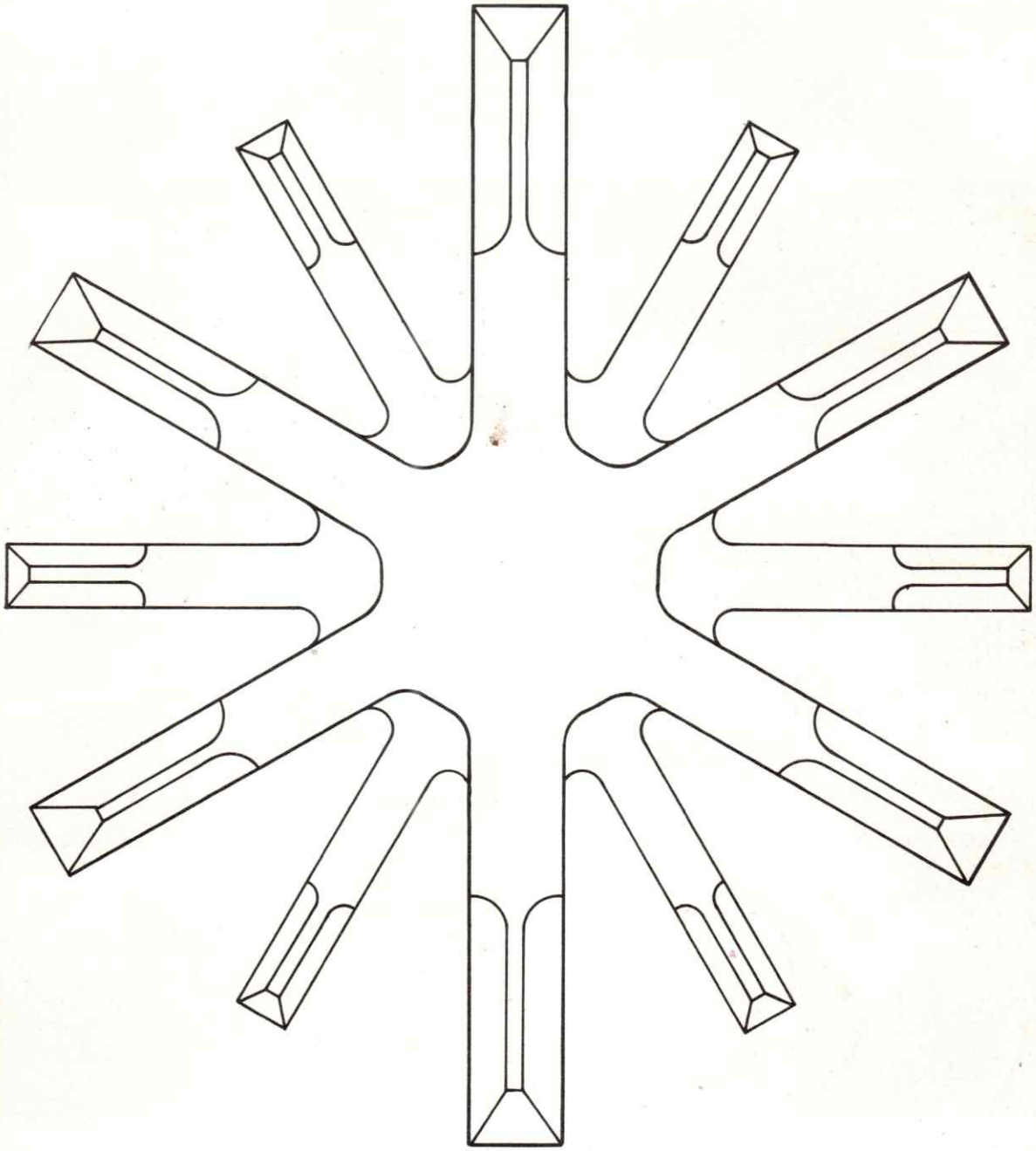

Fig. No. 92 Plan of outer grid vertex hub. Outer layer hubs have six tabs for outer grid members and six tabs for diagonal inner grid members, a total of 12 tabs. Cuts in tab ends provide area for fillit weld. Structure required 83 different hub castings, a total of 5, 900 hubs weighing 120 tons. Approximate weight of steel per square foot of dome surface - 10 pounds per square foot.

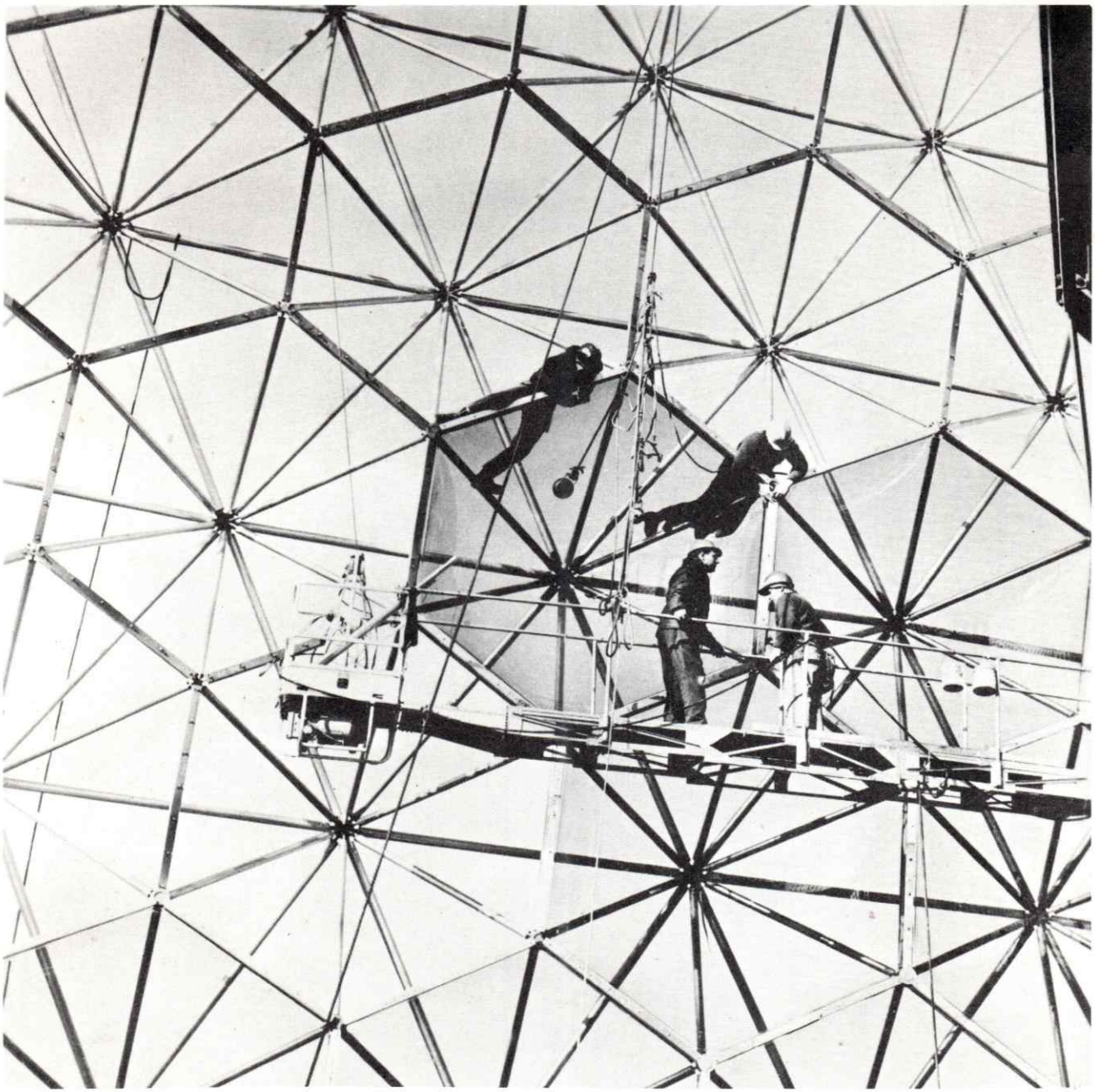

Fig. No. 93 Acrylic dome panels being installed inner grid tubing received a mullion section to which panels were inserted. Project by R. Buckminister Fuller and Sadao, Incorporated and Geometrics, Incorporated.

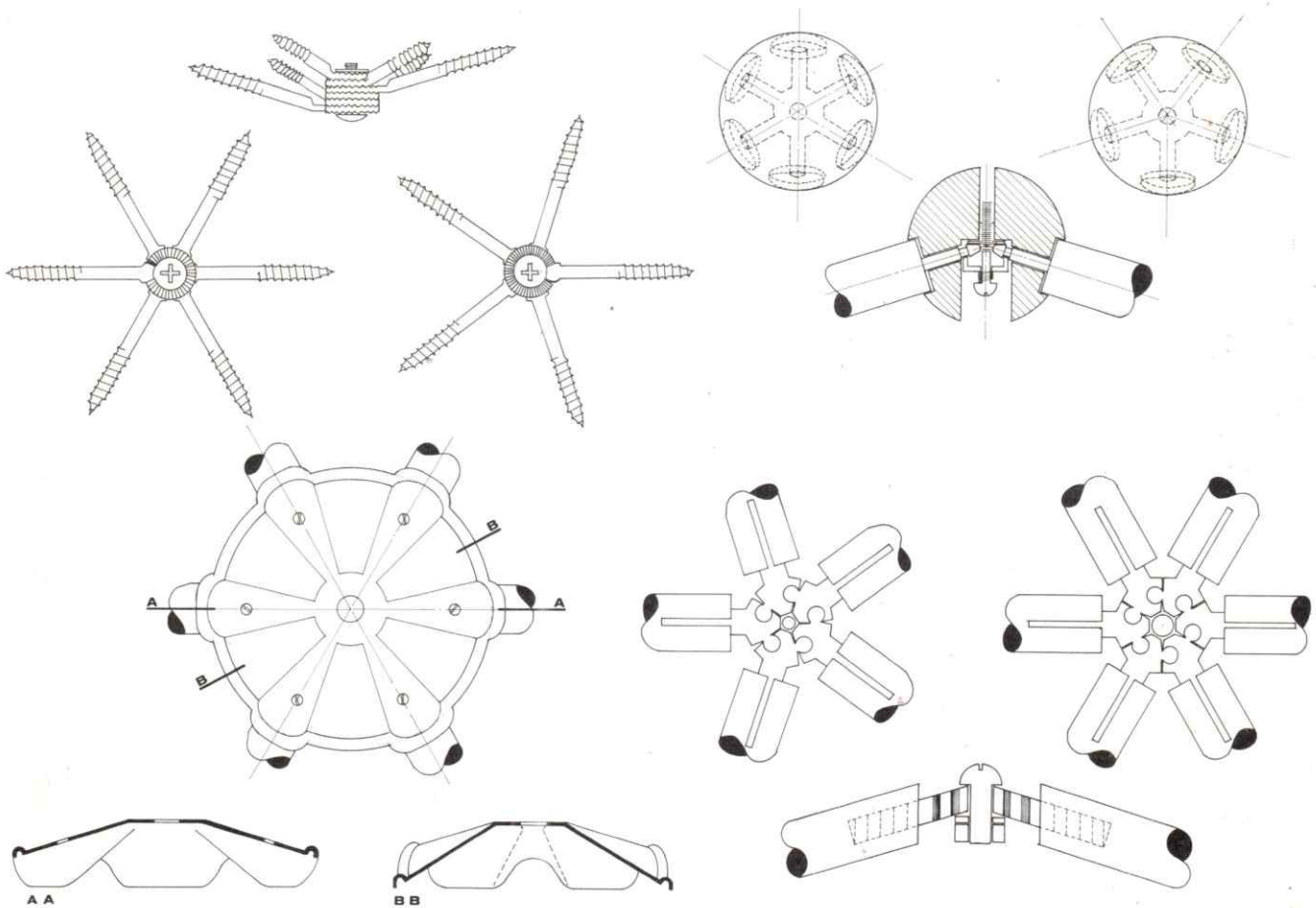

Fig. No. 94 Connection devices for 10' diameter wooden strut 2^V Alternate children's play sphere. Last example is noteworthy extruded as a section, connector is merely cut from lineal stock.

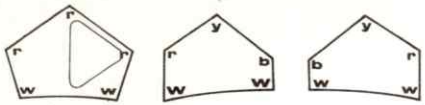

BASE PIECES

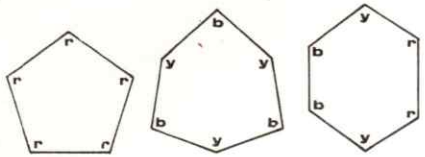

b BLUE
r RED
w WHITE
y YELLOW

DOME PIECES ALL COLOR CODES MATCH AT VERTEXES

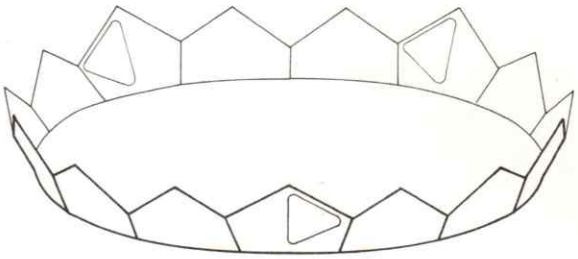

RING 1 5 BASE a
5 BASE b
5 BASE c

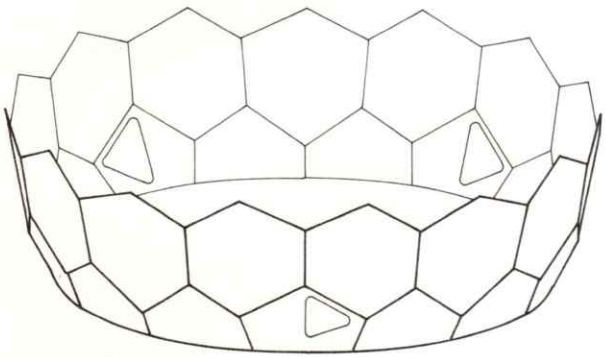

RING 2 5 HEX A
10 HEX B

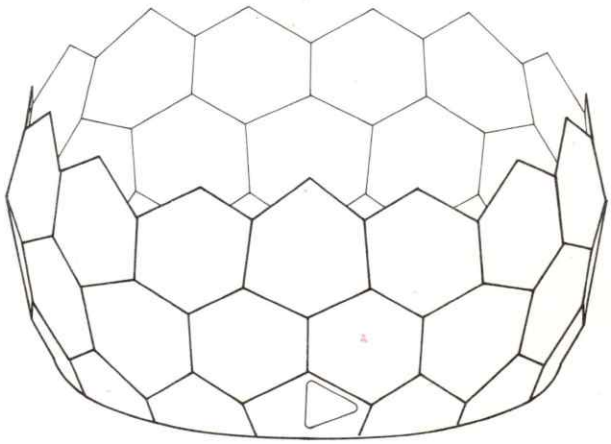

RING 3 5 HEX A
10 HEX B

Fig. No. 95 Concentric ring erection sequence for 6^V Triacon hex-pent dome rings 1-3. In this case, the pure pattern was distorted slightly to give special advantages, namely semi-equal surface area to each of the three different components.

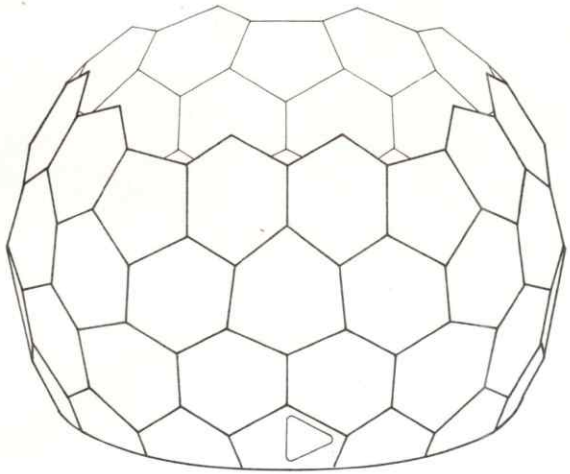

RING 4 5 PENT 10 HEX

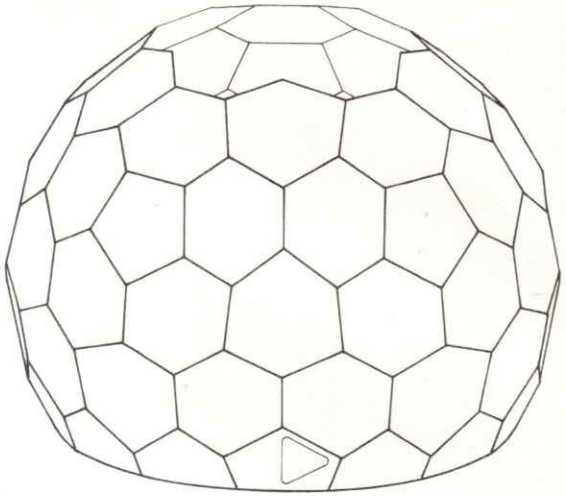

RING 5 5 HEX A 5 HEX B

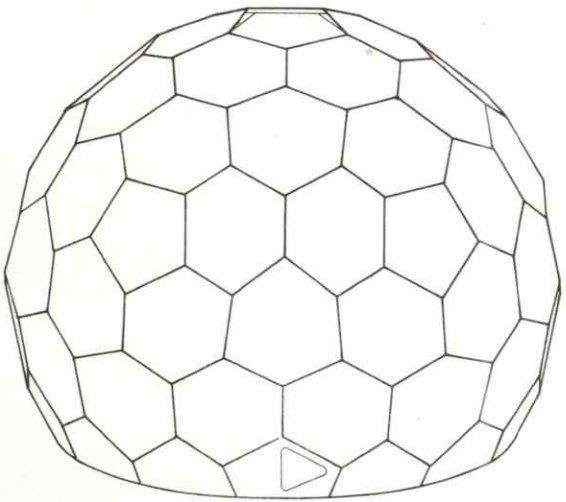

RING 6 5 HEX B

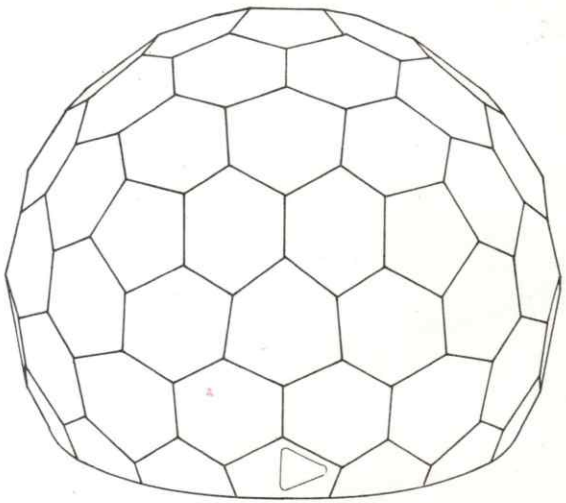

RING 7 1 PENT

Fig. No. 96 Concentric ring erection sequence for 6^V Triacon hex-pent dome rings 4-7. Each successive ring provides necessary stabilization and centering for next ring.

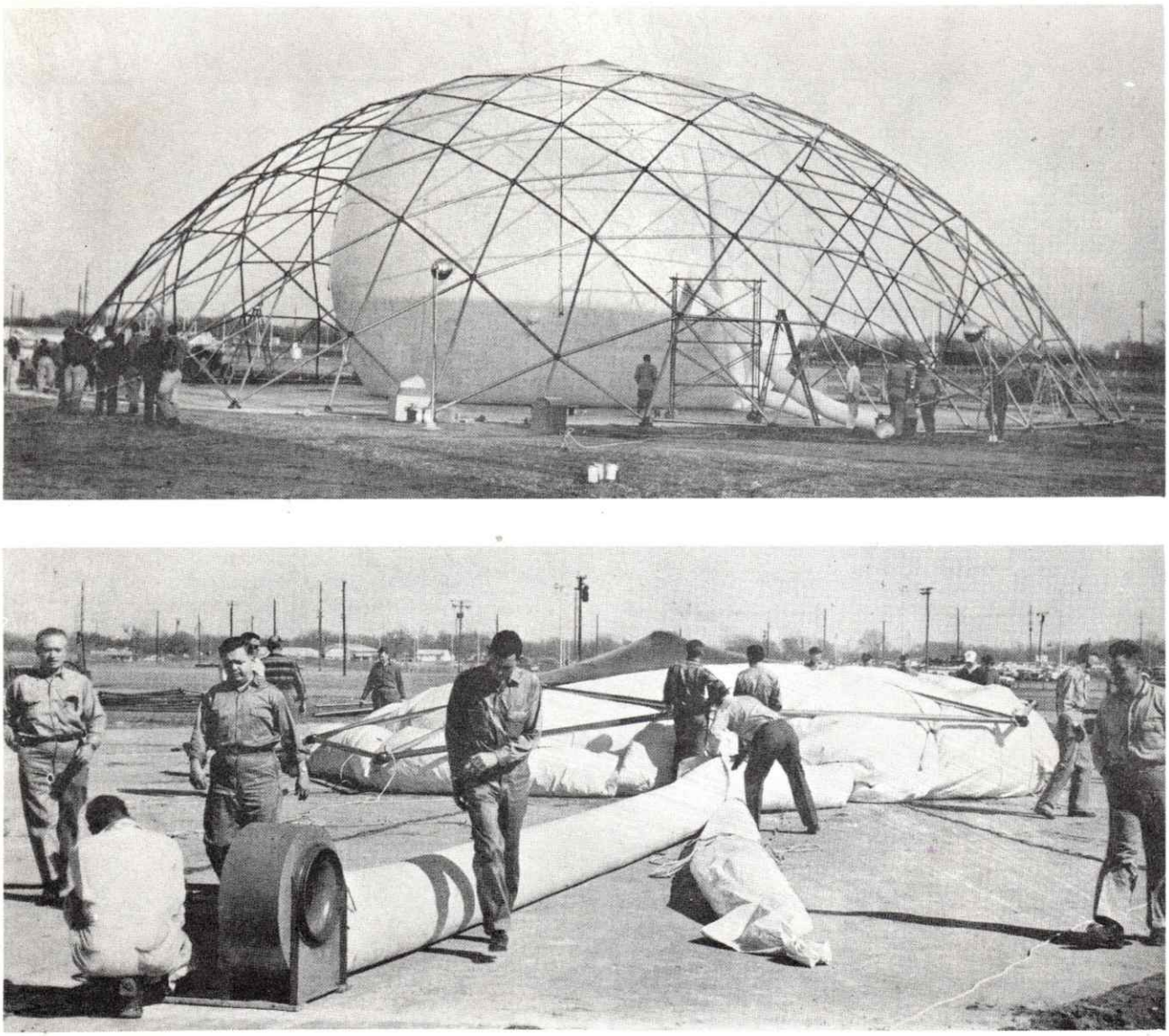

Fig. No. 97 Pneumatic baloon erection of strut dome. Zenith section bottom is anchored by guys to prevent sliding. Method proven highly successful, erectors remain on ground and near supplies. As structure raises increased perimeter enables higher numbers of simultaneous operations to be performed.

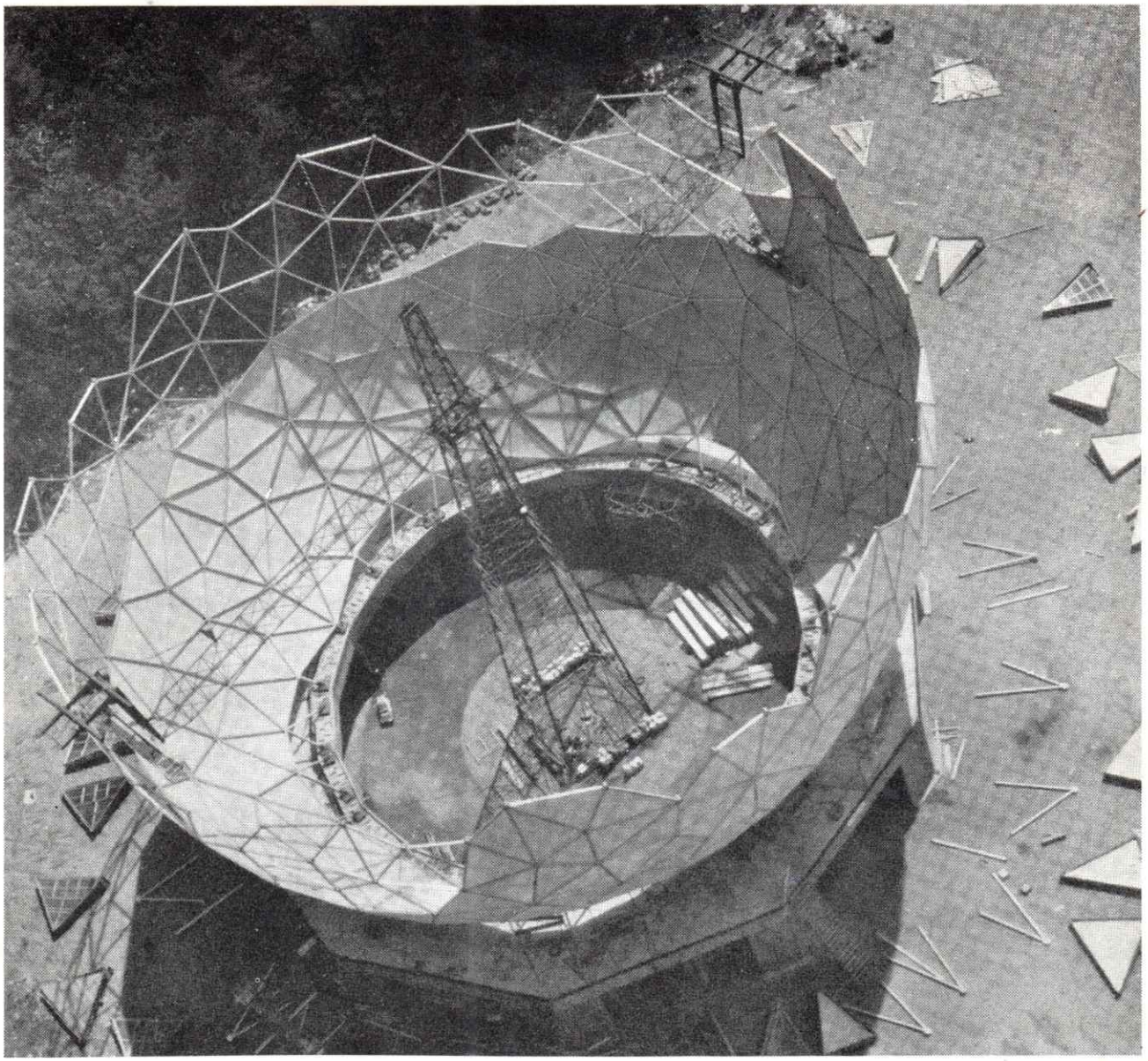

Fig. No. 98 Radome erection by central twin boom mast.

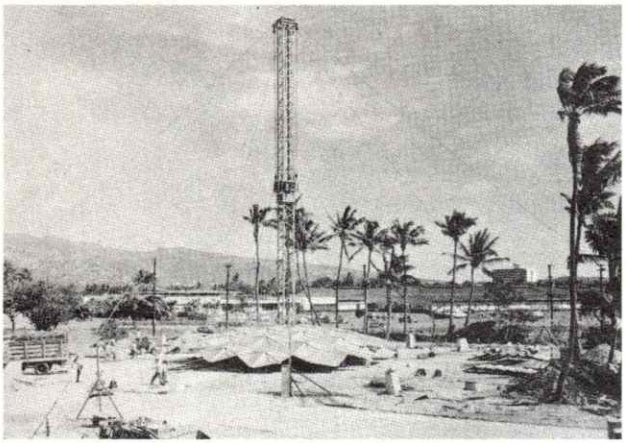

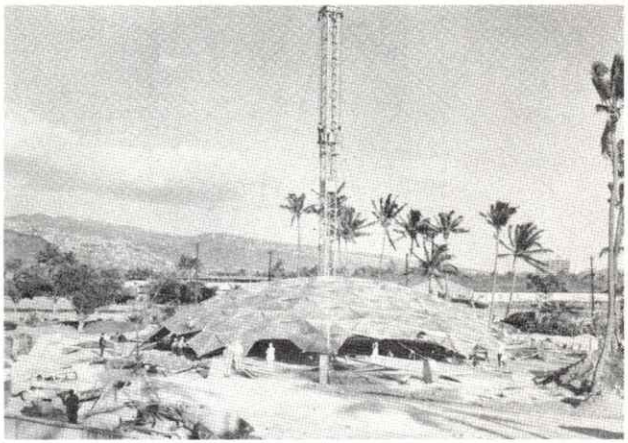

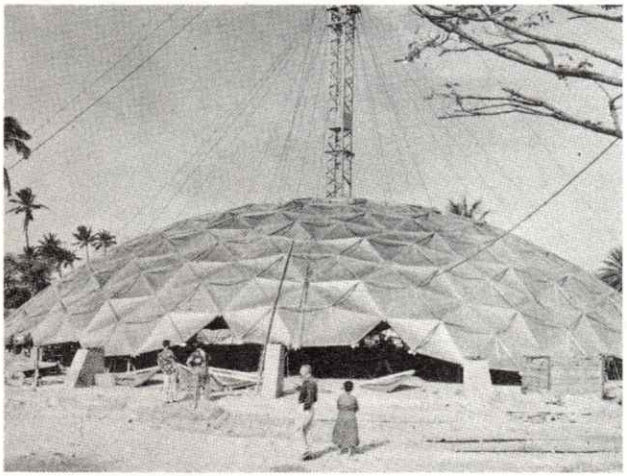

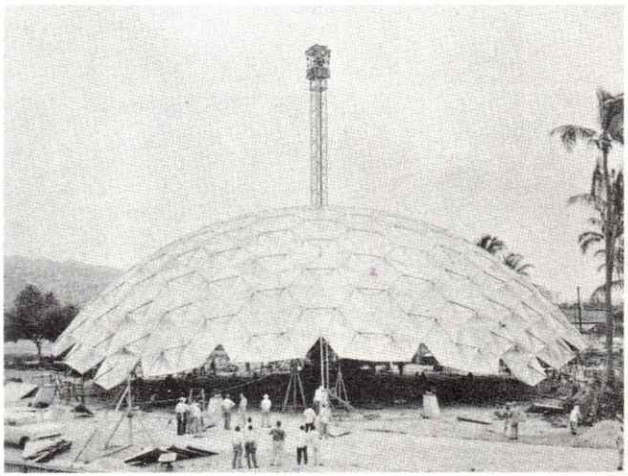

Fig. No. 99 Central mast erection technique Kaiser dome Figs. 79, 80, 81. Compressive and tensile characteristics of aluminum permit a semi-stress reversal in components during erection. Advantages similar to pneumatic technique of Fig. 97. Plywood dome Figs 43, 44, 45 and 46 erection similar.

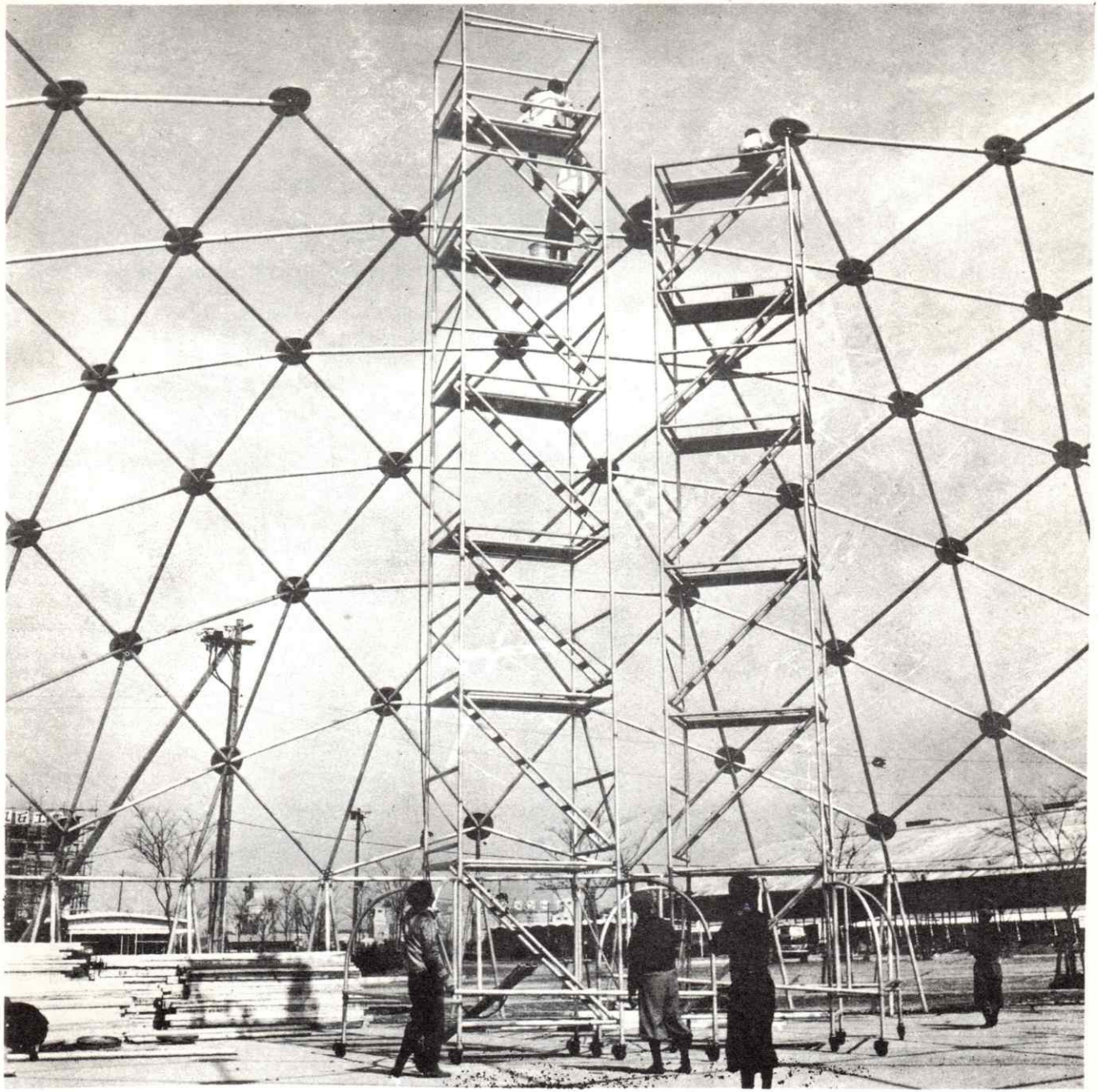

Fig. No. 100 Concentric ring scaffold technique. Limited to heights accessable from tower scaffolds. Material supply and number of simultaneous operations possible reduce approaching zenith.

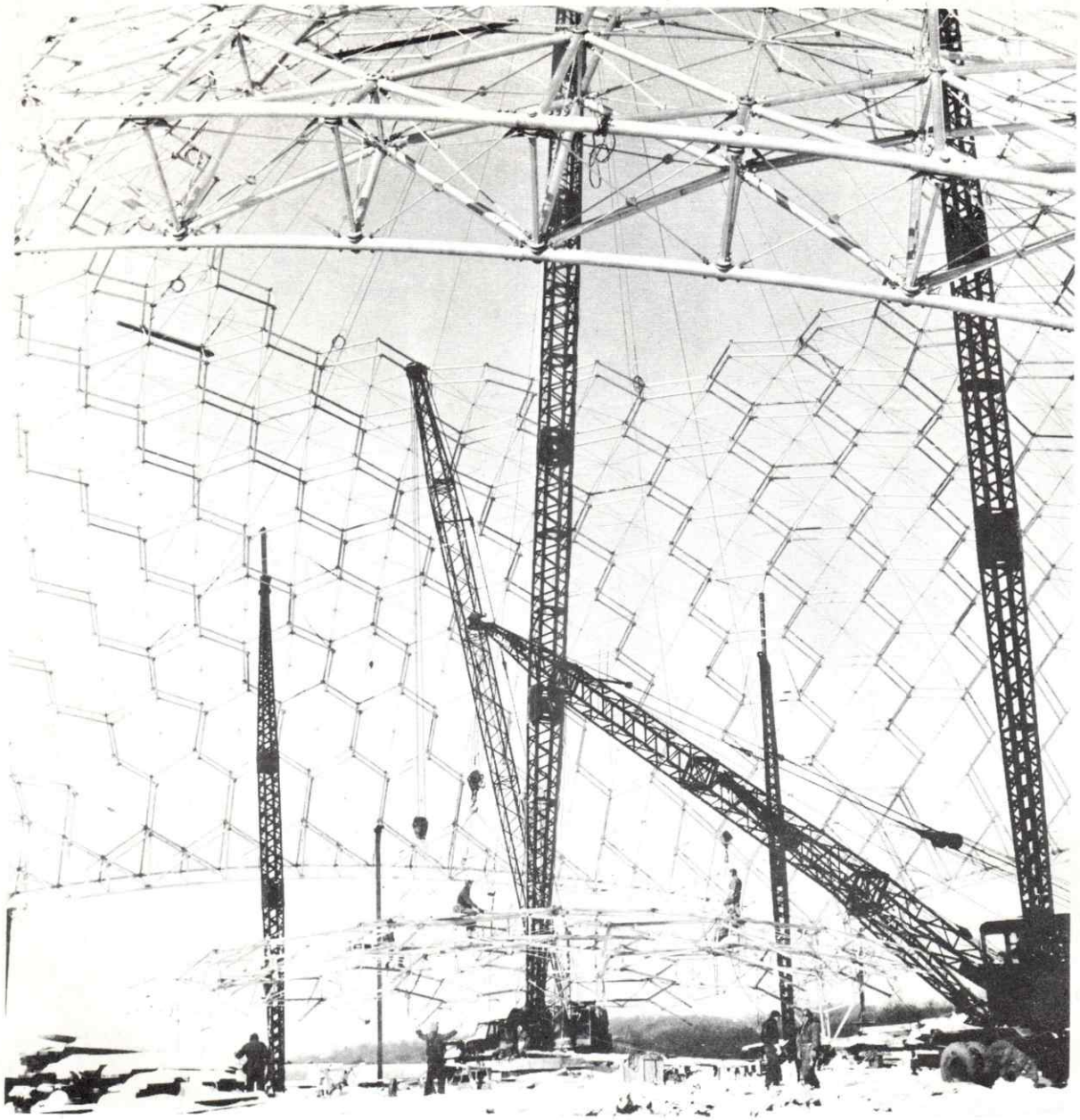

Fig. No. 101 Concentric ring crane technique. Large sections pre-assembled on ground joined in place. Central crane placing zenith section. American Society of Metals dome, Figs. 69, 70, 71, and 72. Similar problems as scaffold technique Fig. 100.

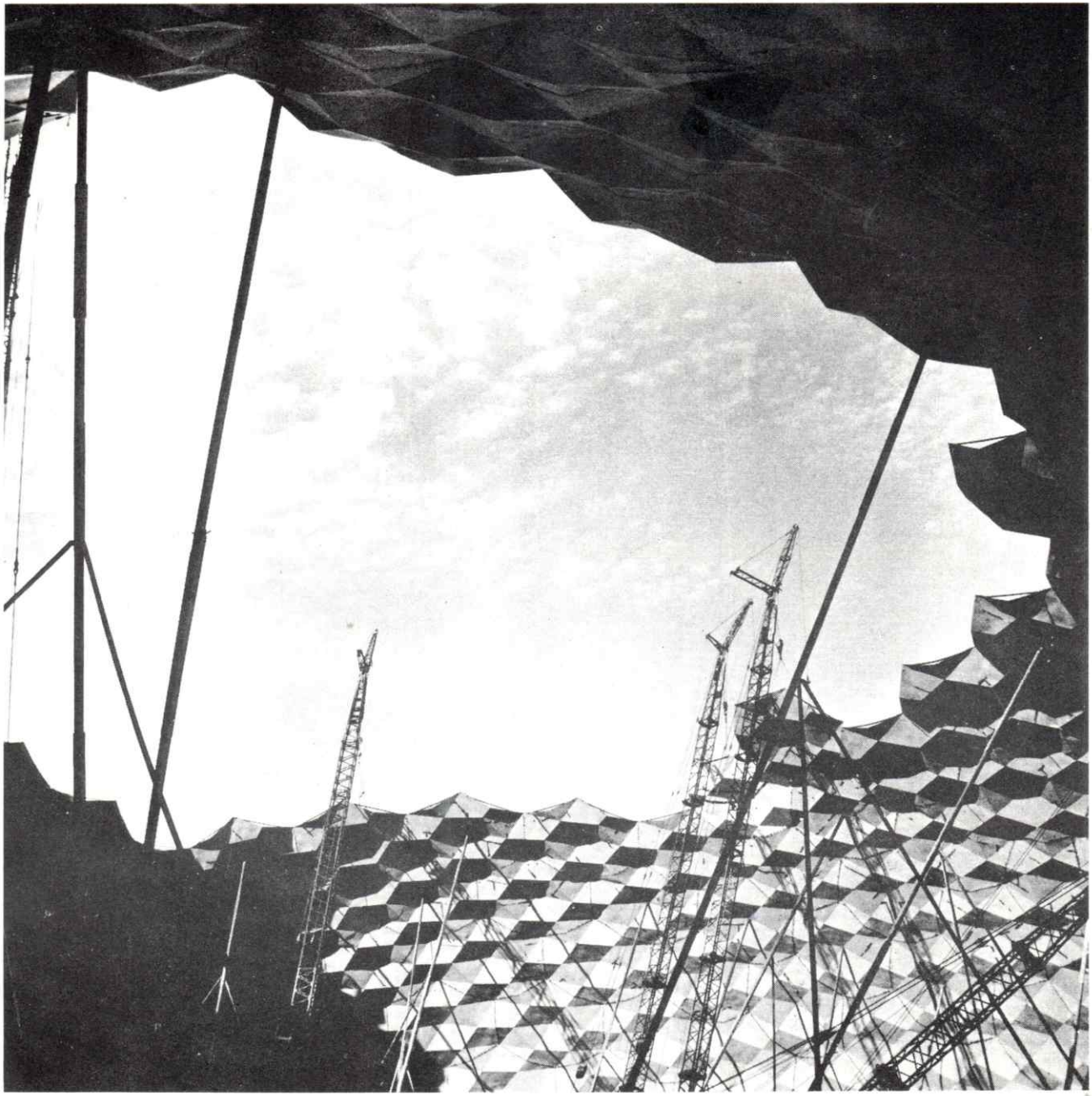

Fig. No. 102 Concentric ring crame technique. Large sections pre-assembled on ground joined in place. Erection of Baton Rouge dome Fig. 77 and 78.

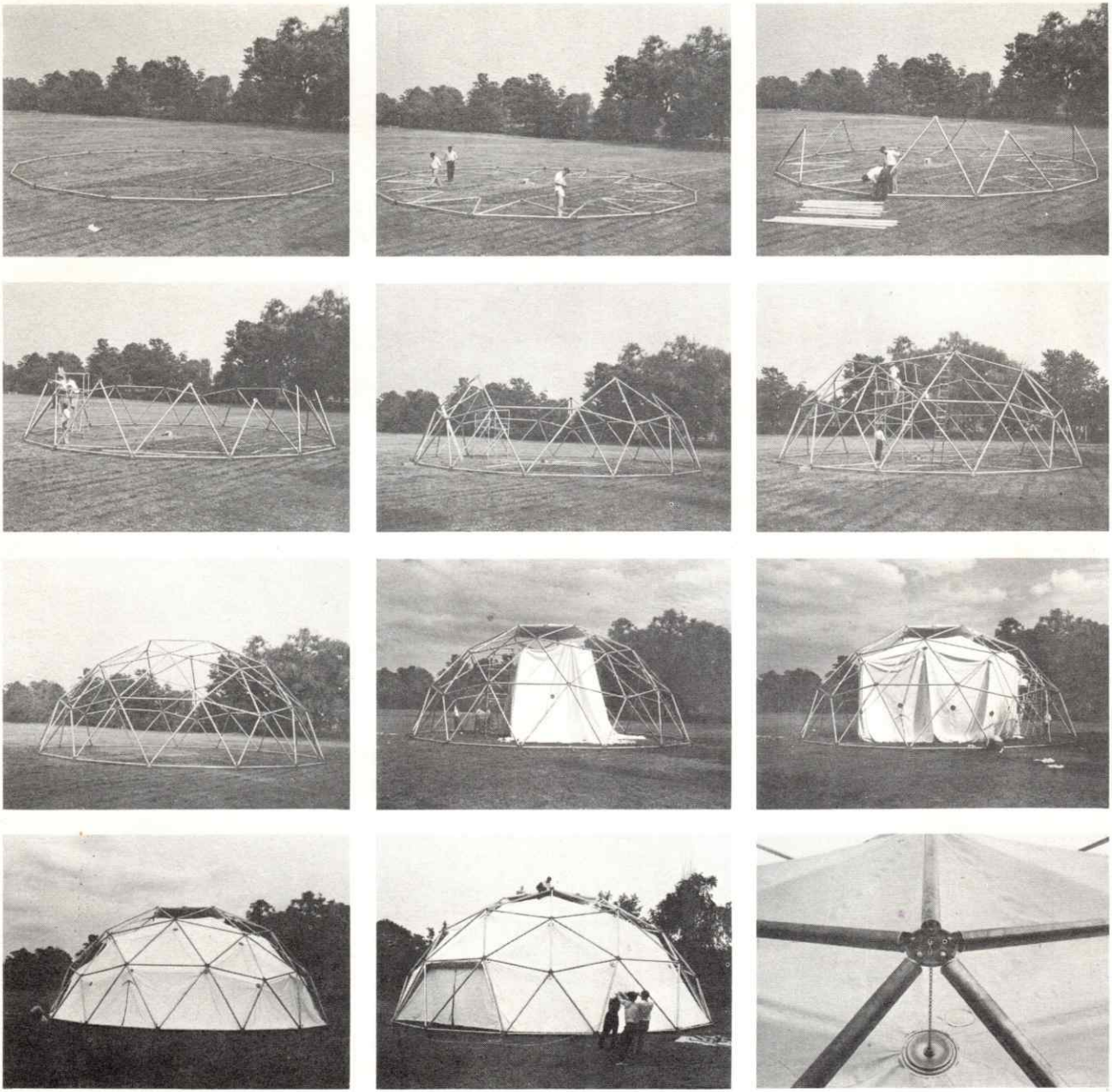

Fig. No. 103 Assembly sequence 55' diameter strut and membrane 3^V Alternate dome. Note suspension sequence and pull chain adjustment at vertex casting.

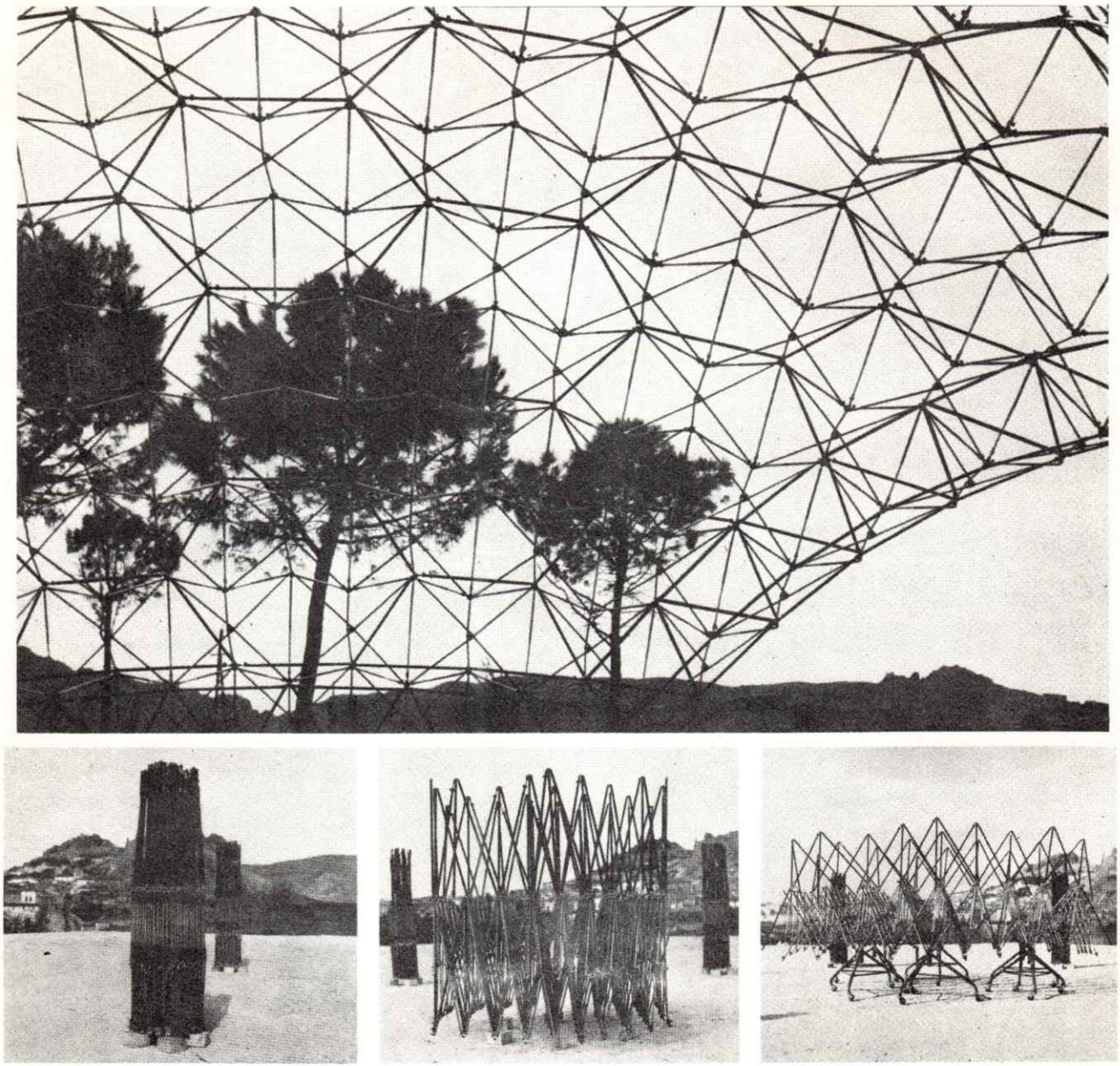

Fig. No. 104 Expandable truss technique developed by Emilio Pinero of Madrid. Segments packaged as compact bundles. Unfolded on wheeled trolleys and joined together to provide dome structures up to 300 feet in diameter.

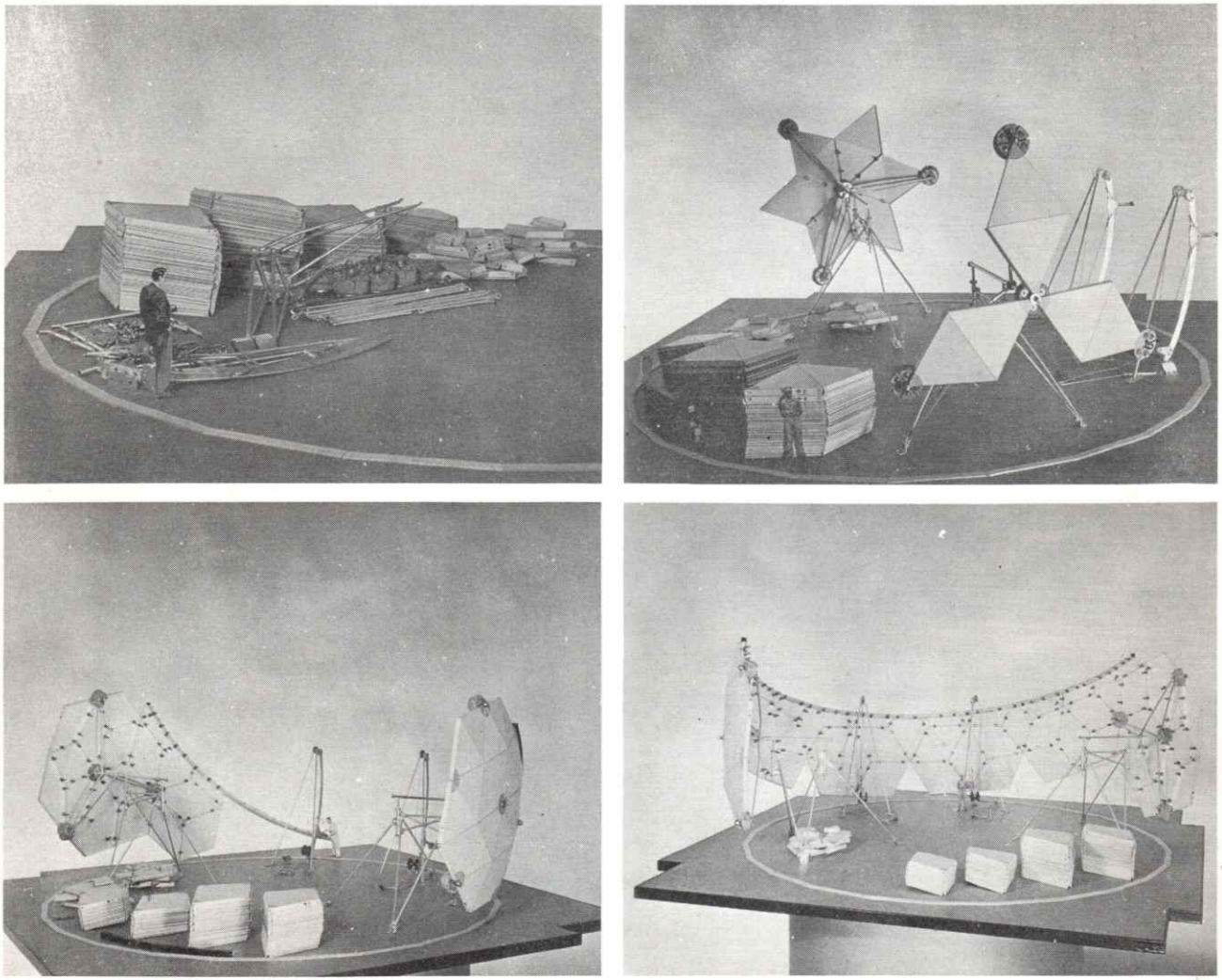

Fig. No. 105 Dome assembly by rotation about a horizontal axis. Overhead rotation on ground during assembly. Sequence: base ring placed, axes tripod and locking panels begun, lifting mast attached to base panels, rings one and two completed.

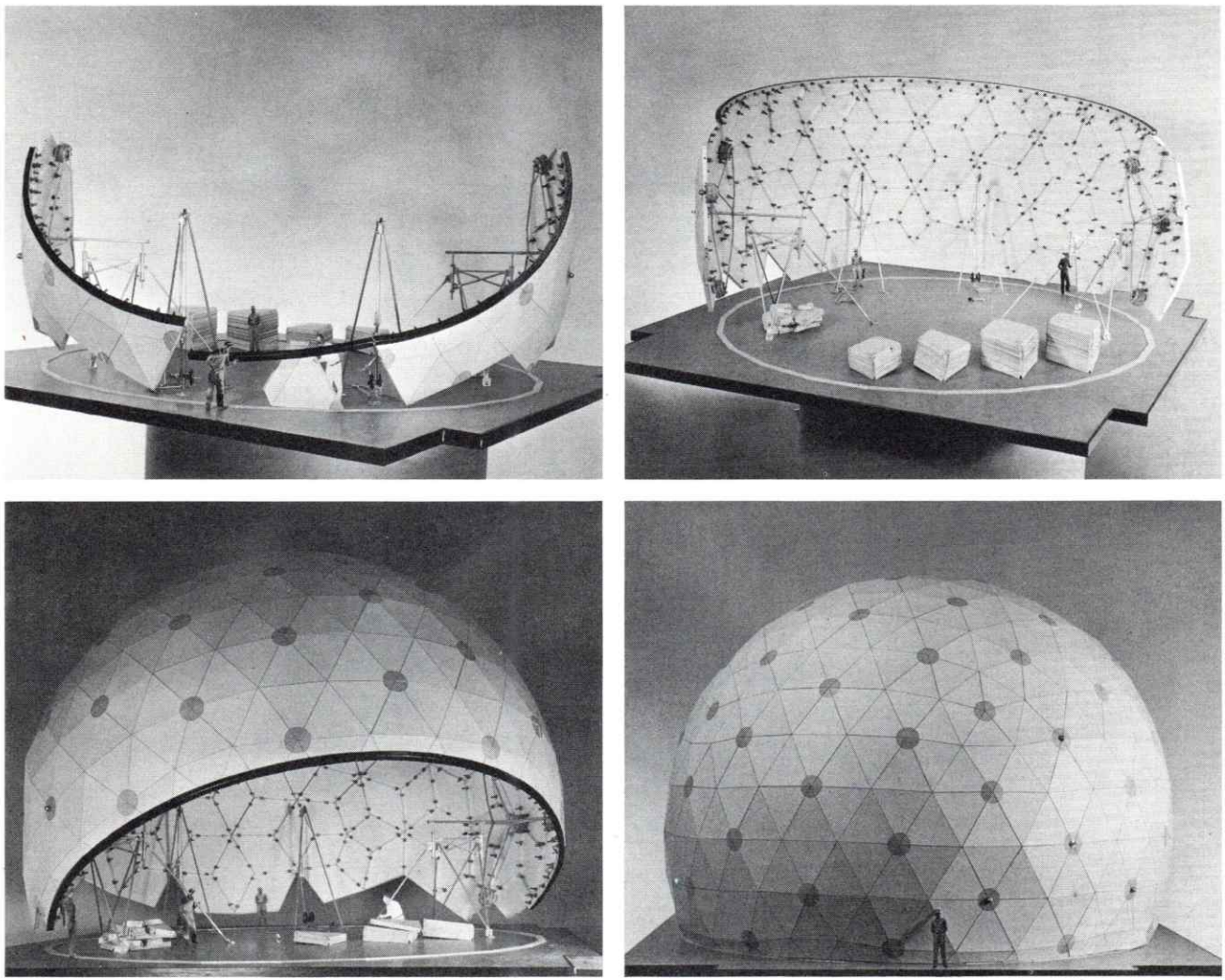

Fig. No. 106 Inverted base rings joined, rings 1-7 complete, 3/4 completion, final erection. Technique developed for Altername method of Dew Line radomes. Construction stresses induced in dome during rock over and sail shape critical in wind restrict use. 6^V Alternate dome similar to Figs. 33, 34, 35, 36, 37 and 38.

SELECTED BIBLIOGRAPHY

History

Marks, R. W., "The Dymaxion World of Buckminister Fuller," Reinhold Publishing Company, New York, 1960.

McHale, J., "Richard Buckminister Fuller," Architectural Design, July, 1961, pp. 290-322.

McHale, J., "Richard Buckminister Fuller," Makers of Contemporary Architecture, George Braziller, New York, 1962.

Fuller, R. B., "Architecture Out of the Laboratory," Student Publication, University of Michigan, 1955, Vol. #1, pp. 9-34.

Geometry

Coolidge, J. L., "A Treatise on the Circle and the Sphere," Oxford University Press, London, 1961.

Cundy, H. M., and Rollett, A. P., "Mathematical Models," Oxford University Press, New York, 1966.

Lyusternik, L. A., "Convex Figures and Polyhedra," Dover Publications, Incorporated, New York, 1963.

Lines, L., "Solid Geometry with Chapters on Space-Lattices, Sphere-Packs and Crystals," Dover Publications, Incorporated, New York.

Steinhaus, Hugo, "Mathematical Snapshorts," Oxford University Press, New York, 1960.

Stuart, Duncan, "On the Orderly Subdivision of Spheres," Student Publication of the School of Design, North Carolina State University (At Raleigh), 1955, pp. 23-33.

Stuart, Duncan, "Polyhedral and Mosaic Transformations," Student Publication of the School of Design, North Carolina State University (At Raleigh), 1963, pp. 3-28.

Structural Behavior

Aguilar, R. J., "A Study of the Stability of Framed Triangulated Geodesic Domes Under the Action of Concentrated Loads," Unpublished Doctorial Thesis Department of Civil Engineering, North Carolina State University, Raleigh, North Carolina, 1964.

Feng, R., "Stresses in Framed Surface Domes," Unpublished Masters Thesis, Department of Civil Engineering, North Carolina State University, Raleigh, North Carolina, 1962.

Uyanik, M. E., "The Design of a Geodesic Dome," Student Publication, The School of Design, North Carolina State University, Raleigh, North Carolina, Vol. #9, Number 2, pp. 47-56, 1960.

R. Buckminister Fuller Geodesic Patents
Geodesic Dome 2,682,235
Geodesic Paper Borad Dome 2,881,717
Geodesic Tent 2,914,074

Special Credits

Fig. 73 Murphey-Mackey Architects
Fig. 88 Shoji Sadao
Fig. 91 B. Mc Donell
Fig. 93 Rohm-Haas Company